Alma Mater Studiorum – Università di Bologna

DOTTORATO DI RICERCA
IN BIOLOGIA FUNZIONALE DEI
SISTEMI CELLULARI E MOLECOLARI
Ciclo XX

Settore scientifico disciplinare di afferenza: BIO 19

INTERAZIONI TRA LE GLICOPROTEINE D, B, H ED L CRITICHE PER LA FUSIONE INDOTTA DAL VIRUS HERPES SIMPLEX

Presentata da: Dott.ssa Cristina Forghieri

Coordinatore del Dottorato

Chiar.mo Prof.
Vincenzo Scarlato

Relatore

Chiar.ma Prof.ssa
Gabriella Campadelli-Fiume

Esame finale anno 2008

TABLE OF CONTENTS

INTRODUCTION

1. INTRODUCTION

1.1 THE HERPESVIRIDAE'S FAMILY TAXONOMY

Herpesviruses are large DNA-containing enveloped viruses widely distributed in nature. Based on biological properties and sequence data, the family Herpesviridae is divided into three subfamilies *Alpha*-, *Beta*-, and *Gammaherpesvirinae* [1,2,3,4].

Alphaherpesvirinae (containing *Simplexviridae*, *Varicelloviridae, Mardiviridae* and *Iltoviridae* genera) were classified by a variable host range, short reproductive cycle, rapid spread in tissue colture and ability to establish latent infections primarily in sensory ganglia. The known human pathogens of this subfamily are: herpes simplex virus 1 and 2 (HSV-1, HSV-2) and varicella zoster virus (VZV).

Betaherpesvirinae (containing *Cytomegaloviridae, Muromegaloviridae* and *Roseoloviridae*) were characterized by a limited host range, long reproductive cycle and slow infection progression in tissue culture. Cells that are infected often become enlarged (cytomegalia) and the virus can maintain latency in secretory glands, lymphoreticular cells, kidneys and other tissues. The human herpesviruses members of this subfamily are: human cytomegalovirus (HCMV or HHV-5), human herpesviruses 6A, 6B and 7 (HHV-6A, HHV-6B, HHV-7).

Gammaherpesvirinae is divided into two genera: *Lymphocryptoviridae* which includes human Epstein-Barr virus (EBV or HHV4) and *Rhadinoviridae* which includes human Kaposi's sarcoma-associated herpesvirus (KSHV or HHV8). They were classified by a very limited host range, actually they are usually specific for T and B cells and establish a latent infection in lymphoid tissues.

All members of the Herpesviridae family share the same virion structure, genomic arrangement and biological properties.

1.2 HERPES SIMPLEX VIRUS (HSV-1)

1.2.1 Epidemiology and Pathogenesis

Herpes simplex virus type 1 infects 60%-80% of people throughout the world. Initial HSV infection usually happens in childhood and is often asymptomatic [5]. Virus transmission occurs between an infected human to a susceptible one, by close contact. The oropharyngeal mucosa is the most common location of primary infection, but incident episodes of genital infection by HSV-1 seems to be increased [6,7]. Generally HSV infections are confined to skin and mucosa but could be severe in immunocompromised host. HSV-1 causes oral, labial and occasionally facial lesions, it may cause keratitis if infects the eye mucosa and is the most common cause of sporadic encephalitis in adults Fig. 1.2. A [5].

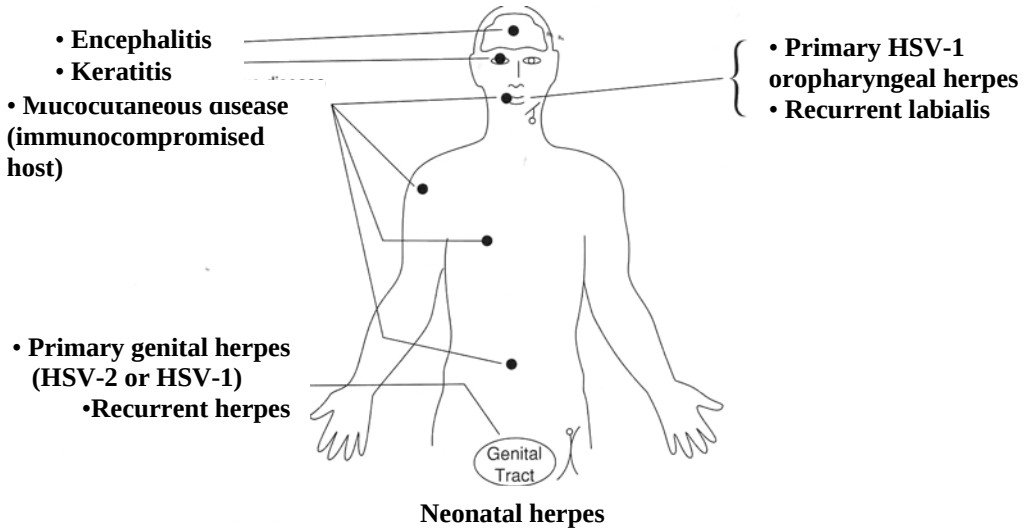

Fig. 1.2.A Sites of HSV infection and disease [5].

During primary infection, HSV-1 replicates at the site of entry then infects nerve endings and translocates by retrograde transport to the nuclei of sensory ganglia [8] Fig 1.2.B. In the majority of the infected neurons, the viral genome remains for the entire life of the host in an episomal state. In some individuals, the virus reactivates and is moved by anterograde transport to a site at or near the portal of entry. Recurrences are spontaneous, but there is an association with physical or emotional stress, fever, exposure to ultraviolet light, tissue demage and immune suppression

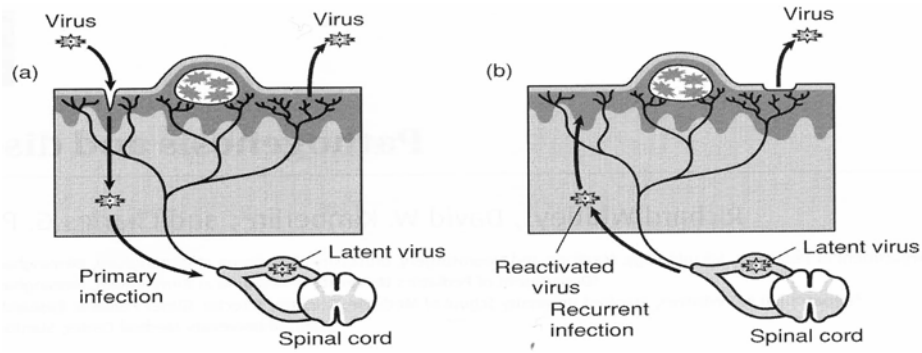

Fig. 1.2.B (a) Primary infection. (b) Recurrent infection. [8]

1.2.2 Structure

Herpesvirus particles consist of four morphologically distinct structures: an electron-dense toroidal core, a highly ordered icosahedral-shape capsid, an amorphous tegument and an outer envelope containing glycoprotein spikes [9] (Fig. 1.2.C).

The core contains a copy of linear double-stranded DNA closely packed into multiple shells [10].

The capsid, about 125-130 nm in diameter, is an icosahedron with 150 hexameric and 12 pentameric capsomers, which are connected in groups of three by the triplexes (asymmetric structures). The hexons consist of six molecules of the major capsid protein (MCP or VP5, *UL19* gene product) together with six molecules of the smallest capsid protein (SCP or VP26, *UL35* gene product). Eleven pentons consist of five MCP molecules and the other one is compound by twelve molecules of the portal protein (PORT, *UL6* gene product). The triplex consist of two copies of the triplex dimer protein (TRI2 or VP23, *UL18* gene product) and one copy of the triplex monomer protein (TRI1 or VP19C *UL3*8 gene product) [11].

The tegument is a proteinaceus layer which contains more than 20 virus-encoded proteins important in various aspects of the virus life cycle [12] .

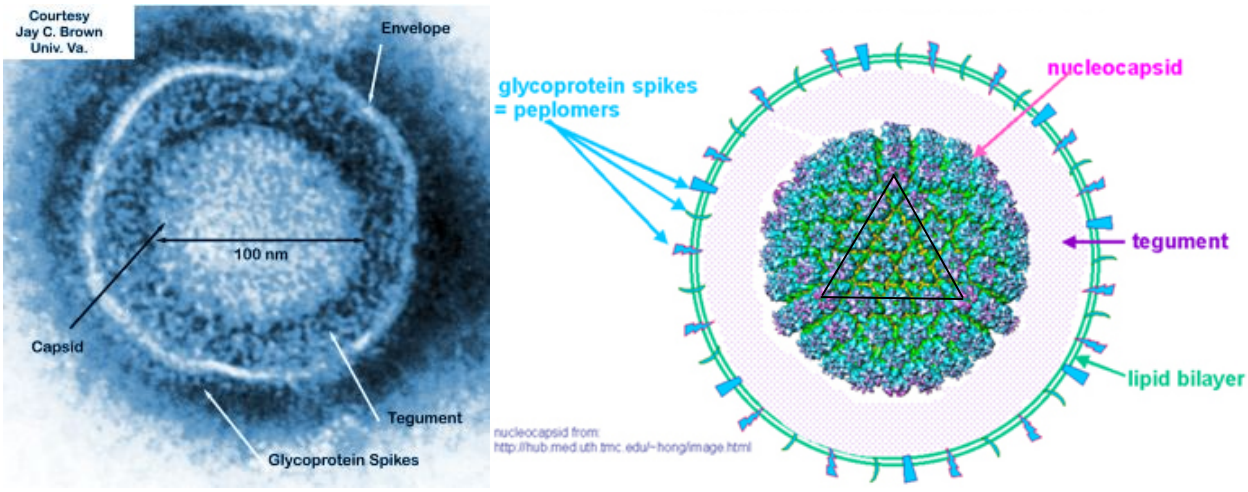

Fig. 1 2.C. Herpes virus structure. On the left image of HSV obtained at electron microscopy. On the right, Herpesvirus capsid at 8 Å resolution [11] surrounded by representation of HSV layers. One of triangular faces is denoted by black triangle.

The most notable proteins include the α-trans-inducing factor (α-TIF or VP16) which induces the transcription of viral immediate-early genes and the virion host shut-off protein (vsh) that degrades most of the host mRNAs during the initial stage of infection.

The HSV envelope contains at least eleven glycoproteins (gB, gC, gD, gE, gG, gH, gI, gJ, gK, gL and gM). Additional membrane proteins not detected in virion envelope are UL20, UL34, UL45 and possibly US9. At the ultrastructural level, HSV glycoproteins form long thin spikes, each made of a single species. The envelope contains 600-750 glycoprotein spikes that vary in length and in the angle at which they emerge from membrane. The distribution suggests functional clustering [13].

1.2.3 HSV-1 genome, organization, replication and transcription

The HSV-1 genome is approximately of 150 kbp with a G+C content of 68%. The genome consists of two unique sequences, designated as L (long) and S (short), bracketed by inverted repeats of different lenghts named *ab* and *b'a'* for the L component and *a'c'* and *ca* for the S one.

The genome can be represented as follows:

$$a_L a_n b\text{-}U_L\text{-}b'a'_m c'\text{-}U_S\text{-}ca_S$$

where the *a* sequence can be variable.

By the inversion of one or both unique sequences four different isomers are originated, these isomers may be purified in equimolar amount from infected cells [14].

The HSV-1 genome encodes for about 90 transcriptional units, and for 84 different gene products [12]. The majority of HSV genes encode for a single protein. Many mRNAs initiate in the middle of an expressed ORF and encode only the C-terminal part of the protein. Few transcripts do not appear to encode expressed ORFs and their function in productive infection is not known e.i. the latency-associated transcripts (LATs) which are expressed in latent infection [14].

The genes of HSV-1 are divided into three classes, according to their kinetic expression after virus entry: α, or immediate early genes, that map near the termini of the L and S components, with the exception of $\alpha 0$ and $\alpha 4$ that map in the inverted repeats sequences; β, or early genes, and γ, or late genes, disseminated long the L and S sequences.

Viral DNA is replicated by the rolling-circle mechanism in the nucleus of the host cell forming concatameric molecules which become cleaved into individual units during their packaging into capsids. At least three virus-encoded gene products are required for viral DNA synthesis: the viral DNA polymerase, the single-stranded DNA-binding protein (ICP8), and the origin-binding protein UL9. The origins of DNA synthesis oriS and oriL, made of palindromic structures, carry a binding site for UL9. UL9 has an ATP-binding and DNA helicase motifs, essential for viral replication. The binding of UL9 induces a bend in the DNA so it forms a single-stranded stem loop structure, and thus ICP8 is recruited. The remaining viral DNA replication proteins, as viral DNA polymerase, are recruited to the replication fork and the viral DNA synthesis initiates.

Viral DNA is transcribed by host RNA polymerase II and gene expression is tightly regulated in a cascade fashion (Fig. 1.2.D).

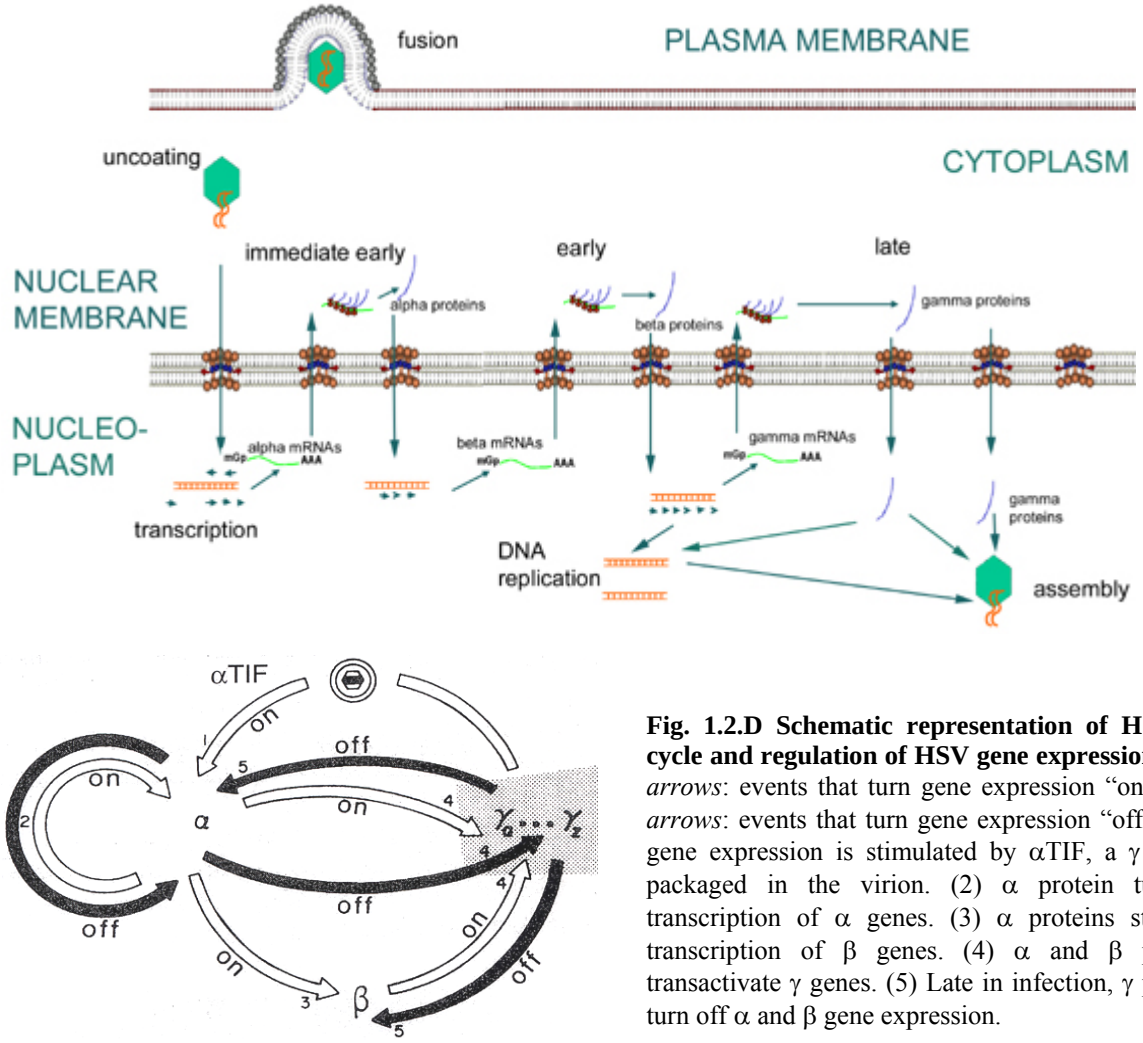

Fig. 1.2.D Schematic representation of HSV cell cycle and regulation of HSV gene expression. *Open arrows*: events that turn gene expression "on"; *filled arrows*: events that turn gene expression "off". (1) α gene expression is stimulated by αTIF, a γ protein packaged in the virion. (2) α protein turn off transcription of α genes. (3) α proteins stimulate transcription of β genes. (4) α and β proteins transactivate γ genes. (5) Late in infection, γ proteins turn off α and β gene expression.

The transcription of *α* genes is transactivated by α-TIF, released in the cytoplasm of the host cell after virus entry, and by cellular transcription factors as Oct-1 and HCF. Proteins encoded by *α* genes, e.g. ICP0 and ICP4, regulate the expression of the other classes of genes. Expression of *α* genes is required for expression of *β* genes which are divided in *β1* and *β2*. The gene products encoded by both *β* subgroups are involved in replication of viral DNA and nucleotide metabolism, and stimulate *γ* gene transcription. *γ* gene products are involved in virion assembly and usually are components of mature virions. *γ* genes are divided into two classes, *γ1* and *γ2*, their expression is dependent of viral DNA synthesis.

In latently infected neurons the viral genome is maintained in episomal form and no replicating virus is observed (Fig. 1.2.E). Latency is established in the absence of *α* gene expression and LAT RNAs are the only transcripts.

Sequence analysis of the LAT domain showed the presence of at least 16 ORFs, two of which, ORF O and ORF P, play some roles. Thus ORF O and ORF P gene products are expressed from a single mRNA, such that they share the same amino-terminal sequence and then diverge. Protein encoded by ORF O binds ICP4 and prevents the transcription of HSV DNA. ORF P protein product co-localizes with spliceosomes and reduces the accumulation of ICP0.

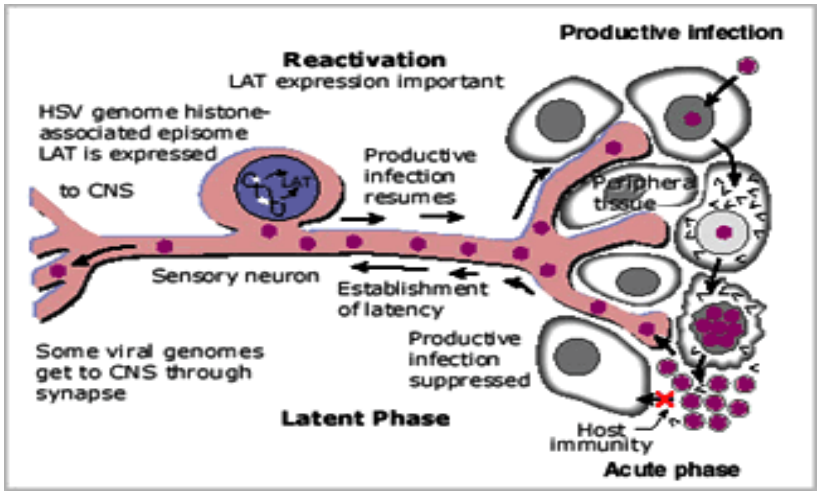

Fig 1.2.E HSV establishment of latency. In productive infection, HSV enters at mucosal surfaces, replicates in epithelial cells at the site of entry and spreads through the tissue. Virus enters nerve endings of sensory neurons and is transported to neuron cell body in the ganglion where virus can either replicate productively or establish a latent infection: viral DNA

1.3 VIRUS MEMBRANE FUSION

Enveloped viruses like HSV enter cell via fusion of their membrane with a host cell membrane. Virus membrane fusion can occur either at the plasma membrane or at an intracellular location following internalization of virus by receptor-mediated endocytosis. Membrane fusion is energetically unfavorable and does not spontaneusly occur. According to the stalk hypothesis, fusion of two lipid bilayers in an aqueous enviroment requires that they come into close contact. This process involves local membrane bending creating a first site of contact. Two forces dominate, a repulsive hydration force arising from water tightly bound to the lipid headgroups, and an attractive hydrophobic force between the hydrocarbon interiors of the membrane. Dehydration of the initial

contact site induces monolayer rupture that allows mixing of lipids from the two outer leaflets, resulting in a hemifusion stalk in which the aqueous inner contents remain distinct. In a next step the radial expansion of the stalk leads to either direct fusion pore opening or to the formation of another intermediate, the hemifusion diaphragm, a local bilayer resulting from the contact between the two internal leaflets of the fusing membranes. The break of the hemifusion diaphragm also result in pore formation. Finally, pore enlargement, leads to complete fusion (Fig. 1.3.A),[15]. In virus entry the energy necessary for membrane deformation and bending is provided by glycoproteins called fusion proteins. Upon appropriate triggering, the fusion protein interacts with the target membrane through a hydrophobic fusion peptide and undergoes a conformational change that drives the membrane fusion reaction. There are a variety of fusion triggers, including various combinations of receptor binding, receptor/coreceptor binding and exposure to the midly acidic pH within the endocytic pathway.

Three different classes of viral fusion proteins have been identified based on their important structural features.

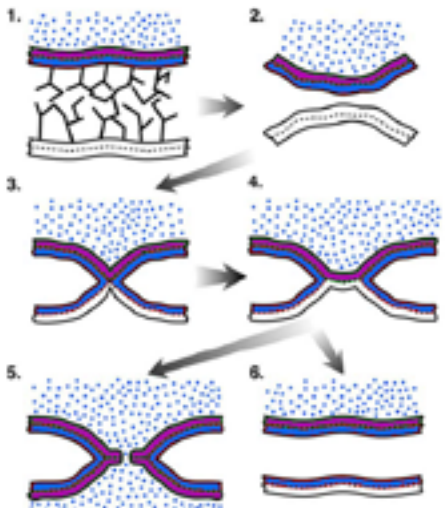

Fig. 1.3.A Fusion-through-hemifusion. The proximal and distal leaflets of the membrane at the top are labeled with purple and blue. In the initial prefusion state (1), membranes are separated by an approximately 10 nm gap determined by the size of the membranedocking proteins. (2) Proteins bring membrane bilayers into close contact. For simplicity, the proteins are not shown at the periphery of the contact zone. (3) The proximal leaflets merge into a fusion stalk, which allows lipid mixing between these leaflets, provided that the lipid flow is not hindered by proteins surrounding the fusion site. (4) The stalk expands into a hemifusion diaphragm that either breaks to form a fusion pore allowing lipid and content mixing (5) or dissociates, yielding separated membranes and interrupting fusion at the stage detectable as complete or partial lipid mixing between the proximal membrane leaflets (6).

1.3.1 Class I fusion proteins

The haemagglutinin protein from influenza virus has provided the model for class I fusion machines, because the atomic structure of three different forms of

this protein have been determined. The class I model, in its essential features, applies to proteins of many unrelated virus families as the HIV gp120, the F proteins from paramyxoviruses, the retroviral SU/TM proteins and the Ebola virus Gp2 protein.

These proteins are homotrimers that project vertically from the virus membrane and contain mostly α-helical structures. They form trimers both before and after the fusion reaction. Type I fusion proteins are frequently synthetized as a single-chain precursor which undergoes cleavage by host proteases. The cleavage generates an N-terminal globular protein and a metastable C-terminal protein. The novel N-terminus contains a hydrophobic sequence (15-30 amino acids), known as "fusion peptide". Downstream of it, it's possible to recognise at least two HR (heptad repeat) regions: one adjacent to the fusion peptide called HR-N and one close to the original trasmembrane domain, called HR-C. After binding to a receptor or exposure to the low pH, the protein forms an extended conformation, in wich HR-N form a trimeric coiled coil, and the fusion peptides insert into the target membrane.Then HR-C fold over the hydrophobic grooves of HR-N trimer in anti parallel direction, thus forming a trimer of hairpins containing a central α-helical coiled-coil structure. In this new conformation the fusion peptide and the original transmembrane domain are juxtaposed. As a consequence, the viral envelope and the target membrane are close (Fig. 1.3.B). The transition from the metastable conformation to the final stable conformation provides the energy necessary for the fusion process, but for many proteins seems that the energy released by the refolding of one trimer is not sufficient. Some observations suggest that the density of influenza virus hemagglutinin is important for fusion and a decrease arrests fusion at hemifusion stage. In contrast to HA, data on HIV-1 env suggest that a single env trimer is sufficient for fusion. On the other hand cellular receptor density, as well as env density, affect the kinetics of HIV-1 env mediated fusion [16].

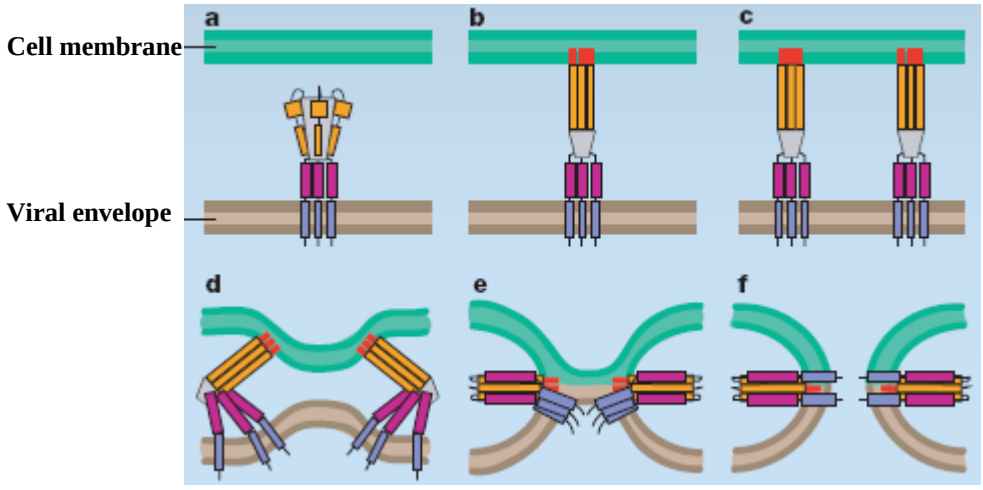

Fig. 1.3.B (from [17]). Proposed mechanism for membrane fusion by class I fusion proteins. **a)** The metastable conformation of a trimeric generalized fusion protein,with helical domain A in orange, helical domain B in pink, and the transmembrane domain in purple. **b)** After binding to a receptor on the cellular membrane, or on exposure to the low pH found in intracellular compartments, the protein forms an extended conformation and the hydrophobic fusion peptide (red) inserts into the target membrane. **c)** Several trimers are thought to be involved. **d)** Protein refolding begins. The free energy thereby released causes the membranes to bend towards each other. **e)** Formation of a restricted hemifusion stalk allows the lipids in the outer leaflets of the membranes to mix. **f)** Protein refolding completes, forming the final, most stable form of the fusion protein,with the fusion peptide and TM domain anti-parallel to each other but in the same membrane.

1.3.2 Class II fusion protein

Representative members of class II fusion protein are the E proteins of the flavivirus tick-borne encephalitis virus (TBE) and dengue virus (DV) and the E1 protein of the alphavirus Semliki Forest virus (SFV) [17-18].

The type II fusion proteins form heterodimers with a regulatory membrane protein maturated by the cellular furin enzyme; in flavivirus, the maturation of the regulatory protein leads the heterodimers to reorganize in homodimers. For both alphaviruses and flaviviruses, furin processing of the companion protein is an important regulatory step without which the virus has decreased infectivity. The dimer of class II fusion proteins do not form spikes but are parallel to the viral membrane. These proteins are elongated finger like molecules with three globular domains composed almost entirely of β-sheets; they are not proteolytically activated. They carry an internal fusion peptide in a loop between two-β-strands. Low pH dissociates the dimers and exposes the fusion loop, than the proteins reorient vertically, insert into the target membrane and trimerize. Structural predictions suggest that the fusion loop insert only peripherally into the bilayer, projecting their aromatic side chains into the aliphatic region of the

outer leaflet of the target membrane. After the trimerization a further rearrangement bring the original transmembrane domain juxtaposed to the fusion peptide thanks to a flexible region, adjacent to the trasmembrane domain called stem region. The type II fusion proteins are not predicted to form a coiled coil, their post-fusion state is characterized by trimers of hairpins composed of beta structures (Fig. 1.3.C).

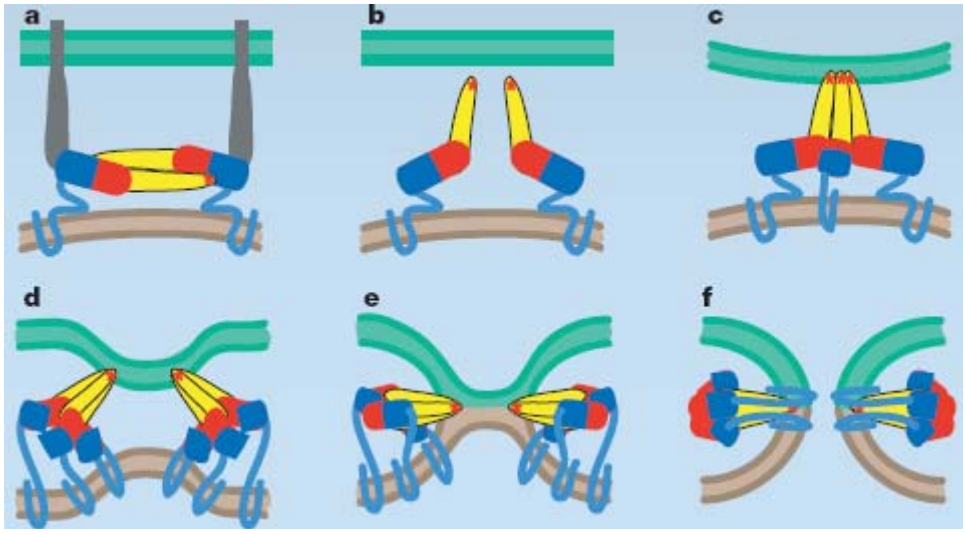

Fig. 1.3.C (from [17]) Proposed mechanism for fusion by class II proteins, **a)** The dimeric E protein binds to a cellular receptor (grey) and the virus is internalized to endosomes. Membrane fusion,which will release the virus into the body of the cell, takes place within endosomes. Domain I is in red, domain II in yellow, and domain III in light and dark blue (the lighter blue shows a predicted but unsolved structure). **b)** The acidic pH inside endosomes causes domain II to swing upward, permitting E monomers to rearrange laterally. **c)** The fusion loop (red dot) inserts into the outer leaflet of the host-cell membrane, enabling trimer formation. **d)** The formation of trimer contacts extends from the top to the bottom of the molecule. Domain III shifts and rotates to create contacts, bending the membrane. **e)** The formation of further contacts leads to unrestricted hemifusion. **f)** The final most stable form of the protein**.**

1.3.3 Class III fusion protein

The distinct structural features of vescicular stomatitis virus (VSV) glycoprotein (G) from class I and II have resulted in the creation of a third class of fusion protein, class III. In this class are also enclosed proteins of other Rhabdoviridae and gB of HSV. The VSV G protein oligomerizes into a homotrimer during the transport to the cell surface and is not subject to proteolytic priming for fusion activation. G forms spikes that protrude from the viral surface, it is responsible for viral attachment to specific receptors and for membrane fusion after endocytosis of the virion. Unlike the other two type of fusion protein G have not an irreversibile metastable pre-fusion state. The VSV G conformational

change induced by its exposure to low pH in endosomes is reversible. G can adopt at least three conformational states: the native pre-fusion state detected at the viral surface above pH 7 (Fig 1.3.D); the activated hydrofobic state, which interacts with the membrane as a first step of the fusion process; finally the fusion–inactive post-fusion conformation that is antigenically distinct from the other two. The post-fusion conformation displays the classic hairpin conformation of other viral fusogenic proteins, that is an elongated structure with the fusion domain and the TM domain at the same end of the molecule. As in class I fusion proteins, the post-fusion trimer displays a six-helix bundle with the fusion domains at the N terminus of the central helices and the TM domains at the C-terminus of the antiparallel outer helices. However, each fusion domain exposes two fusion loops located at the tip of an elongated β-sheet revealing a striking convergence with class II fusion proteins [19-20]. It isn't clear how VSV G catalyzes the fusion process, it has been proposed that a concerted cooperative change of a large number of glycoproteins, perhaps organized in a hexagonal lattice, is used to overcome the high energetic barrier encountered during fusion.

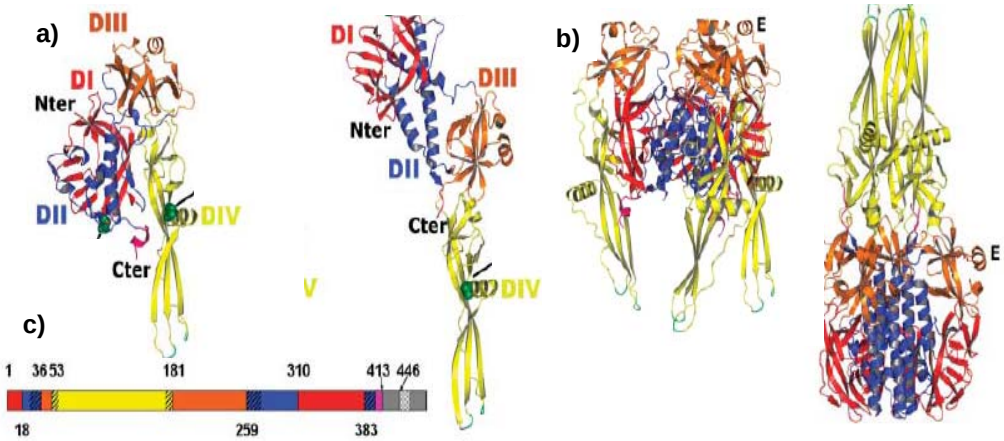

Fig. 1.3.D a) View of the G protomers structures in pre- and postfusion conformations, colored by domain. b) View of corresponding G trimers. C) Domain architecture of VSV G plotted on a linear diagram with domain boundaries numbered. [20]

1.4 HSV ENTRY INTO HOST CELLS

The current model of HSV-1 entry consists of three stages: the first step involves virus attachment to the cell surface, the second step involves the

interaction of glycoprotein D (gD) with an entry receptor, and the third step involves fusion of the viral envelope with the host membrane followed by releasing of the capsid-tegument complex into the cytoplasm of the infected cell, or involves endocitosys followed by fusion with endosomal membrane. The site of entry is cell type dependent, but in both cases the fusion is driven by four essential glycoprotein gD, gB, gH and gL.

1.4.1 The attachment

The attachment of the virus to cell membranes is mediate by gC (non essential glycoprotein encoded by *UL44* gene), and possibly gB, which interact with glycosaminoglycans (GAGs) [21]. The attachment is reversible, ensures that virions are tethered and concentrated on the cell surface but even if enhances infectivity by approximately 10 fold, is not strictly required.

Some reports have suggested that three different pathways are implicated in HSV-1 entry into different cell types: via direct fusion with the plasma membrane, via fusion within an acidic or a neutral endosome [22-24]. Furthermore in each pathways are required gD, gB, gH, gL and a gD receptor.

1.4.2 Receptors

gD interacts with three alternative entry receptors, nectin1, HVEM (herpesvirus entry mediator, also named HveA for herpesvirus entry mediator A) and specific *O*-sulphated (3-*O*-S) moieties on HS generated by the enzymatic activity of certain D-glucosaminyl *O*-sulfotransferases on HS [25-30].

The three receptors belong to structurally unrelated molecular families [30-32]. HVEM belongs to the tumor necrosis factor receptor (TNFR); it seemed to be restricted to T-lymphocytes in human tissues, but its distribution may be wider, at least as judged from cultured cells. The interaction with gD involves two of the four typical cysteine-rich domains (CRD) of TNFRs. Like other TNFRs, HVEM has in the cytoplasmic tail a death domains or TRAF (TNFR-associated

factor) interacting motifs with which may trigger intracellular transduction pathways.

Nectin1 belongs to a family of intercellular adhesion molecules, whose ectodomain is made of three immunoglobulin (Ig)-structured domains. Nectins mediate cell adhesion by forming *cis*-homodimers (e.g. nectin1-nectin1) on the cell surface, and *trans*-dimers with other nectins located on adjacent cells. *Trans*-dimers are formed between nectins of the same molecular species, but also between nectins belonging to different species (e.g. nectin1 to nectin3), in highly specific associations. Nectin1 is broadly expressed in human tissues, including tissues and organs targeted by HSV, like CNS, ganglia and muco-epithelia [33-37] and is expressed in virtually all human cell lines [31-32].

3-*O*-sulfated Hepara Sulfate derived from heparan sulfate proteoglycans modified by the enzymatic activity of certain D-glucosaminyl *O*-sulfotransferases which are present in a number of human cells, including neuronal and endothelial cells, and corneal fibroblasts. There is limited information regarding the interaction of HSV with 3-*O*-S HS.

It is unclear why HSV interacts with multiple alternative receptors. The gD affinity to nectin1 and HVEM is of the same order of magnitude (10^{-6} M); hence, affinity is not a basis for preferential usage [38]. Because clinical isolates use both nectin1 and HVEM, it appears that this property favours successful infection and spread in the human host [39].

A type 2 glycoprotein, designated B5, was identified by its ability to render otherwise resistant porcine cells more susceptible to HSV entry [40]. The same cells were rescued by HVEM, and it was thus proposed that B5 serves as HSV receptor. However, the ability of B5 to bind virions, or, even more so, a specific glycoprotein was not documented.

Recent data suggest, that also gB may interact with an own receptor on the cell surface. Thus a soluble truncated form of gB is able to bind in a saturable manner to the surface of different cell types, including cells deficient in heparan sulfate proteoglycan or even after heparin treatment to remove gB bound to HS. Besides

the soluble gB inhibits HSV-1 entry into HS deficient cells in a dose-dependent manner. The nature and the role in the entry of HSV-1, of this receptor is still unknown [41]. A molecule that associate with gB and seems to serve as co-receptor in HSV-1 entry may be PILR (paired immunoglobulin-like type 2 receptor) [42].

1.4.3 HSV fusogenic glycoprotein

1.4.3.1 gD

HSV-1 glycoprotein D is a type I membrane glycoprotein of 369 aa, after signal sequence cleavage, with a single transmembrane segment located between aa 317 and 339 (fig. 1.4.A) and three glycosylation sites.

The crystal structure of a soluble form of gD (up to aa residue 259) alone or in complex with the ectodomain of HVEM was solved [43].

gD's ectodomain structurally consists of three regions: the central core consist in a V-like domain of the immunoglobulin fold (residues 56-184) and a 17 aa long helix; the N-terminus (residues 1-37), that is unstructured in the crystal of gD alone, but forms a hairpin (bending at residue 21) in the crystal of the complex with HEVM; the C-terminus folds back towards the N-terminus [44].

The contacts of gD for HVEM have been localized within the N-terminal hairpin [43; 45],

The nectin1-binding site remains poorly defined, determined by means of insertion-deletion or substitution mutants appears to be more widespread than that of HVEM, it seems to be formed by several discontinuos sequences [46-47]. Deletion of the first 32 aa of gD abrogate the interaction with HVEM but not with nectin1. Critical aa residues for nectin1 binding include V34, Y38 and the cluster D215, R222, F223, all of which occupy a same surface of the molecule [48-50].

Functionally, the endodomain of gD is dispensable: a soluble form of gD, deprived of the TM and C-tail regions, is sufficient to complement the infectivity of a noninfectious gDnull virus and gD is functional even when anchored to the virion envelope through a GPI anchor [51-52]. Hence, the

activity of gD reside completely in the ectodomain which may be divided into two functional domains, a N-terminal domain with receptor binding activity that takes up the first 250-260 residues and a C-terminal domain with the pro-fusion domain (PFD), which lies in 250-310 residues [53]. It is not clear the activity of PFD domain but its replacement by heterologous sequences and some aminoacids substitutions impair infection and cell-cell fusion, without affecting gD binding property.

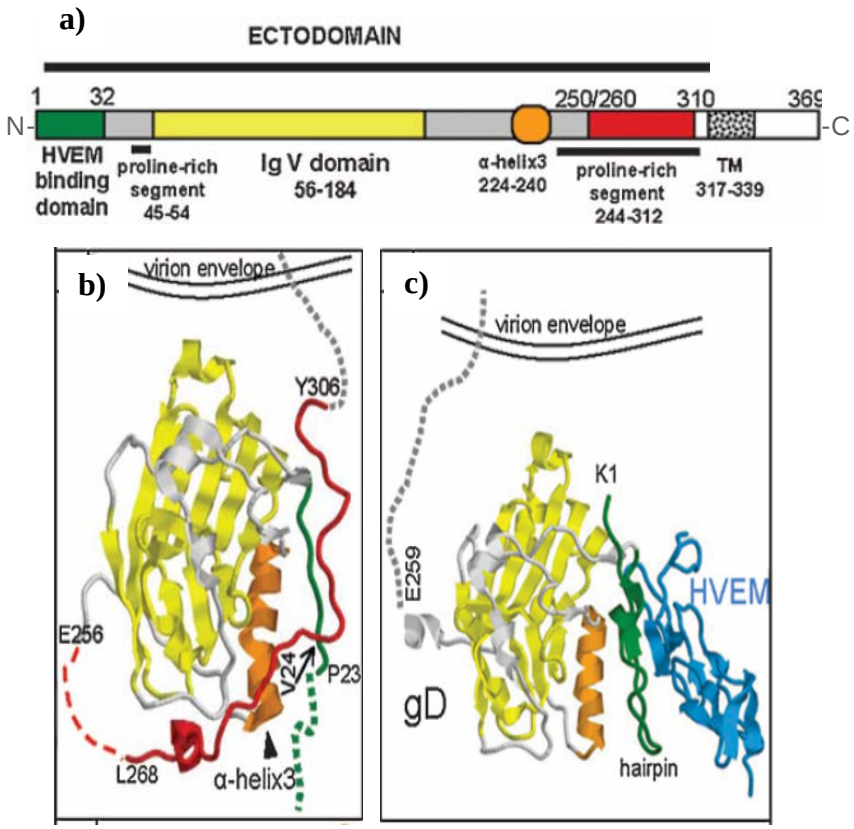

Fig. 1.4.A gD Structure a) Domain architetcture of gD b) Ribbon diagram of gD derived from crystal data. c) Ribbon diagram of gD HVEM-bound derived from crystal data.

An interesting feature of PFD is its high content of prolines which exibhit defined spacings. Substitution of some prolines reduced HSV infectivity indicating that they represent necessary residues. The frequent presence of proline rich regions in cassettes that function in protein-protein interaction, suggests that the PFD may interact with target proteins.

Whereas soluble gD is able to mediate the entry of a gDnull virus, the interaction with its receptor is not used to anchor the virion to the cell surface but probably to trigger conformational changes in gD which lead to the envelope

fusion. Structural studies and before biochemical studies done with GST pull down experiments had shown that gD may adopt almost two different conformations: closed and opened [44 and 54]. In the closed conformation, present when gD is not ligated to a receptor, the C-terminal portion of the ectodomain folds back on itself and wraps the N-terminal region; in the opened conformation, the binding with a receptor displaced the C-terminus. It is not clear how and if this change from closed to opened conformation triggers fusion and if the free terminus of opened gD may act binding other proteins.

The Ig-like domain in the ectodomain of gD seems to play the role of connecting the N-terminal receptor-binding region to the C-terminal region carrying the PFD but does not appear to encode executable functions required for viral entry into cells at least when the HVEM and nectin1 binding sites are substituted by uPA (urokinase plasminogen activator) as noticed in an isolated obtained modifying an HSV retargeted to uPA [55]. This isolate had gD split into two polypeptides (A and B), as a consequence of frame shifts and stop codon insertions. Polypeptide A was made of uPA fused to gD_{33-60}. Polypeptide B started at methionine 219, and thus was $gD_{219-369}$; it included the α-helix3 plus the downstream proline-rich flexible region. It was demonstrated that the uPA moiety of polypeptide A could mediate physical interaction with polypeptide B. Attempts to generate a split gD in which the polypeptide A lacked the uPA moiety and instead consisted entirely of gD sequences (gD_{1-60}) did not yield any virus. Possibly the polypeptides A and B are unable to interact one with the other in the absence of uPA.

1.4.3.2 gH.gL

Glycoprotein H, a 110 kDa glycoprotein encoded by UL22, is essential for virion infectivity [56] Neutralizing antibodies to gH block virus entry but permit attachment, indicating a role of the protein in a post-attachment step [57].

Bioinformatic predictions of structural motifs show that gH ectodomain carries elements typical of class I fusion glycoproteins, in particular a highly

hydrophobic α-helix (named α-H1) which has features of an internal fusion peptide and two heptad repeats (HR-1 and HR-2) that could interact and adopt a coiled-coil conformation, in addition to a less hydrophobic region (named α-helix2), and a membrane-to-interface hydrophobic sequence [58-61].α-Helix1 can be functionally exchanged with heterologous fusion peptides (e.g. from HIV gp41 and VSV-G), and interacts with lipids of natural and artificial membranes [58, 61-62]. Furthermore a mimetic peptide may adopt an α-helical conformation. The predicted α-helix is positionally conserved in all examined gH orthologs from human and animal herpesviruses, suggesting that it may constitute a critical element in the conserved mechanism of herpesvirus fusion.

Heptad repeats are predicted in all gH orthologs and occupy a canonical position typical of class I fusion glycoproteins. A mimetic peptide to heptad repeat-1 can adopt an α-helical conformation, and forms a stable complex with the heptad repeat-2 mimetic peptide. Peptides mimicking HR-1 or HR-2 block infection [59, 60 and 62].

The ectodomain of HSV-1 gH also carries a RGD motif (residues 176, 177, and 178) that is used by several viruses to attach to integrin molecules and mediate the entry into the cells. gH binds integrins [63] but mutation of the RGD to RGE seemed not alter the HSV ability to bind and penetrate cells in vitro [64].

gH's function depend on forming a heterodimer complex with gL, whic acts as a gH chaperon for its proper processing and trafficking to the viral envelope. The non covalent interactions occur between the first 323 amino acids of gH and the first 161 amino acids of gL. gL is a soluble glycoprotein of 224 amino acids encoded by UL1 gene. It is unclear that it only enables gH to adopt a correct conformation, or plays own specific roles in HSV entry and fusion.

1.4.3.3 gB

gB encoded by HSV-1 *UL27* gene is highly conserved among the Herpesviridae family. It is a homotrimeric, 904-aminoacid type I glycoprotein composed of a 696-aa ectodomain that is N-glycosilated at multiple sites [65-68, 5], a 69-aa

transmembrane domain, and 109-aa carboxy-terminal domain [69-70]. The transmembrane domain was proposed to have three segments corresponding to residues 727-746, 752-772 and 775-795 which can traverse the membrane three times. The third segment was suggested to be the membrane anchoring domain, while the first and the second may be peripherally associated with the membrane [71]. The cytoplasmatic tail of gB is the longest among HSV-1 glycoprotein and has a negative control on fusion. In fact the gB endodomain carries at least two functional endocytosis motifs, one di-leucine based (LL871) and one thyrosine based (YTQV889-892) [72-74]. They traffic gB from the plasma membrane to small endocytic vacuoles which after coalesce, subtracting the amount of gB exposed on the plasma membrane and decreasing the ability of the cells to fuse with adjacent ones [73, 75]. Besides gB C-tail is the site of *syn* mutations (*syn* 3). Cell infected with *syn* mutants form syncytia differently from cell infected with wild type virus. *Syn* mutations are thought to affect genes which negatively regulate fusion but the mechanism is unknown [76].

On the other hand, gB still exerts a positive role in fusion, may be through the ectodomain. The requirement of gB in HSV fusion is inferred by numerous lines of evidence: HSV-1 mutants lacking gB are not able to enter the cells due to a post-attachment defect; gB is necessary in in the cell-cell fusion assay; neutralizing antibodies map on gB; mutants temperature-sensitive with affected rate entry reside in the gB ectodomain [69-70, 76-84]. The crystal structure of part of the ectodomain (from D103 to A730) was recently solved, showing a homotrimeric spike made up of five distinct domains in each protomer [84]. There isn't an unique trimerization domain but several contacts between protomers, throughout the molecule, contribute to trimer stability. The ten cysteines per subunit form only intramolecular bonds. The rod-shaped trimer organised around a coiled-coil central core resembles closely to that of VSV G in its post-fusion conformation [19]. Domains I and II, the 'base' and the 'middle', (similar to domains IV and III of G), adopt a fold similar to pleckstrin homology (PH) domains. PH domains are found in cytosolic proteins involved

in intracellular signaling, where they mediate both protein-protein and protein-lipid interactions [85]. gB domain I is structurally homologous to the domain IV of VSV G containing two fusion loops at the tip of an elongated four-strand β-sheet. In gB the two loops lie, the first, at residues 173 to 179 and the second at residues 258-265. Three residue of these loops, W174, Y179 and A261, are essential for gB's function in cell-cell fusion [86].

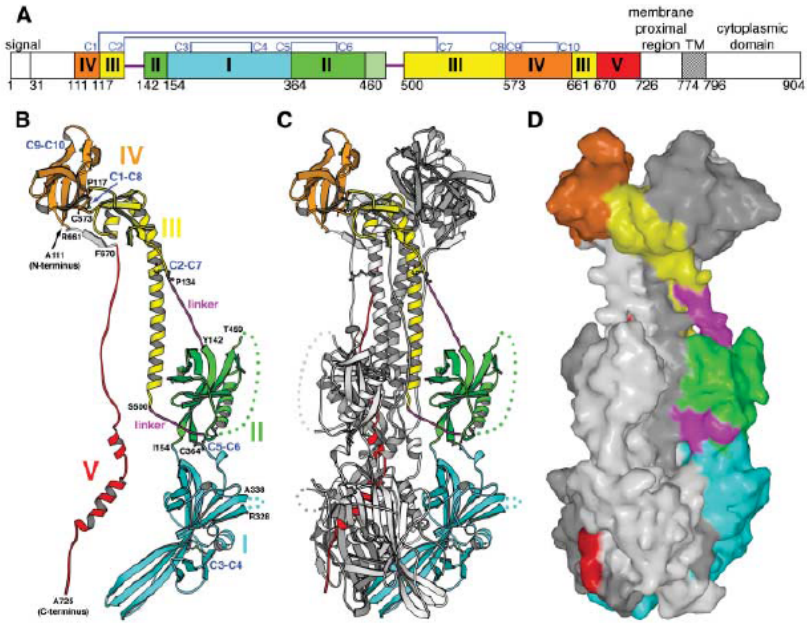

Fig. 1.4.C (A) Domain architecture of gB; (B) Ribbon diagram of a single gB protomer; (C) gB trimer; (D) Accessible surface area representation of gB trimer [84].

Domain III (VSV G domain II) is composed by the long α-helix that forms the coiled-coil core followed by a short helix and a small β sheet. Domain IV (corresponding to domain I of VSV G), the "crown", doesn't show homology with structures previously described; it is fully exposed on top of the trimeric spike. Domain V, the "arm", is a long extension that spans the full length of the protomer and makes contact to other two protomers.

Antibodies with neutralizing activity bind to different regions on the gB surface and are against both continuos and discontinuos epitope. Recently functional regions (FR) based on neutralizing Mabs had been reclassified holding in consideration the solved structure into: FR1 is composed of residues of domain I and the C-terminus of domain V; FR2 comprises three overlapping epitopes

within domain II; FR3 includes amino acids located between domain III and domain IV and FR4 that lie at a unresolved region (Fig 1.4.B) [87].

Glycoprotein B together with glycoproteins H and L form the core fusion machinery conserved throughout the herpesvirus family. In Varicella-Zoster virus (VZV), cytomegalovirus (CMV) and human herpesvirus 8 (HHV-8) the action of gB or the gH/gL complex alone could result in fusion, although at a very lower level than when all 3 glycoproteins are present [88-90].

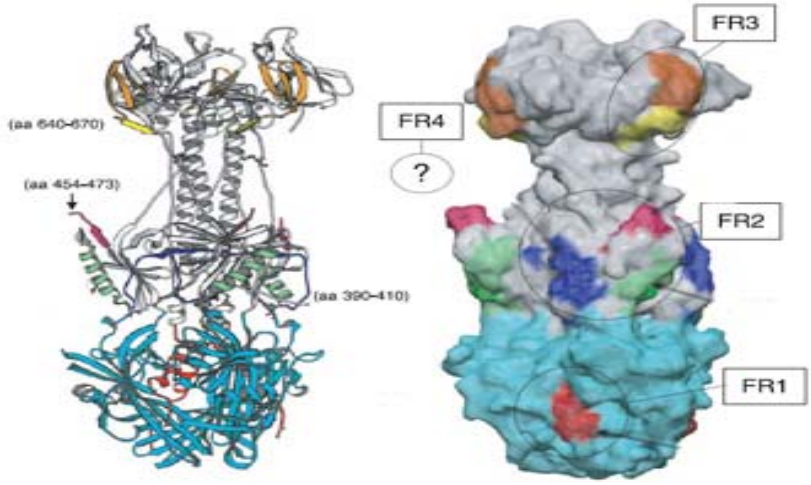

Fig. 1.4.B Location of the epitopes of neutralizing MAbs and of FRs on the surface of the crystal structure of gB. On the left ribbon diagram of a gB trimer showing in color the epitopes of representative neutralizing MAbs. On the right accessible surface area representation of the gB trimer. FR1 to FR3 are indicated with circles. Since FR4 is present in an unresolved region of gB, it is symbolically represented with a question mark [87].

HSV-1 gB exhibits 86% identity with HSV-2 gB while shares the 27 % identity and 46 % similarity at the protein sequence level with HHV8 gB.

In the experimental work of this thesis amino acid sequences from HHV8 were used so gB HHV8 is dealt with details.

1.4.3.3a gB of human herpes virus 8

Human herpes virus 8 (HHV8) or Kaposi's sarcoma associated virus (KSHV) is a gammaherpesvirus etiologically linked to the pathogenesis of Kaposi's sarcoma, peripheral effusion lymphoma, and multicentric Castelman's disease. These pathologies occur more frequently in people with severe

immunodeficiency. KSHV has been detected in B cells, endothelial cells, monocytes and epithelial cells in vivo. In vitro HHV8 can infect a variety of human cell types and several animal cells but infection usually evolves as a latent infection making difficult to study the virus. Very little is known about the entry of HHV8. It has been shown that HHV8 enters in human foreskin fibroblast cells (HFF) through clathrin-mediated endocytosis [91] and that HHV8 gB, gH and gL (homologues of HSV-1 gB, gH and gL) could mediated the fusion of CHO cells with embryonic kidney cells and B lymphocytes [90]. HHV8 is able to bind to heparan sulfate, thus infectivity is reduced by enzymatic removal of cell heparan sulfate, virus binding is blocked or displaced by soluble heparin and binding is drastically reduced on CHO cells that are deficient in HS [92]. Probably like HSV-1, the attachment allowes to concentrate the virus on the cell surface and is followed by the binding to one or more cell receptor molecules. Several lines of evidence indicate that attachment is mediated by two glycoproteins gpK8.1A and HHV8 gB. HHV8 gB is a type I membrane glycoprotein 845 amino acids in lenght, with a cleavable signal sequence of 23 residues, a predicted transmembrane domain between residues 710-729 and 13 putative N-glycosylation sites. There is a potential proteolytic cleavage site (RKRR/S) at amino acid position 440-441, and cleavage at this site would result in two proteins with predicted masses of about 48 and 45 kDa [93, 94]. The cellular distribution and processing of gB depend on the cell type in which the protein is expressed; it is not cleaved when expressed transiently in CHO and COS-1 cells while in BCBL-1 cells is synthesized as a 112 kDa precursor protein, undergoes cleavage and processing, and the envelope-associated form consist of 75 and 59 kDa polypeptides that form disulfide-linked heterodimers and multimers [92, 94].

HHV8 gB may also bind cell integrins thanks to an integrin-binding RGD motif that lies near the signal sequence. Soluble gB induces the integrin-mediated activation of FAK (focal adhesion kinase) [95]. KSHV infectivity but not

binding of fibroblast and endothelial cells is neutralized by RGD peptides and by antibodies to α3 and β1 integrins.

A recent study showed that KHSV utilizes the dendritic cell-specific ICAM-3 grabbing nonintegrin (DC-SIGN; CD209) as a receptor for infection of myeloid DCs and macrophages [96]. It is a type II C-type lectin that is expressed on myeloid DCs, IL-4-treated monocyte-derived DCs, macrophages and IL-13-activated monocyte-derived macrophages. DC-SIGN and other C-type lectins act as pathogen recognition receptors that alert macrophages and DCs to take up and process pathogens for Ag presentation to T cells. Certain viruses, parasites, yeast, and bacteria can subvert this immune function by using DC-SIGN as a receptor.

Another receptor used by KSHV is the 12-transmembrane transporter protein xCT for entry into adherent cell but doesn't seem involved in infection of B cells which are important target for KSHV infection [97].

1.5 HSV EGRESS

The assembly of herpesviruses begins in the nucleus of an infected cell, where newly synthetized genomes are packaged into preformed capsids. In a second time nucleocapsids contact the inner nuclear membrane and bud into the perinuclear space. In this process HSV UL31 and UL34 proteins interact with the nuclear envelope and recruit cellular protein kinase that partially dissolve the nuclear lamina providing the sites for envelopment. The subsequent steps of egress have been extensively debated. An earlier model, reffered as the single envelopment model, suggested that perinuclear enveloped virions are transported to the cell surface via the secretory pathway and the envelope glycoproteins are processed in situ [98]. In this pathway the virion manteins the tegument acquired in the nucleus as well as the envelope acquired at the inner nuclear membrane. More recently it was proposed that capsids pass across the nuclear envelope through enlarged nuclear pores into the cytoplasm and undergo their first envelopment at TGN [99]. Critics raised against this models are that it

is based solely on electron microscopic observations and that other groups have not seen dilated pores at the late stages of infection or the exit of capsids through nuclear pores. However the current widely accepted model, supported by biochemical and morphologic evidence, is the de-envelopment re-envelopment egress. In this model virions fuse their primary envelope with the outer nuclear membrane such that unveloped nucleocapsids are released into the cytoplasm where capsid-proximal tegument proteins assemble at the capsid. After that they acquire other tegument proteins and a second envelope with mature glycoproteins by budding into the trans-Golgi network (TGN) or into a endosomal compartement [100] (Fig 1.5.A). It isn't clear how the de-enveloped nucleocapsid can travel through the cytoplasm to TGN. An other question is why it was found that perinuclear virions carry immature oligosaccharides, intracytoplasmatic virions carry both intermediate and mature type of oligosaccharide and extracellular virions carry only mature oligosaccharides if the secondary envelope is taken at TGN. If the secondary envelopment occour at the *cis*- or *medial*-Golgi is difficult to understand how the virions travel from these to farther compartments of the exocytic pathway to obtain their final envelope.

It is also unclear how primary envelope fuses with the outer nuclear membrane. HSV mutants lacking any one of the four glycoprotein essential for entry, are not substantially compromised in virus egress yet cannot enter cells. Otherwise recently an HSV mutant lacking both gB and gH was shown to accumulate as enveloped virions in the perinuclear space and in the nucleoplasm. While viruses lacking just one of the two proteins do not exhibit substantial defects in nuclear egress suggesting that they are required also for fusion at the outer nuclear membrane and act in a redundant manner [101].

Other viral proteins, notably gK and UL20, seem to be involved in subsequent steps after primary envelopment, thus in their absence virus particles accumulate in the perinuclear space or cytoplasm. These proteins, however, appear to inhibit fusion performed by the quartet [73].

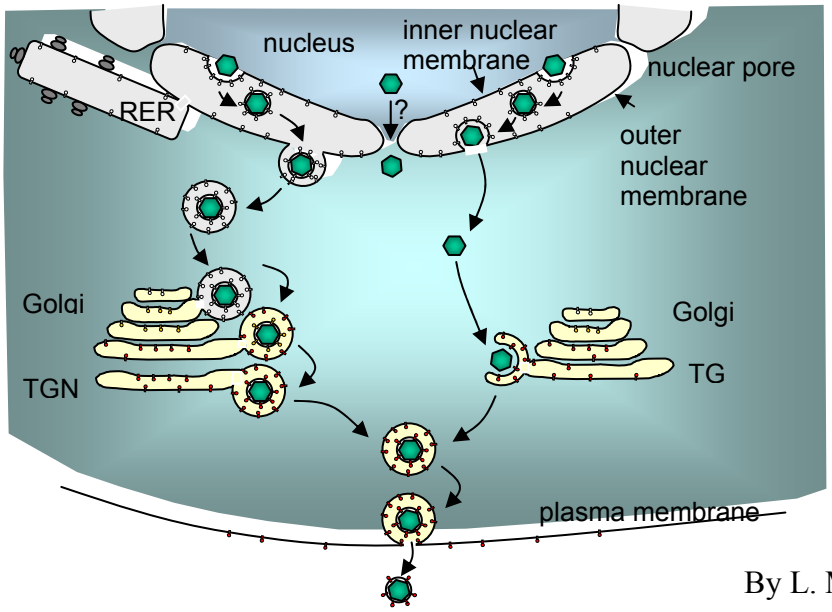

Fig. 1.5A Alternative pathways of HSV egress from infected cells. The single envelopment pathways is depicted to the left, and the double envelopment to the right. Perinuclear virions and nuclear membranes are decorated with glycoproteins of different color than virions at level of the Golgi apparatus and TGN, as well as extracellular virions, to emphasize that the oligosaccharide moieties of the viral glycoproteins are of the immature type in early exocytic compartment, but are of the mature type in the late exocytic compartments and in extracellular virions. The drawingconsiders also the possibility that nucleocapsids exit the nucleoplasm through modified nuclear pores, without transiting across the perinuclear lumen.

In the final envelopment seems to have a role the glycoproteins gE, gI and gD. In PrV the simultaneous deletion of gE-gI and gM drastically inhibits plaques formation and replication and induces intracytoplasmatic aggregation of capsids surrounded by tegument proteins. In HSV similar defects are obtained with deletions of gD and gE or gD, gE and gI. It was proposed that gD and the gE-gI act in a redundant fashion [102]. Also several viral tegument proteins are thought to play critical roles in cytoplasmic envelopment. These include homologues of the HSV-1 UL11 and UL36 genes [103-106] the alphaherpesvirus UL48 and UL51 genes [107-110] and the CMV UL32 gene [111]. It has to be explored the requirement of cellular proteins, recently it has been shown that HSV-1 cytoplasmatic envelopment requires functional Vps4 that is a cellular enzyme essential for multivescicular endosome (MVE) biogenesis [112]. Otherwise whichever egress model is correct, the identity of the membranes that serve as platforms for secondary envelopement is still unclear as well as if the enveloped virus reach the extracellular space directly by budding across the plasma membrane or by budding into the lumen of cellular

organelles, with luminal virions released into the extracellular enviroment via an exocytic mechanism or both. Many enveloped virus i.e. HIV seems to use for this process the cellular MVE budding machinery.

1.6 INTRACELLULAR TRAFFICKING AND THE MULTIVESCICULAR BODIES LATE ENDOSOME

In eukariotic cells cell, surface lipids, proteins, ligands and other solutes can be internalized by endocytosis and undergo opposite fates, some being routed towards lysosomes for degradation and others being retrieved for reutilization. In the sorting of endocytosed molecules a key role is held by multivescicular bodies [reviewed in 113-116].

The multivescicular body (MVB) was described by electron microscopists as an organelle that consist of a limitating membrane enclosing many (sometimes several hundred) internal vescicles of 40-90 nm. Later was shown that it represent an intermediates of the endocytic pathway and sometimes on refers to it as multivescicular endosome MVE. MVBs are formed by invagination and budding of vescicles from the limiting membrane of sorting (early) endosomes into the lumen of the compartment. During this process, proteins destined for degradation are sorted into the forming intralumenal vescicles (ILVs). Mature MVBs fuse with the lysosomes and deliver the ILVs to the lysosomial lumen where the vescicles and cargo are degradated. Transmembrane proteins may also are retained on the limiting membrane of MVBs and are either recycled to the *trans*-Golgi network and plasma membrane or are delivered to the limiting membrane of lysosomes. MVBs not only contain molecules endocytosed but also receive biosynthetic cargo from TGN including precursor of lysosomial enzymes. In specialised cell types, MVEs serves as intermediates in the formation of secretory lysosomes that fusing with the plasma membrane released the intraluminal vescicles (Fig. 1.6.A) [114].

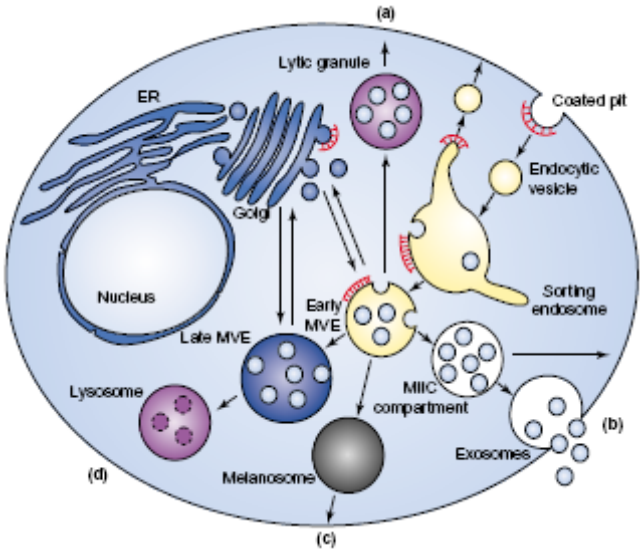

Fig. 1.6A Formation and functions of MVEs. Multivesicular endosomes are formed after invagination of the limiting membrane of the sorting endosome. They can serve different functions in different cell types, such as being precursors for (a) lytic granules in T lymphocytes, (b) MHC class II compartments and exosomes in antigen-presenting cells, (c) melanosomes in melanocytes, and (d) late MVEs/lysosomes in most nucleated cells. Both endocytic and biosynthetic proteins are sorted in and out of MVEs, indicated by arrows. Clathrin-coated buds are found at the plasma membrane, the TGN and on tubular regions of the sorting endosome, whereas flat clathrin coats are found on early endosomal compartments. Clathrin is indicated in red.

1.6.1 The role of ubiquitination in sorting

Ubiquitination causes sorting toward lysosomes from a number of compartments, including the Golgi (where ubiquitin serves as a signal to divert proteins to endosomes), the cell surface (where promotes internalization), and the MBV (where mediates incorporation into ILVs). The transfer of ubiquitin (Ub) to substrate proteins involves the sequential action of three classes of enzymes: an activating enzyme E1, a conjungation enzyme E2, and a ligase E3 [117]. Ub is typically attached to lysine side chains of substrate proteins and forms an isopeptide bond, but can also be covalently linked to other Ub moieties on target proteins to form polyubiquitin chains. E3 can interact directly with its substrate or uses other adaptor proteins to target its substrates. The majority of Ub is removed from proteins, by Ub-specific proteases or deubiquitinating enzymes (DUbs), just prior to the delivery of cargo into ILVs. Although certain Ub-dependent functions involve the formation of long polyubiquitin chains, MVB targeting does not; the fusion of a single Ub is sufficient to direct ILV targeting, and there are few long polyubiquitin chains on MVB cargo proteins [118-119]. Generally polyubiquitinated proteins are targeted to proteasomes but

polyUb might also function as an MVB targeting signal i.e. the yeast Gap1 becomes polyubiquitinated in the TGN and this signal its entry into MVBs [120]. Besides some proteins like yeast Sna3 or mammalian LRP don't require ubiquitination for sorting into ILVs [121-122]. Ub is recognized by an expanding group of endosomal proteins, which may act as Ub-sorting receptor responsible for binding and directing cargo.

1.6.2 MVBs biogenesis

The formation of lumenal membranes so the MVBs biogenesis depends on the function of a group of at least 18 conserved proteins originally described in yeast as class E Vps (Vacuolar Protein Sorting) proteins [115]. Loss of class E protein function rapidly leads to the accumulation of endosomal cargo in a anormally enlarged, higly tubulated endosome membrane compartment that fails to mature normally into MVBs, called the 'class E compartment'. For each known component of the yeast MBV sorting machinery, one or more mammalian homologues have been identified suggesting a higher complexity (Tab.1.6.A). Furthermore in mammalian cells the depletion of individual E Vps proteins causes varying phenotypes probably because they have more intermolecular connections than in yeast and that may compensate for the loss of a single component. The majority of the class E Vps proteins are constituents of three separate heteromeric protein complexes called ESCRT-I, ESCRT-II and ESCRT-III (Endosomal Sorting Complex Required for Transport). These protein complexes are transiently recruited from the cytoplasm to the endosomal membrane where they function sequentially in the sorting of transmembrane proteins into the MVB pathway and in the formation of MVB vesicles.

Initially, the ESCRT-I protein complex, recruited from the cytoplasm by Vps27, binds to ubiquitinated endosomal cargo and in some way activates ESCRT-II. ESCRT-II in turn initiates the oligomerization of at least four small coiled-coil proteins (Vps2, Vps24, Vps20, Sfn7), resulting in the formation of a large endosome-associated structure, like a lattice, the ESCRT-III complex. ESCRT-

III concentrates the MVB cargo and recruits additional factors such as Bro1 and Vps4.

Yeast gene	Mammalian gene	Motifs	Binds to	Modification	Complex
Vps23/Stp22	TSG101	UEV, Coiled-coil	Ubiquitin	Ubiquitinated	
Vps28	VPS28				ESCRT-I
Vps37	VPS37A-D	Coiled-coil			
Vps22	EAP30	Coiled-coil			
Vps25	EAP25				ESCRT-II
Vps36	EAP45	NZF	Ubiquitin		
Vps2/Did4	CHMP2A, B	Coiled-coil			
Vps20	CHMP6	Coiled-coil		Myristoylated	ESCRT-III
Vps24	CHMP3	Coiled-coil			
Sfn7/Vps32	CHMP4A-C	Coiled-coil			
Vps27	HRS	UIM, FYVE,VHS	Ubiquitin, PI3P	Ubiquitinated	Vps27/HRS
Hse1	STAM1, 2	UIM, VHS, SH3	Ubiquitin	Ubiquitinated	
Vps4	VPS4A, B	AAA, Coiled-coil			Vps4
Bro1/Vps31	A1P1/ALIX	Coiled-coil	LBPA		not known
Vps60/Mos10	CHMP5	Coiled-coil			not known
Fti1/Did2	CHMP1A, B	Coiled-coil			not known
Vta1	SBP1				not known

Tab. 1.6.A. Class E Vps proteins (modified from ref. 115)

Bro1 recruits the deubiquitinating enzyme Doa4, which removes the ubiquitin tag from the cargo protein prior to sorting into the MVB vesicles. In mammalian cells, the homologues of the yeast Bro1, called AIP1 (ALG2-interacting protein 1) or Alix (ALG2-interacting protein X), appears to serve as a bridge between ESCRT-I and ESCRT-III complexes and also to regulate the interaction of ILVs with the limiting membrane of lysobisphosphatidic acid (LBPA)-containing endosomal membranes.

Vps4 is a multimeric AAAtypeATPase, that after protein sorting has been completed, binds to ESCRT-III and disassembles the complex in an ATP-dependent manner. The dissociation of the ESCRT machinery is a prerequisite for vesicle formation.

The ubiquitination seems to have not only a function in sorting of cargo but also in MVB formation. The impairing of ubiquitin binding of the yeast ESCRT-II subunit Vps36 and of the yeast ESCRT-I subunit Vps23 affects MVBs formation. One possible explanation is that the interaction of ESCRTs

complexes with ubiquitinated cargo notonly serves to sort cargo but also has a regulatory function
in activating downstream events, such as the formation of ESCRT-III. Another possibility is that ESCRTs complexes, might interact not only with ubiquitinated cargo but also with ubiquitinated proteins of the MVB sorting machinery itself, promoting the formation of a functional sorting complex. However, a study on TSG101 (mammalian Vps23 homologue) has shown that its ubiquitination results in decreased MVB sorting and in its solubilization from the endosomal membrane, suggesting that in case of ESCRT-I at least, ubiquitination plays a negative regulatory role. Also Vps27 (mammalian HRS), that recruits ESCRT-I from the cytoplasm to endosome, has a Ub binding activity, but in this case mutations only affect sorting of ubiquitinated cargo but not the formation of MVBs.
The formation of MVB vesicles is unique in that it is directed toward the lumen of the compartment, rather than the cytosol. It is not easy to imagine how the ESCRT proteins could be directly involved in the invagination of the endosomal membrane
without getting trapped in the lumen of the forming vesicle and which role have lipids in this process. Differential lipid sorting render ILVs susceptible to degradation and the limiting membrane resistant to hydrolase, but the lipid composition and localized lipid remodeling may also control the organization of the protein sorting machinery and perhaps the budding. Consistent with this, phosphatidylinositol 3-phosphate (PI3P) recruits Hrs to endosome, antibodies against lyso-*bis*phosphatidic acid (LBPA) inhibit MVBs formation and sphingomyelin and cholesterol are candidates for mediating protein sorting to MVBs.

1.6.3 Viruses and MVBs

The production of various enveloped RNA viruses such as HIV depends on some of the same protein machinery that controls MVB formation (Fig.1.6.B).

Topologically, the budding of viruses out of the cytosol (either from tha cell surface or from endosome) is similar to the budding of endosomes from the limiting membrane to form ILVs.

Gag, the major structural protein of retroviruses, can assemble and bud from cells in the absence of any other viral factor [123]. Mutational analyses of Gag have defined short sequences motifs required for efficient particle release termed late or L domains to reflect their function late in the virus budding process [124-125].

Three classes of motifs have been defined in viral L domains: P(T/S)AP, PPXY (where X usually is a proline), and $YP(X)_nL$. Late domain have been identified in retroviruses, rhabdoviruses, filoviruses, arenaviruses and probably also in ortho- and paramyxoviruses. It's now clear that different L domains bind different cellular factors and in particular proteins of the MVBs biogenesis machinery. PTAP late domains function by recruiting TSG101, $YP(X)_nL$ domain seems to facilitate virus budding by binding AIP1/Alix, PPXY motifs interact with proteins containing WW domains (two Trp separated by about 40 amino acids) like Nedd4 family of ubiquitin E3 ligases. Mutations in TSG101 and AIP1 affect the release of retroviruses which have PTAP and $YP(X)_nL$ late domains.

Mutants on VPS4A and B proteins are also potent inhibitors of retrovirus budding and block the release of retroviruses that leave the cell via all three known late domains, suggesting that retroviruses all enter the MVB pathway upstream VPS4, regardless of which class E proteins they bind.

Ubiquitin transfer also plays importants roles in the budding of virus that utilize P(S/T)AP and PPXY late domains. Mutations in Ub can inhibit the release and it is known that several retrovirus incorporate high level of Ub into their particles.

Gag proteins are monoubiquitinated at multiple sites and the levels of ubiquitination are altered by the presences or not of L domains. Althought ubiquitin transfer is clearly important for retrovirus release, it has not been established that Gag proteins are the functional targets for ubiquitination, indeed

it has been reported that amino acid substitutions which prevent Gag from being ubiquitinated do not impair virus budding [126].

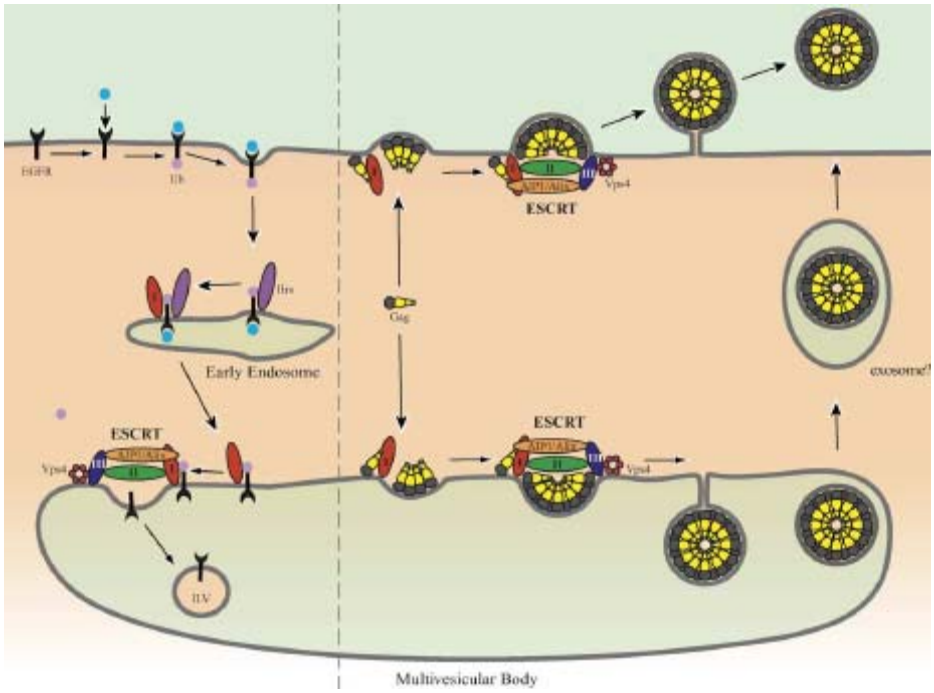

Fig. 1.6.B (from ref. 125) **Model for retrovirus release**. On the left, schematic representation of endocytosis and MVB sorting of an activated growth factor receptor. An Hrscontaining complex (dark purple) recognizes and sequesters ubiquitylated cargo (Ub, light purple) at clathrin-rich regions of the early endosomal membrane. Hrs recruits ESCRT-I (I, red) through a direct interaction with Tsg101. ESCRT-I in turn recruits additional components of the MVB pathway, i.e., ESCRT-II (II, green) and ESCRT-III (III, blue), to assemble into a functional sorting complex. AIP1/Alix (brown) is recruited to the assembled complex and in mammaliancells bridges ESCRT-I and -III. The AAA ATPase Vps4 (red) is critical for disassembly of the complex following inward budding of vesicles into the endosomal lumen. On the right is depicted the hijacking of MVB sorting machinery for virus release. HIV-1 Gag is believed to mimic Hrs in triggering membrane recruitment of ESCRT-I. Virus particles are shown to assemble and bud at the plasma or to be released (e.g., from macrophages) through the exosome pathway following assembly in the MVB.

The MVB machinery is not only hijacked by viruses to egress from cell, but some viruses like VSV use it to entry. VSV envelope fuse with the membrane of ILVs leading the release of the nucleocapsid into the lumen of these vescicles to be safely transported across the cytoplasm then back-fusion events allow its final release with a mechanism that require LBPA and AIP1 [127].

Several lines of evidence indicate that MVB biogenesis machinery has a role in HSV envelopment.Vps24 and Vps4 are critical for efficient HSV-1 assembly/release, very likely for HSV envelopment [112 and 128]. The MVB compartment was morphologically altered in HSV-infected cells, and appeared to be enlarged compared to that of uninfected cells. gB accumulates at MVB

membranes and its intracellular trafficking requires a correct MVB biogenesis process. gB is ubiquitinated in infected cells and in its ubiquitination seems to be involved in part K63, a residue implicated in endocytosis and not in proteasome-dependent degradation [128]. A gB mutant lacking the 37 most C-terminal amino acids of the cytoplasmic tail ($gB_{\Delta 867}$) and impaired in its ability to accumulate at cytoplasmic vesicles [73], is significantly less ubiquitinated than the wt protein [128]. Virions carrying in their envelope $gB_{\Delta 867}$ are impaired most likely in cytoplasmic envelopments and egress [128]. The site of gB accumulation as well as its ubiquitination makes it likely that the membranes of the MVBs serve as platforms for HSV envelopment, at least in some cells. Alternatively, the site of envelopment may be membranes other than those of the MVBs, to which components involved in MVB biogenesis are recruited through the intervention of gB and possibly additional viral proteins; candidates are the tegument proteins, predicted to contain L-domain motifs [112 and 128].

OBJECTIVES AND EXPERIMENTAL DESIGN

2. OBJECTIVES AND EXPERIMENTAL DESIGN

2.1 DETECTION OF HSV-1 GLYCOPROTEINS INTERACTIONS

The entry of herpes simplex virus (HSV) into cells takes place in 3 steps. In the first, two viral glycoproteins, gC and gB bind to heparan sulphate proteoglycans. In the second step, another glycoprotein, gD, interacts with at least one of three alternative receptors: nectin 1, herpesvirus entry mediator (HVEM) or modified heparan sulfate. In the third step, gH, gL and gB execute the fusion of viral envelope with the cell membranes, either plasma or endosomal.

A key question in HSV entry/fusion centres on how gD signals the encounter with one of its receptor to the others virion glycoproteins required to execute fusion.

The gD ectodomain is organized in two distinct regions, a N-terminus (aa 1-260) carrying the receptor binding sites, and the C-terminus (aa 260-310) carrying the profusion domain required to trigger fusion but not for receptor binding. In the unliganded state, the virion gD adopts a conformation in which the flexible C-terminus of the ectodomain folds back, wraps the N-terminus and masks receptor-binding sites. At receptor binding, the C-terminus is displaced leading gD to adopt an open conformation. This conformational change and/or the exposed residues trigger the fusion process in some ways [129]. Our working model envisions that, after receptor binding, gD forms complexes with downstream glycoproteins, or a subset of them.

The fusion between cells induced by co-expression of the all four fusogenic glycoproteins might be an useful surrogate of viral envelope-cell membrane fusion.

A method that allows to detect protein interactions in living cells is the bimolecular complementation assay. This method is based on observation that many reporter proteins, including green fluorescent protein (GFP), β-Lactamase, dihydrofolate reductase, firefly and *Renilla* lucferase, can be divided into

fragments that neither of them retains significant activity by themselves but can refold in a functional complex when they are brought into sufficient closeness. Therefore is possible restores and detects the fluorescence emission of a split GFP protein if its two halves are fused to two proteins that are destined to interact each other and only when they do it [130] . The objective of this study was to investigate, in intact cells, the interactions that occur among the quartet of membrane glycoproteins required for HSV entry into the cells

To this aim:

- we searched evidence that the bimolecular complementation assay was suitable to the detection of membrane-bound protein interactions fusing two fragments of the enhanced green fluorescence protein EGFP to two known interacting partners, gD and its receptor nectin 1.
- We fused the N- and the C- portions of EGFP to the endodomains of HSV glycoproteins to investigate their supposed interactions.

2.2 CHARACTRIZATION OF MUTANTS IN THE gD PRO-FUSION DOMAIN

The molecular events that follow receptor recognition by gD and precede the execution of fusion, referred to as triggering of fusion, are poorly understood. The gD ectodomain seems to encode two functions: the receptor binding and a signaling activity of receptor binding to downstream glycoproteins. The second activity may be carried by the region from aminoacid 260 to 310, which is required for viral infectivity and fusion but not for receptor binding. This region was called pro-fusion domain (PFD). The pro-fusion domain has an high content of prolines which exhibit somewhat regular spacings, feature often present in protein-protein interacting domains.

The substitution of some prolines reduced HSV-1 infectivity in a complementation assay, indicating that prolines represent critical residues.

The objective of this study was to define the regions/sequences involved in the pro-fusion activity of gD more accuratly.

To this aim:

- we mapped subregions of the pro-fusion domain testing the activity of mutants in which half domain was substituited by sequences from CD8;
- we mutated proline-glutamic acid doublets in the N-terminal portion of PFD to investigate their activity.

2.3 CONSTRUCTION OF gB CHIMERAS TO IDENTIFY FUNCTIONAL DOMAINS.

To enter the cell HSV-1 requires the quartet made of glycoproteins D, B, H and L. The roles of each component of the quartet are poorly understood. Available evidence indicates that, in the receptor-bound conformation, gD recruits, or activates the fusion executors gB and or gH/gL heterodimer. Of the three executors, gH appears to contain elements associated with fusion proteins, e.i. a hydrophobic α-helix that exhibits the properties typical of a fusion peptide and two heptad repeats, capable to form coiled coils and to interact with each other. On the other hand gB has features typical of viral fusion protein as showed from the crystal structure recently solved. gB structure is similar to that of the postfusion form of vescicular stomatitis virus (VSV) glycoprotein G, the sole responsible for VSV entry. Thus, comparison between G and gB domains does not explain how gB functions in concert with the other three glycoproteins of the HSV-1 fusion machinery. Furthermore VSV-G needs low pH for its trigger, while gB is required for fusion even when HSV-1 enters into cell in a pH independent way.

The current model of HSV entry envisions that the four glicoproteins interact with each other before or during fusion, the details of the interactions are not understood. The ectodomain of gB is known to be involved in entry. Temperature sensitive virus and a mutation that alters the rate of entry map to

gB ectodomain. Furthermore, gB ectodomain harbors the epitopes of several neutralizing antibodies.

gB has homologs in all herpesviridae family and in particular the position of ten cysteines in the ectodomain is highly conserved. In the past linker-insertion mutagenesis has been applied to gB to identify functional domains; however insertions exerted a detrimental effect on its folding [77, 83]. It is likely that point mutations would be less disruptive to protein structure, but the size of gB makes it impratictical to identify functional domains by this approach. When this work started the crystal structure was not solved and the only information available was that the conservation of the cysteines position was critical.

The objective of this study was to define the sequences involved in the fusion activity of gB and, in particular, the domains involved in the interaction with gD, gH and gL.

To this aim:

- we inserted the 5E1 epitope in the poly-lysine region of gB; we truncated the c-ter tail that carries the endocytoses motifs to enable cellular accumulation of the protein.
- we inserted restriction sites adjacent to two consecutive cysteines of gB to substitute, the sequences embedded, with homologous sequences derived from the HHV8-gB.
- we tested the chimeras obtained for their activity in cell-cell fusion assay, in the complementation of a gB -/+ virus and in a pull-down assay from gH or gD fuse to the *Strep*-Tactin affinity tag.

MATERIALS AND METHODS

3. MATERIALS AND METHODS

3.1 CELLS AND VIRUSES

Baby hamster kidney (BHK) cells, 293T and COS cells were grown in Dulbecco's modified Eagle medium (DMEM) supplemented with 5% fetal bovine serum (FBS). The receptor-negative J, J-nectin 1, and J-HVEM cells were described in refs. 33 and 53.

HSV-1(F) is described in ref. [131]. In gD-minus F-gDβ virus, the gD gene was replaced with *Lac-Z* gene [132]. The virus was grown in R6 cells to obtain ($gD^{-/+}$ stock). R6 cells express HSV-1 gD under control of UL26.5 promoter [11]. ΔgB-KΔT mutant was grown and titrated in gB-expressing D6 cells to produce complemented $gB^{-/+}$ stock.

3.2 PLASMID CONSTRUCTION

3.2.1. Generation of plasmids for spilt-EGFP complementation assay

The mammalian expression plasmids for gH in the MTS vector, and gD and nectin1 in pcDNA3.1 [33 and 47] were site-directed mutagenized 0 to 10 aa upstream of the stop codon, in order to generate restriction sites for the insertion of N or C amplimers. The sites were SphI for gH and BglII for gD or nectin1. Where necessary, the BglII site of pcDNA3.1 was preliminarily eliminated by digestion, filling in by T4-DNA polymerase and religation. N and C sequences were PCR amplified from pCMS-EGFP (Clontech) with the primer pairs (or variations thereof) 5'CCCAGATCTCCATGGTGAGCAAGGGCG AGGAGCTGT plus 5'GGGAAGCTTCTACTTGTCGGCCATGATATAGACGTTG or 5'CCCGCTAGCTCAGAAGAACGGCATCAAGGTGAACT plus 5'GGGAGATCTTAC TTGTACAGCTCGTCCATG CCGAGA, respectively.

N amplimer was ligated with BglII-HindIII-digested gD plasmid or SphI-BglII-digested gH plasmid, generating gD_N and gH_N. The C-EGFP amplimer

was ligated with digested nectin1 (BglII-XhoI) and gH (SphI-BglII) plasmids, generating $Nect_C$ and gH_C. The gC gene sequence was PCR amplified from DNA of HSV type 1 (F) with primers 5'AGATCTAGGCCTATGGCCCCGGGGC GGGTGGGCCTTGCCGTGGTCCTGTGGAGCCTG and 5'GAAGATGCGGCCGCTTA GCTAGCCGCCGATGACGCTGCCGCGACTGTGATGTGCG. The StuI-NheI-digested gC amplimer and the NheI-BglII-digested C amplimer were ligated with StuI-BglII-digested MTS vector. The gB-encoding plasmid in pcDNA3.1 was deleted of the endodomain sequences that carry endocytosis motifs, from aa 867 to the stop codon ($gB_{\Delta 867}$), in order to maximize gB expression [73]. The gB_C chimera was generated by mixing $gB_{\Delta 867}$ and C amplimers, generated with primer pairs 5'GGCTGGATCCTCCCCGTAGTCCCGCCATGC3' plus 5'CCTTGATGCCGTTCTTCTGAGATCTCTTCTTCTTGGCCTTGTGTTC3' and 5'GAACACAAGGCCAAGAAGAAGAGATCTCAGAAGAACGGCATCAAGG plus 5'GGGAAGCTTTTACTTGTACAGCTCGTCCATGCCGAGA3', followed by ligation with BamHI-HindIII-digested pcDNA3.1.

3.2.2 Generation of plasmids used to define functional subdomains in gD-PFD

First, we derived gD-PFD/2; the $gD_{1\text{-}260}CD8$ construct was amplified up to amino acid 285 with primers 5′-CCCTCTAGACTCGAGCGTTCCGGTATGGGGG-3′ and 5′-CAAGTTTGGTGGGATTTGCGGCGCCACCTGCGACGCGATGGTGGGCG CCGGTGT-3′. Amplimer 2, derived by amplification of the gD gene with primers 5′-CTCTTGGAGGACCCCGTGGGGACGCCCCTGTCCCTGCGCCCAGA GGCG-3′ and 5′-GCGGTTTAAACTGAATTCTCTAGTAAAACAGGGG-3′, contained the gD amino acid 285-stop codon. Each amplimer contained overlapping sequences (contained in the primers) with the other amplimer. The amplimers were mixed and further amplified with the external primers. The product was cloned into pcDNA3.1(-) at the XhoI and EcoRI sites. To generate $gD_{\Delta PFD}$ and gD-PFD/1, we inserted an Asp718 site at amino acid 310 of $gD_{1\text{-}260}CD8$. Digestion with Asp718 and EcoRI removed the

transmembrane (TM) and cytoplasmic tail (C-tail) of CD8, which were replaced with the TM and C-tail gD sequences, and amplified with primers 5′-CATCCCCCGGGTACCCCGAACAACATGG-3′ and 5′-GCGGTTTAAACTGAAT TCTCTAGTAAAACAGGGG-3′, thus generating $gD_{\Delta PFD}$. To generate gD-PFD/1, the latter construct was PCR-amplified from amino acid 285 to the stop codon with primers 5′-GGTCTCTTTTGTCTCGAGCGTTCCGGTATGGGGG-3′ and 5′-CGCCTCTGGGCGCAGGGACAGGGGCGTCCCCACGGGGTCCTCCAAGAG-3′.

A second amplification product, containing gD amino acids 1-285 plus the natural gD signal sequence (amino acids -25 to -1), was derived with primers 5′-CTCTTGGAGGACCCCGTGGGGACGCCCCTGTCCCTGCGCCCAGAGGCG-3′ and 5′-GCGGTTTAAACTGAATTCTCTAGTAAAACAGGGG-3′. The two amplimers contained overlapping sequences and were mixed and amplified with external primers. The final product was cloned in pcDNA3.1(-) at the XhoI and EcoRI sites.

gD mutants E259A-P261L (1), PE266-267LA (2), PE270-271LA (3), and PED273-274-275LAA (4) were obtained by site-directed mutagenesis of wt-gD-encoding plasmid described in ref. 33. Mutagenesis was performed with the following primers: (1) 5′-GCTGCCCCCGGAGCTCTCCGCGACCCTCAACG CCACGCAG; (2) 5′-CCCAACGCCACGCAGCTAGCACTCGCCCCGGAAGC; (3) 5′-GCAGCCAGAACTCGCGCTAGCAGCCCCCGAGGATTC; and (4) 5′-CTC GCCCCGG AAGCGCTAGCGGCTTCGGCCC TCTTGGAG.

3.2.3 Generation of plasmids encoding gB chimeras

a) gB_{5E1N}

To generate $gB_{5E1N,}$ two restriction sites, BamHI and EcoRI, were inserted at residues 68 and 77, respectively, by site-directed mutagenesis of plasmid for gB in pcDNA3.1. Mutagenesis was performed with the following primers: BamHI, 5’CCAACGGGGGACACGGATCCGAAGAAGAA CAAA; EcoRI, 5’GAACAAAAAACCGAATTCCCCACCGCCGCCGCGCCC. An amplimer of 5E1 epitope [133] was generated by extension of two synthetic partially overlapping oligonucleotides: 5’CTATTCGGAT

CCGAGTCGACCAGGAAGCACTACACCCTCTGGGAACTCTGCAAGATATGGG plus AGTAATGAATTCGGAGTTATACTTCTAGGTGTGTTATTCCCATATCTT GCAGAGTTCCCAG. The amplimer was cleaved with BamHI and EcoRI, and ligated in predigested gB.

b) $gB_{5E1N\Delta867}$

To remove the endocytosis motifs located in the cytoplasmic tail, downstream of aa 867 of gB, a stop codon was inserted at the corresponding aa of gB_{5E1} by site-directed mutagenesis performed with primer described in ref. 73. The resulting construct was named $gB_{5E1N\Delta867}$.

c) gBC3C4

XbaI and HpaI restriction sites were inserted at aa 217 and aa 270 (we always refer to amino acid position in wt-gB) respectively, by site-directed mutagenesis of $gB_{5E1N\Delta867}$ with the following primers: 5'GTACGTGCGCAA CAATCTAGAGACCACCGCGTT and 5' GTACGGGACGACGGTTAACTGCATC GTCG. Both mutations were silent. The restriction sites inserted were adjacent to the third and the fourth cysteines of gB ectodomain after cleavage of the signal sequence thus the construct obtained was named gBC3C4. This kind of nomenclature was used for all mutants.

d) gBC1C3C4

A HindIII restriction site was inserted by site-directed mutagenesis in gBC3C4 generating the substitution N112S. The primer used was the following: 5'GAACACCGATGCAAGCTTTTACGTGTGCCC. The construct was named C1C3C4.

e) gBC6

To generate gBC6, a XhoI site was introduced by site-directed mutagenesis in $gB_{5E1N\Delta867}$ by means of the oligonucleotide 5' CCTGGGGGA CTGCCTCGAGAAGGACGCCCGCGA. The mutagenesis inserted the following substitutions: I412L and G413E.

f) gBC5VC6

A XbaI restriction site was inserted by site-directed mutagenesis in gBC6 with primer 5'GCCCGTCGGTCTGCTCTAGAACCAAGTGGCAGG generating the substitution T365S and M366R.

g) gBC5MC6

To generate gBC5MC6, an Asp718 restriction site was introduced by site-directed mutagenesis in gBC6 with primer 5' TCATGGTGCAGAGGTAC CGGCGCTTTGGCAC. The mutagenesis inserted the following substitutions: P361R, S362Y and V363L.

h) gBC6C7

To generate gBC6C7 an EcorV restriction site was inserted in gBC6. The site-directed mutagenesis was performed with primer 5' CGCGTGG TGCGATATCCAGAATCACGAGCTG and introduced the substitutions E530D and L531I.

i) gBC4C5

Asp718 and HpaI restriction sites were inserted at aa 362 and aa 270 respectively, by site-directed mutagenesis of $gB_{5E1N\Delta867}$ with primers previously described in c) and g).

j) gB13H8

To generate gB13H8, the sequence encoding amino acid residues 65 to 167 of HHV8-gB was PCR amplified from plasmid pAB38 that carries HHV8-gB in pcDNA3.1(-)Myc/HisA vector (gift of F. Neipel), with primers 5'TTTTAAAGCTTCAGAGTGTGTAGTGC and 5'AGTAAATGTGTTTTCTAG ACCGTTG.

The amplified fragment was digested with HindIII and XbaI and cloned into gBC1C3C4 digested with the same endonucleases.

k) gB34H8

To generate gB34H8, the sequence encoding amino acids 169 to 221 of HHV8-gB was PCR amplified from plasmid pAB38 with the primer pairs 5'CAACGGTCTAGAAAACACATTTACTGAC plus 5'AACGGTGGTCCTAACTC

TGTATATGCC that was phosphorylated at its 3' end. The amplimer was digested with XhoI and cloned into gBC3C4 digested with XhoI and HpaI.

l) gB45H8

To generate gB45H8, the sequence encoding amino acids 223 to 311 of HHV8-gB was PCR amplified from plasmid pAB38 with primers 5' CCG TTAACTGCGAGATAGTCGACATGAT and 5' CACAGGTACCTGGTCTTGC TCTCGGA. The amplified fragment was digested with HpaI and Asp718 and ligated in HpaI/Asp718-predigested gBC4C5.

m) gB56H8

The construction of gB56H8 followed essentially the same strategy. The sequence encoding amino acid residues 316 to 361 of HHV8-gB was PCR amplified from plasmid pAB38 with primers 5' GACCAGGTACC TGTGTCCGCTAGCACTGTGG and 5'CCGACTCGAGACAAGAGTACGTGT CGGTAAA. The amplimer was digested with Asp718 and XhoI and cloned into gBC5MC6 digested with the same endonucleases.

n) gB67H8

To generate gB67H8, the sequence encoding amino acids 365 to 485 of HHV8-gB was PCR amplified from plasmid pAB38 with primers 5' CTCTTGTCTCGAGTCGGATATCAACAC and 5' GTCCCTGACCTGAGGCCTA CACCAT. The amplimer was digested with XhoI and StuI and ligated in gBC6C7 peviously digested with XhoI and EcorV.

3.2.4 Generation of plasmids useful for pull down experiments

To generate gH_{Strep} an amplimer that carried the sequence encoding the V5-epitope, the One-STrEP™ tag (trademark of IBA GmbH) and the factor Xa Protease recognition site, was generated by extension of two synthetic partially overlapping oligonucleotides: 5' GGAGACGCATGCTAATCGAAG GGCGAGGTAAGCCTATCCCTAACCCTCTCCTAGGCCTCGATTCTACGAGCGCTT GGAGC-3' and 5'GGTAGTAGATCTCATTTTTCGAACTGCGGGTGGCTCCACGA TCCACCTCCCGATCCACCTCCGGAACCTCCACCTTTCTC-3'. The fragment was digested with SphI and BglII and cloned into plasmid gH_{5E1} predigested with

the same endonucleases. gH_{5E1} plasmid (gift of Gianni T.) encodes HSV-gH with a 5E1-epitope inserted in frame at residue 837. The amplimer inserted replaced 5E1-epitope.

5E1-epitope was displaced from gH_{5E1} also by V5 epitope to generate gH_{V5}. An amplimer encoding the epitope V5 and the His-Tag was obtained by extension of the partially overlapping oligonucleotides: 5'GGAGACGCATGCTAGGATCCGGTAAGCCTATCCCTAACCCTCTCCTCGGTCT CGATTCTACGC and 5'TTAGCGAGATCTCAATGGTGATGATGGTGATGATGA ACGGTACGCGTAGAATCGAGACCGAGGAGA. The fragment was digested with SphI and BglII and cloned into predigested gH_{5E1}. The construct obtained was named gH_{V5}.

To construct gD_{Strep} , an amplimer that carried the sequence encoding One-STrEP Tag™ was generated by extension of the partially overlapping primers 5'GGAAGATCTCTGGCTGGAGCCACCCGCAGTTCGAGAAAGGTGGAGGTTCCG GATCGGGAGGTGGATCG and 5'CCCAAGCTTCCCGGATCCTCATTTTTCGAAC TGCGGGTGGCTCCACGATCCACCTCCCGATCCGGAACCT. The amplimer was digested with BglII and HindIII and ligated in BglII/HindIII-digested gD_N (see chapter 3.2.1).

3.3 OTHER PLASMIDS

pEA99 carries the gD gene cloned in pcDNA 3.1(-) [134].

The gB, gH, and gL genes were cloned in pMTS-1, a vector derived from pAcSG2 (Pharmingen) by the insertion of CMV IE promoter [11 and 47]. gL_{V5} encodes for gL with V5 epitope fused at C-terminus. gB in pcDNA3.1 contained a StuI/BglII fragment subcloned from gB in pMTS-1. EGFR2Δ (named Erb-2) carries the extracellular domain and transmembrane sequences of rat HER-2/neu and is deleted of the tyrosine kinase domain [135]. Plasmid pCAGT7 containing the T7 RNA polymerase gene under control of the CAG promoter, and the pT7EMCLuc plasmid expressing the firefly luciferase under the T7 promoter were decribed in ref. [79 and 136]. pCF18 carries

nectin1β cDNA, cloned into BstXI and NotI of pcDNA3.1(+) [33]. pBEC10 encoding HVEM was described in ref. 25. pcDNA3.1(-)Myc-His/Lac vector (Invitrogen, Milan, Italy), encodes βgalactosidase.

3.4 ANTIBODIES

Monoclonal antibody (MAb) H170 is directed to the N-terminal of gD (Goodwin Institute, Plantation, FL and ref. 137). Polyclonal antibody (PAb) R8 is directed to gD [138]. MAb H1817 is directed to the first 20 residues of gB ectodomain, the latter at the N-terminus (Goodwin Institute, Plantation, FL and ref. 139). MAb 53S recognizes a discontinuous epitope of gH and strictly requires gL for reactivity [137].
MAb R1.302 is directed to hNectin-1 (gift of M. Lopez) [140]. H633 to gC was from Goodwin Institute (Plantation, FL). Anti-V5 antibody was from Invitrogen (Milan, Italy) and was used to recognize gH_{V5} and gL_{V5}. Monoclonal antibody 5E1 is an HHV-7-specific MAb directed to pp85(U14) herein used to recognize gB_{5E1N} and other gB-mutants in which the specific epitope was inserted.
Anti-rabbit or anti-mouse IgG-FITC (fluorescin-isothiocyanate) or -TRITC (tetra-methyl-rhodamine isothiocyanate) conjugated antibodies were from Jackson Immunoresearch. Coupled to peroxidase anti-mouse and anti rabbit secondary antibodies were from Sigma-Aldrich or GE Healthcare.

3.5 INDIRECT IMMUNOFLUORESCENCE (IFA)

COS cells were grown on glass coverslips and transfected with the indicated plasmids by means of Polyfect (Qiagen), according to manufacturers instructions. 293T cells were transfected by means of Arrest-in (OpenBiosystem, Celbio, Milan, Italy). After 24 h the cells were fixed with either 4% paraformaldehyde in PBS for 10 min at room temperature followed, when requested, by permeabilization with 0.1%Triton X-100 in phosphate-

buffer saline (PBS), or fixed with -20°C-cold methanol. Samples were incubated for 1h with the following monoclonal antibodies (MAbs): MAb H170 (1:400) to gD; MAb 53S (1:200) to gH; MAb R1.302 to nectin-1 (1:100); MAb H1817 (1:400) to gB. Alterwards, the appropriate anti-mouse or anti-rabbit IgG-FICT (fluorescein-isothiocyanate) conjugated antibody (1:1000) (Jackson Immunoresearch) was added and incubate for 45 minutes. Samples were observed with a Zeiss microscope, and micrographs were taken with a Kodak DC290 digital camera.

3.6 SPLIT EGFP COMPLEMENTATION ASSAY

COS or 293T cells were grown on glass coverslips and transfected with the indicated combination of plasmids gD_N, $Nect_C$, gH_C, gH_N, gB_C, and gC_C by means of Arrest-in (OpenBiosystem, Celbio, Milan, Italy). At 24-48 h post transfection cells were mounted without fixation with Fluoromount and observed with Leica TCS-SL confocal microscope, set at 100% excitation at 488 nm and emission between 490-540 nm. Images were collected with a 63X1.62 Leica oil immersion objective. Confocal slices were 1.7 to 2.3 µm thick. For each experimental series images were collected on the same day, under the same settings, applying 1,024- by 1,024-pixel resolution and an 8-bit intensity scale. Specifically, the first sample to be analyzed was the negative one, containing gCc; for subsequent observations of the samples belonging to the same series, the settings were then kept unmodified.

3.7 CELISA (cell enzyme linked immunosorbent assay)

CELISA was performed as described [141]. Briefly, subconfluent cultures of COS cells in 48-well plates were transfected with plasmids encoding wt-gD or gD mutants (125, 250, or 375 ng per well), or with 125 ng of plasmids encoding wt-gB or gB mutants. The Erb-2 plasmid DNA was used to make the amounts of DNA equal. After 24 h cells expressing gD were reacted with

MAb H170, HVEMt, or nectin 1-Fc and cells expressing gB were reacted with MAb H1817 . Subsequently, cells were fixed with 4% formaldehyde in PBS, followed by anti-mouse peroxidase, anti-His6-peroxidase, or anti-human peroxidase and o-phenylenediamine substrate. The optical density (OD) was read at 490 nm.

3.8 CELL-CELL FUSION ASSAY

β-galactosidase-based cell–cell fusion assay

Subconfluent cultures of BHK cells, grown on glass coverslips in 24 well plates, were transfected by means of Fugene (Roche Applied Science, Milan, Italy) with DNA mixtures that contained the expression plasmids for gD, gH, gL, gB, plus pcDNA 3.1(-) Myc-His/Lac vector (Invitrogen, Italy), for constitutive expression of ß-Galactosidase (80 ng of each plasmid). When necessary the wt-gB was replaced with gB mutants or Erb-2. After incubation at 37° for 48 h, cells were fixed with 0.2% glutaraldehyde and 0.2% paraformaldehyde in PBS. Syncytia were detected by light microscopy observation of ß-Gal expressing cells after staining with 5-bromo-4chloro-3-indolyl-ß-galactopyranoside (X-Gal) with a Axioplan Zeiss microscope equipped with a Kodak DC120 digital camera.

Luciferase-based cell-cell fusion assay

The luciferase-based cell-cell fusion assay was performed as detailed [141] using the Luciferase Assay System from Promega. Effector COS cells were transfected with 80 ng of plasmids for gH, gL, gB, plus 80 or 240 ng of plasmid for chimeric or WT-gD or Erb-2 and 107 ng of pCAGT7. Target cells [COS, J-nectin 1, and J-HVEM were transfected with pT7EMCLuc. The extent of fusion was express as luciferase units (L.U.) reading the sample in a luminometer TD-20/20 (Turner designs version 2.5) at 560 nm. The negative control lacked gD and its value was the subctracted background. The total amount of transfected

plasmid DNA was made equal by addition Erb-2 plasmid DNA. All samples were run three times and in triplicates.

3.9 INFECTIVITY COMPLEMENTATION ASSAY

Cells in T_{25} flasks were transfected by means of Polyfect (Qiagen) with the indicated plasmids. The total amount of plasmid DNA transfected per flask was made equal by addition Erb-2 plasmid DNA. Four h later cells were infected with with $gD^{-/+}$ FgDβ (3 PFU/cell). Unpenetrated virions were inactivated by washing two times with PBS, followed by a 1 min rinse with 40 mM sodium citrate, 10mM KCl, 135 mM NaCl, pH 3. The monolayers were then rinsed twice with PBS and overlaid with medium containing 1% FBS and frozen 24 h after transfection. Progeny virus was titrated in gD-expressing cells (R6) or was quantified as β-galactosidase activity in BHK, J-nec1, or J-HVEM cells by staining with o-nitrophenyl-β-D-galactopyranoside (ONPG) and reading the optical density (OD) at 405 nm or by light microscopy observation of β-gal-expressing cells after staining with X-gal.

Infectivity complementation assay of $gB^{-/+}$ KΔT virus followed esentially the same protocol but progeny virus was titrated in gB-expressing cells (D6)

3.10 *STREP*-TAG PULL DOWN EXPERIMENTS AND WESTERN BLOT ANALYSIS

293T cells (~2,8 x 10^6 cells/T25 flask) were transfected by means Arrest-in (OpenBiosystem, Celbio, Milan, Italy) with plasmids encoding gH_{V5}, gL_{V5}, $gB_{5E1ND867}$, gD (1,5 μg each, all together or combination of them) and HVEM (3 μg) or when necessary $gB_{5E1ND867}$ was replaced with HSV-HHV8 gB chimeras, wt-gD with gD_{STREP} or gH_{V5} with gH_{STREP}. 24 h after transfection cells were solubilized in $EA1^+$ (250 mM NaCl, 50 mM hydroxyethylpiperazine-ethanesulfonic acid and 0,1% Nonidet P40, pH 8) added with N_α-*p*-Tosyl-L-lysine chloromethyl ketone hydrochloride (TLCK) and N-*p*-Tosyl-L-

phenylalanine chloromethyl ketone (TPCK) (final concentration 0,3 mM each). Cell lysates were centrifuged at 14000 rpm for 1h. The supernatants were incubated with Protein A-Sepharose resin (Sigma Aldrich, Milan, Italy) for 1 h at 4 °C. After incubation the beads were recovered by centrifugation and then the complexes were harvested by incubation with the *Strep*-Tactin Sepharose (IBA GmbH, Gottingen, Germany) 1 h at 4 °C with gentle mixing. *Strep*-Tactin is an engineered streptavidin [142]. The beads were washed five times with Buffer W (100 mM Tris-Cl pH 8.0, 150 mM NaCl and 1 mM EDTA) and then the absorbed proteins were eluted by the addition of SS (solubilizing solution) containing SDS and β-mercaptoethanol. The proteins were separated by denaturing polyacrylamide gel electrophoresis (PAGE) and transferred to Hybond ECL nitrocellulose membrane (Amersham Biosciences, Milan, Italy). The membranes were blocked 1 h at RT with ECL Advance Blocking Agent (GE Healthcare, Milan, Italy) incubated overnight with the appropriate antybody and then with anti-mouse or anti-rabbit peroxidase-conjugated antibody (1:80000) (GE Healthcare, Milan, Italy). The blot was developed by ECL Advanced Western Blotting Detection Kit (GE Healthcare, Milan, Italy), according to manufacturer's instructions.

3.11 BIOINFORMATIC ANALYSIS

The sequences of HVS-HHV8 chimeras were submitted to SWISS-MODEL server (http://swissmodel.expasy.org//SWISS-MODEL.htm). SWISS-MODEL provides a fully automated comparative protein modelling service. To build the homology model, SWISS-MODEL identified a structural template, aligned the target sequence and the template structure, generated the model and minimized the energy of the model. For each steps SWISS-MODEL used specialized software and protein databases. SWISS-MODEL also provided a model quality evaluation [143].

RESULTS DISCUSSION AND CONCLUSIONS

4. RESULTS, DISCUSSION AND CONCLUSIONS

4.1 DEVELOPMENT OF A SPLIT EGFP COMPLEMENTATION ASSAY TO DETECT INTERACTION BETWEEN gD, gB, gH.gL

4.1.1 RESULTS

4.1.1.1 gD-Nectin1 complex detection.

To investigate HSV glycoproteins interaction we used the split enhanced green fluorescent protein (EGFP) complementation assay. EGFP is a humanized red-shifted variant of wilde type GFP from *Aquorea victoria*, incorporating mutation for optimal expression in mammalian cells and brighter fluorescence. EGFP is composed of 11 strands of β sheet that form an anti-parallel barrel with short α helices forming lids in each end. The fluorescent-active center of EGFP is located inside the barrel. In the complementation assay (CA), EGFP is split into two fragments that, if brought to an 8- to 10-Å proximity of ach other, refold together and emit fluorescence [144 and 145] Fig. 4.1.1

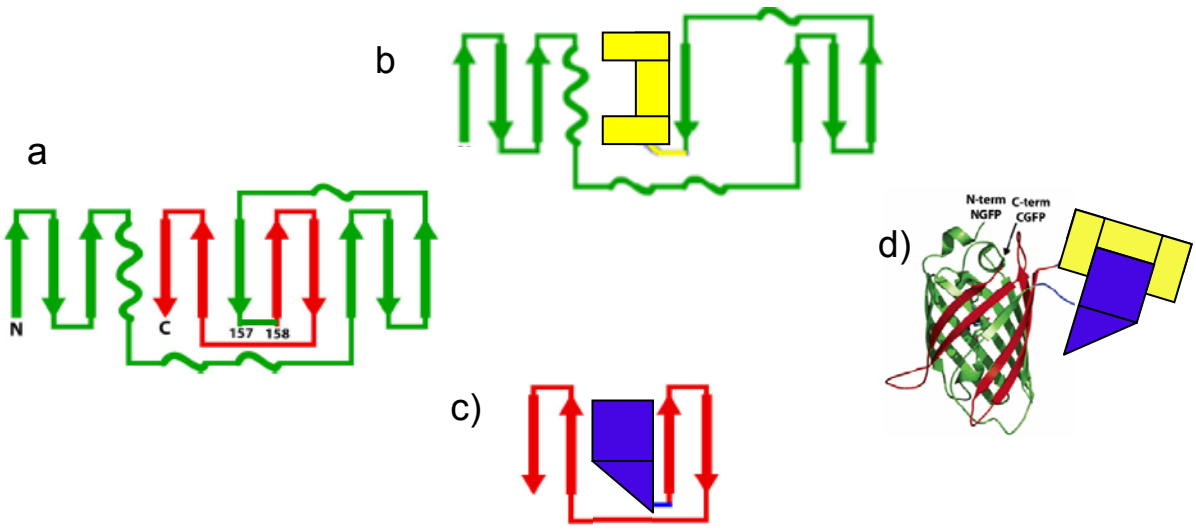

Fig. 4.1.1 Schematic of EGFP dissection. In a) a schematic of the secondary structure topology of EGFP is shown and the site of dissection is indicate. In b)c) and d) the interaction partners fused to EGFP fragments are depicted as geometrical drawings (yellow and blue). In d) is represented the EGFP recostitution after proteins interactions (modified from ref.146).

Inasmuch EGFP-CA has been applied mainly to analysis of soluble mammalian or bacterial proteins [144], we first validated its application to membrane proteins - in particular to HSV glycoproteins - by analysis of gD and its nectin1 receptor. We fused the N- and C- fragments of EGFP (EGFP N-term corresponds to aa 1-157 and C-term corresponds to aa 158-239) to the endodomains of gD and nectin1 respectively, the constructs were named gD_N and $Nect_C$. Fig. 4.1.2 C and M, documents complex formation between gD_N and $Nect_C$ as fluorescence emission from EGFP-CA in transfected 293T and COS cells, and the specificity controls. Cells were observed 36 h after Arrest-in-mediated transfection. Results with the two cell lines were essentially similar, although the level of expression and number of fluorescent cells was higher in 293T cells. In agreement with previous reports, the overall fluorescence emitted by complementation of split EFGP fragments was lower than that from the unsplit protein [144]. The specificity controls that validated the assay were as follows. First, neither gD_N nor $Nect_C$ emitted fluorescence when transfected singly (Fig. 4.1.2 A, B, K, L), or in combination with the wt alleles of nectin1 or gD (not shown), ruling out autofluorescence. Second, fluorescence was reconstituted only when the EGFP chimeric proteins were in a specific complex, and not simply present in the same subcellular compartment. For this control, we selected gC, which is involved in virus attachment but not virus entry and is present in the same subcellular compartments as gD. Coexpression of gD_N and gC_C resulted in no significant fluorescence (Fig. 4.1.2 D and N), ruling out the possibility that proteins that exhibit no specific interaction, but that are abundantly present in the same cellular compartment, give rise to EGFP complementation. We took advantage of the lack of EGFP complementation by gC_C-containing samples and, in all experiments, used the gC_C-containing sample to adjust the confocal microscope settings. The settings were then kept constant throughout the observation period of a same series of samples. Third, we ascertained by immunofluorescence assay (IFA) that all proteins were expressed, even those expressed singly (gD_N, $Nect_C$)

(Fig. 4.1.2 E, F, O, and P) or in the gD_N-gC_C combination that did not yield EGFP fluorescence (Fig. 4.1.2 I, J, S, and T).

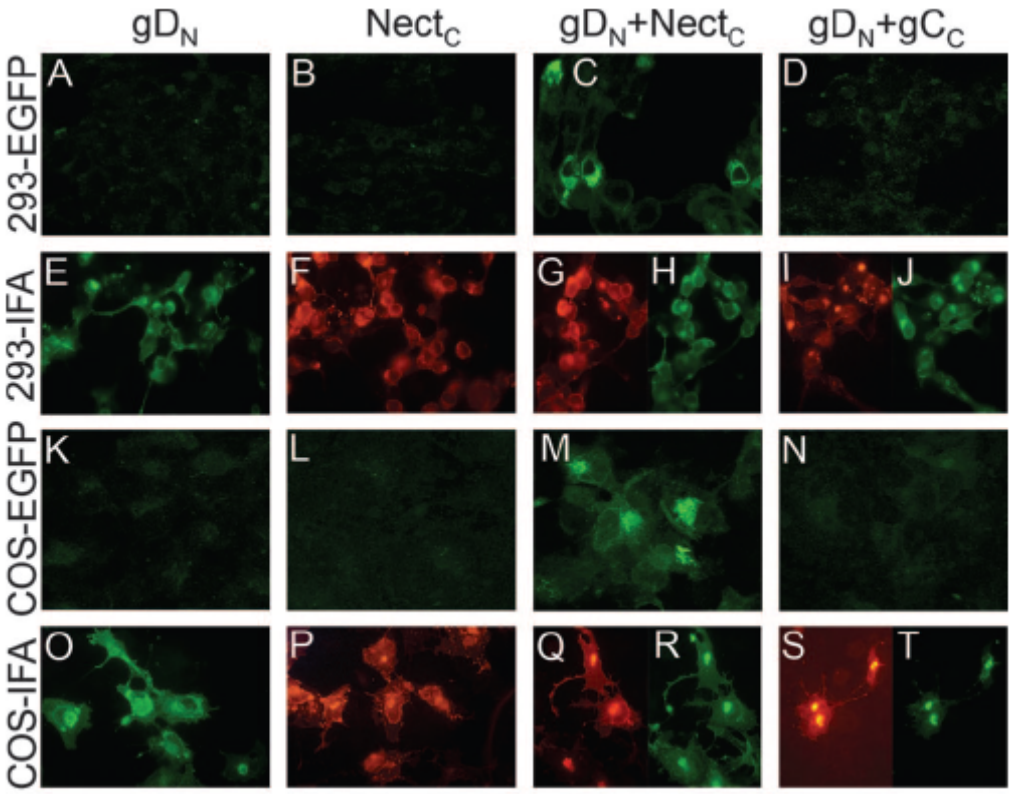

FIG. 4.1.2 EGFP CA (A to D and K to N,) **and IFA** (E to J, and O to T)**.** EGFP CA between gD_N and $Nect_C$ and lack of complementation between gD_N and gC_C. COS or 239T cells were transfected with the indicated plasmids, gD_N (A, E, K, and O), $Nect_C$ (B, F, L, and P), gD_N_$Nect_C$ (C, G, H, M, Q, and R), and gD_N_gC_C (D, I, J, N, S, and T). IFA: Green, gD; red, Nec_C or gC_C. Antibodies used were R8 to gD, R1.302 to nectin1 and H633 to gC.

Importantly, the EGFP-glycoprotein chimeras were not hampered in plasma membrane localization (Fig. 4.1.2). We conclude that EGFP-CA fulfills the criteria for detection of specific interactions between membrane-bound proteins, particularly HSV gD and its receptor.

4.1.1.2 Complexes between HSV glycoproteins.

The second series of experiments was performed with 293T and COS cells tranfected with three membrane proteins in combinations that included: $gD_{N+}gB_C$, $gD_{N+}gB_{\Delta 867}$, gD_N+gH_C+wtgL, gD_N+wtgH+wtgL, and gD_N+gC_C. We used a form of gB deleted for endocytosis motifs, to maximize its espression and localization in exocytic and plasma membranes [73]. Transfection mixtures were made equal in DNA amounts (900 ng/well, 300 ng/plasmid) by addition of

plasmid encoding epidermal growth factor receptor 1 deleted in signalling sequences [135]. This control ensured that exocytic membranes were loaded with comparable amounts of proteins. In both cell types observed 36 h after transfection, the gD_N+gH_C+wtgL combination resulted in a readily detectable fluorescence (Fig. 4.1.3 B and E). The gD_N+gB_C combination gave rise to a somewhat weaker fluorescence (Fig. 4.1.3 A and D) that nonetheless was much higher than the background fluorescence emitted by the gD_N+gC_C combination (Fig. 4.1.3 C and F). Even though the subcellular localization cannot be clearly defined, EGFP appeared to localize to a perinuclear position, consistent with a Golgi compartment localization, to a cytoplasmic reticular compartment, consistent with endoplasmic reticulum, and to nuclear membranes. By IFA, all proteins resulted to be expressed, even those that did not yield EGFP fluorescence (not shown). We infer that gD can recruit gH to a complex. gD can also recruit gB to a complex. The gD-gH combination results in a stronger EGFP fluorescence than the gD-gB combination, possibly reflecting a stronger interaction, a more stable or longer half-life complex, a higher number of complexes at steady state, or peculiar behaviors of the fusion proteins.

Cells transfected with the quartet of gD, gB, gH, and gL form syncytia [79]. A series of experiments was designed to verify whether the glycoprotein-EGFP chimeras were still functional in cell-cell fusion, and whether complexes were detectable under conditions that lead to cell-cell fusion. 293T or COS cells were cotransfected with combinations of five plasmids (1.25 µg/well, 250 ng/plasmid) encoding gD, $gB_{\Delta 867}$, gH, gL, and gC or their EGFP chimeras. The transfected combinations included gD_N+gB_C+wtgH+wtgL+wtgC, gD_N+gH_C+wtgL+$gB_{\Delta 867}$+wtgC, and gD_N+$gB_{\Delta 867}$+wtgH+wtgL+gC_C. Cells were observed 24 h (293T) or 40 h (COS) after transfection. The results in Fig. 4.1.3 G to L show that syncytia were formed for any combination, indicating that the EGPF-glycoprotein chimeras were not hampered in fusion activity. The strongest fluorescence was observed with the combination that included gD_N+gH_C (panels H and K).

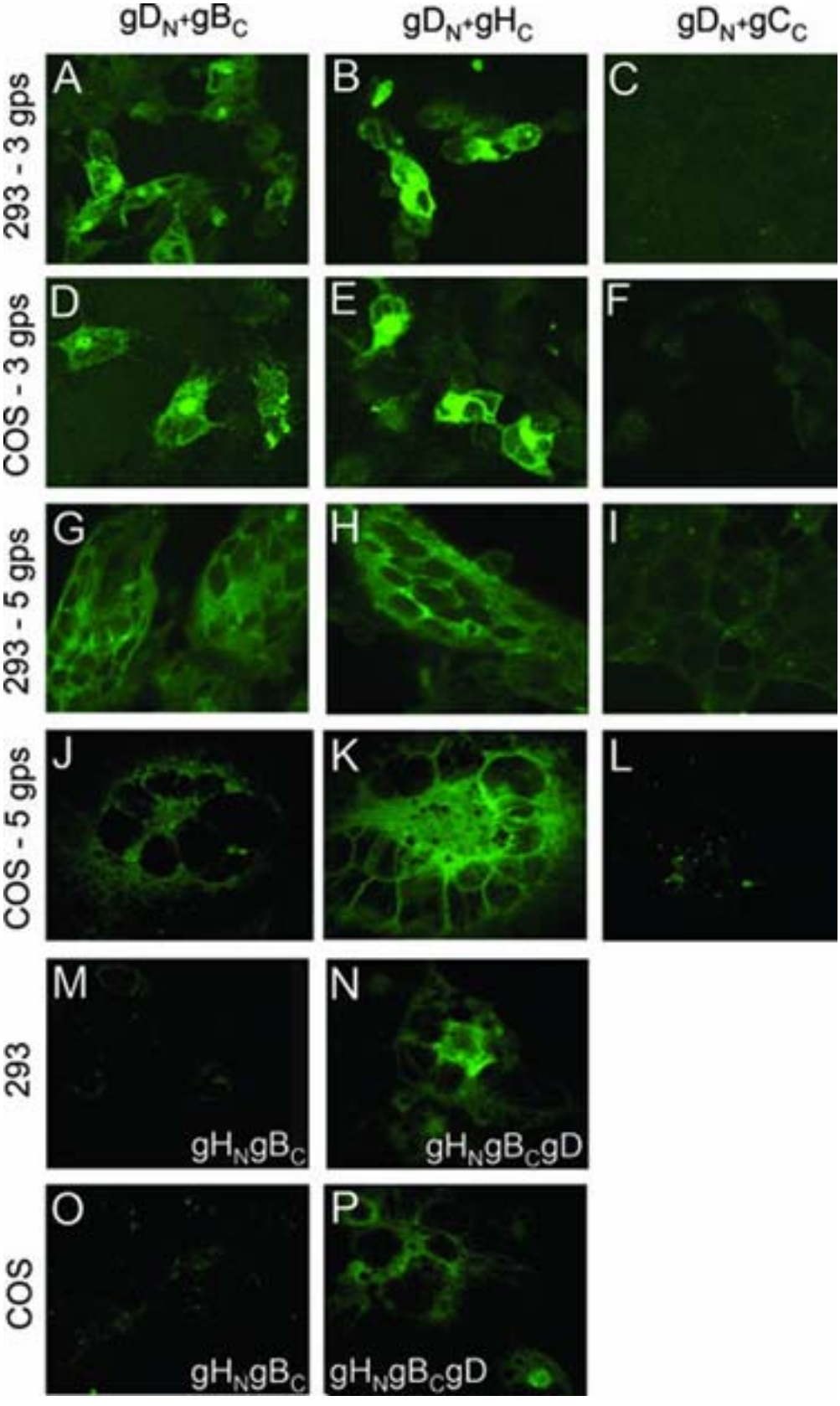

FIG. 4.1.3. EGFP CA between HSV glycoproteins. COS or 239T cells were transfected with the indicated plasmids, gD_N + gB_C (A, D, G, and J), gD_N + gH_C (B, E, H, and K), gD_N + gC_C (C, F, I, and L), gH_N + gB_C (M and O), and gH_N + gB_C + gD (N and P). Cells transfected with three glycoproteins (gps) received, in addition, plasmids encoding wtgL or epidermal growth factor receptor, as appropriate. Cells transfected with five glycoproteins received gD, $gB_{\Delta 867}$, gH, gL, and gC as the wild type or EGFP chimeras, as indicated.

A somewhat weaker fluorescence was observed with the combination that included gD_N+gB_C (panels G and J), particularly in COS cells. No fluorescence above background level was observed with the combinations that included gD_N+gC_C (panels I and L).

The stronger fluorescence in panels B relative to H and in panels E relative to K reflects (i) higher amounts of transfected DNA for each plasmid, (ii) a longer time interval after transfection (panels B versus H), (iii) the lack of dilution of complemented EGFP molecules consequent to fusion of transfected fluorescent cells with adjacent untransfected nonfluorescent cells, or (iv) possibly a longer half-life of the complexes when cell-cell fusion does not ensue.

We next tested whether gH and gB interact with each other and whether the interaction was dependent on the presence of gD. Cells were transfected with gH_N+wtgL+gB_C in the absence or presence of wtgD. Interaction between gH_N-gB_C (Fig. 4.1.3 M and O) of gD.

4.1.2 CONCLUSIONS

We validated the adaptation of the EGFP-CA to membrane proteins by first applying it to the gD-nectin1 interaction. The fluorescence emitted from the gD_N-$Nect_C$ combination was readily detectable, whereas that from the gD_N-gC_C combination was detected at only background levels, testifying to the assay specificity. For every series of observations, the gC_C-containing sample was therefore used to adjust the confocal microscope settings. Samples exhibiting readily detectable fluorescence under these conditions were considered positive.

We detected a complex made of gD and gH, in agreement with coimmunoprecipitation data [40]. The complex formed even in the absence of gB. In addition, we detected a complex made of gD and gB that formed even in the absence of gH·gL. We further documented the interaction between gH and gB; its gD dependence suggests that the interaction is triggered by gD. A notable property of the EGFP-CA as applied here was that complex formation between HSV glycoproteins was detected in intact cells, i.e., in the intracellular

compartment and microenvironment and under the very conditions in which the interactions do occur. Importantly, the EGFP chimeric glycoproteins were not hampered in cell-cell fusion activity. Hence, the detected interactions were a faithful mirror of the interactions that take place under conditions that lead to cell-cell fusion. Inasmuch as EGFP reconstitution from split portions is an irreversible reaction, the assay does not allow us to infer whether the complexes between the HSV glycoproteins were stable or transient.

Cumulatively, the current assay provides in situ evidence for the following.

(i) gD recruits gH·gL and gB to complexes.

(ii) gH and gB can be recruited to gD independently of one another. Thus, gD carries binding sites for both gH·gL and gB. The independent recruitment of these glycoproteins to gD is consistent with and substantiated by the observation that, at the outer nuclear membrane, virions deleted for gB but carrying gD+gH, or deleted for gH but carrying gD+gB are capable of fusion [101].

(iii) Once gH·gL and gB are recruited to gD, they possibly interact with each other. (iv) gH·gL and gB are not necessarily recruited in a sequential order or one to the other. Current data support a model of HSV entry-fusion whereby gH and gB exert their activity through complex formation with gD, or following activation mediated by complex formation with gD.

4.2 ROLE OF gD PRO-FUSION DOMAIN IN THE RECRUITMENT\ACTIVATION OF gB AND gH.gL

4.2.1 RESULTS

4.2.1.1 Functional Subdomains in gD-PFD.

To identify functional subdomains of PFD, we generated two gD chimeric proteins that carried, downstream of residue 259, either PFD/1 (amino acids 260-

285) or PFD/2 (amino acids 285-310) (Fig. 4.2.1). In the constructs, gD-PFD/1 and gD-PFD/2, the TM and C-tail regions were from gD, and the gD missing sequences were replaced by the corresponding sequence of CD8. A chimera in which the entire PFD was replaced by the corresponding sequences of CD8 ($gD_{\Delta PFD}$) differed from $gD_{(1-260)}$CD8 [53] in that the TM and C-tail regions were from gD but not from CD8. The chimeric forms of gD, cloned in pcDNA3.1(-), were analyzed for their ability to reach the plasma membrane, and in three functional assays, i.e., the binding to soluble forms of HVEM (HVEMt) and nectin 1 (nectin 1-Fc) [33 and 38], the cell-cell fusion, and the infectivity complementation. All chimeric gDs reached the plasma membrane as measured by CELISA (Fig. 4.2.2) and by immunofluorescence of paraformaldehyde-fixed cells (data not shown). In the case of gD-PFD/2, 3-fold higher amounts of plasmid (3×) were transfected to achieve a WT level of plasma membrane expression; gD-PFD/2 was transfected at 3× higher concentrations relative to WT-gD in all subsequent experiments, except when otherwise stated. The binding to HVEMt and nectin 1-Fc, measured by CELISA, showed an extent of binding similar to that of WT-gD (Fig. 4.2.3).

For the cell-cell fusion assay, baby hamster kidney cells were cotransfected with the gD-PFD chimera or WT-gD plus gB, gH, gL, and β-galactosidase plasmids [73, 79] and were stained with 5-bromo-4-chloro-3-indolyl β-galactopyranoside (data not shown). For the luciferase-based cell-cell fusion assay [141], each chimeric gD or WT-gD was cotransfected with gB, gH, gL, and the T7 polymerase in COS cells. The target COS, J-nectin 1, or J-HVEM cells were transfected with a T7-promoter-driven luciferase gene; COS cells were transfected at either 1× or 3× the amounts of plasmids (Fig. 4.2.4A). The two assays concordantly showed that gD-PFD/1 was partially active in the fusion assay; the activity increased when the plasmid amounts were increased 3×. By contrast, gD-PFD/2 was inactive at either concentration. $gD_{\Delta PFD}$ was inactive at either concentration, in accordance with the analogous $gD_{(1-260)}$CD8 [53]. The results suggest a certain degree of differentiation in fusion activity between the

two PFD subdomains, and only subdomain 1 was in part sufficient for this function, in agreement with ref. 149.

Next, we determined whether the same chimeric forms of gD were capable of complementing infectivity. Each chimera, or WT-gD, was transfected into COS cells, and 4 h later, the cells were infected with the gD-deletion virus FgDβ [131]. When the virus is grown in noncomplementing cells, noninfectious gD-/- progeny are produced. When the virus is grown in cells expressing gD, gD complements the virus (gD-/+ stock) and confers infectivity. If gD is partially defective, the complemented virions exhibit a reduced infectivity. As shown in Fig. 4.2.4B, gD-PFD/1 was partially active in the infectivity complementation, consistent with the partial cell-fusion activity. The complementation activity did not change whether the gD-PFD/1-encoding plasmid was transfected at 1× or 3× amounts (data not shown). Surprisingly, gD-PFD/2, which exhibited no cell-fusion activity, partially complemented infectivity. Similar results were obtained irrespective of the cell line and of the receptor expressed in the cells where the complemented virions were titrated. The results indicate that PFD cannot be narrowed down, because subdomain 1 (amino acids 260-285) exhibits partial cell fusion and infectivity activities. The subdomain 2 (amino acids 286-310) is not sufficient for cell fusion but is sufficient for partial complementation of infectivity, in agreement with the finding that Pro residues 288, 291, 292, and 305 were critical residues for infectivity [53]. The discrepancy between the results of the cell-cell fusion and infectivity complementation assays indicates that the two assays mirror each other but are not necessarily identical.

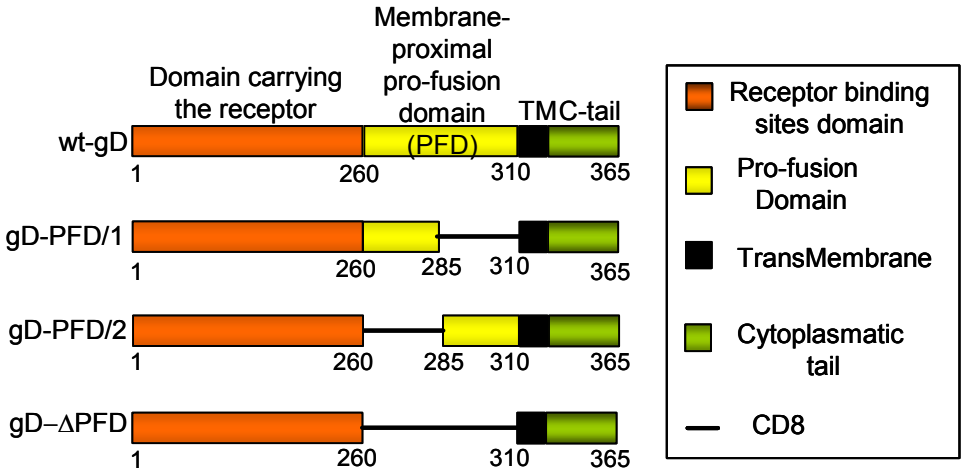

Fig. 4.2.1 Schematic diagram of gD constructs. At the top, linear map of WT-gD, with N terminus (amino acids 1–260) carrying receptor-binding sites (orange) and C terminus (amino acids 260–310) carrying the PFD (yellow), the transmembrane (TM) (black), and the C-tail (green) regions. The black bold line in the chimeras represent the region of gD replaced by sequence derived from CD8.

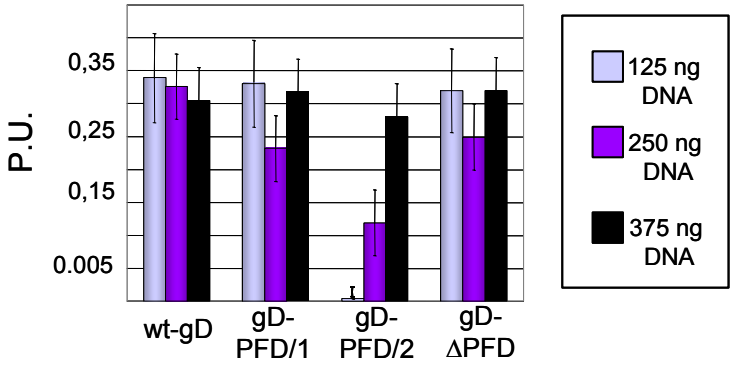

Fig. 4.2.2 Cell surface expression of gD chimeric proteins quantified by CELISA.
COS cells, in 48 wells, were transfected with plasmids encoding wt or chimeric forms of gD at the indicated amounts, corresponding to 1x, 2x, or 3x the regular amount. Cells were fixed with 4% paraformaldehyde at 24 h after transfection and were reacted with mAb H170, anti-mouse IgG peroxidase, and *o*-phenylenediamine. Results are expressed as peroxidase units (P.U.). Vertical bars denote SD. Columns represent the average of triplicates. Three independent experiments were run.

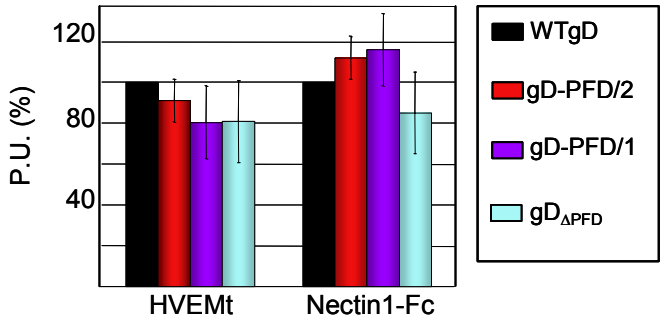

Fig. 4.2.3 Binding of COS cells expressing the chimeric or WT-gD to HVEMt and nectin 1-Fc. Details were as in Fig. 4.2.2, except that cells were reacted with the soluble receptors, anti-His6-peroxidase or anti-human peroxidase, to detect HVEMt and nectin1-Fc, respectively, and *o*-phenylenediamine.

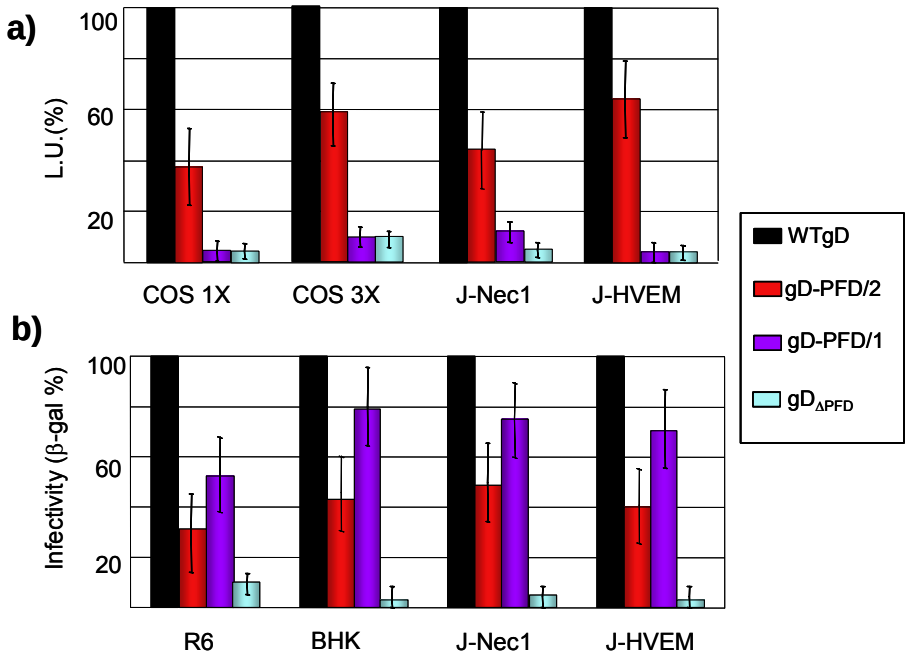

Fig. 4.2.4 Cell– cell fusion and infectivity complementation of chimeric gD proteins. a) Luciferase-based cell–cell fusion assay. Effector COS cells, in 24 well-plate, were transfected with 80 ng/well of plasmids encoding gH, gL, gB, 107 ng/well of plasmid encoding T7 polymerase and 80 or 240 ng of plasmids encoding chimeric or wt-gD, corresponding to 1X and 3X regular amounts. Target cells [COS, J-nectin 1 (J-Nec1), and J-HVEM] were transfected with T7-luciferase-expressing plasmid. The negative control lacked gD (data not shown). The luciferase activity was expressed as luciferase units (L.U.). **b) Infectivity complementation**. COS cells were transfected with chimeric or wt-gD and infected 4 h later with a gD stock of FgDβ (3 PFU/cell). Progeny virus was titrated at 24 h in gD-expressing cells (R6) or was quantified as β–galactosidase in BHK, J-nec1, or J-HVEM cells.

4.2.1.2 Effects of Pro and Glu Substitutions in Subdomain 1.

The PFD sequence (Fig. 4.2.5) reveals a high content of Pro residues, most of which are adjacent to Glu residues in PFD/1. Some prolines in PFD/2 (amino acids 288, 291, 292, and 305) are critical for infectivity [53]. Here, the prolines of PFD/1 were replaced by leucines and the glutamic acids by alanine residues (both are nonconservative substitutions). The mutants 1-4 carried the following substitutions, E259A-P261L, PE266-267LA, PE270-271LA, and PED273-274-275LAA, respectively. Their cell-surface expression, as determinated by CELISA, showed no major defect (Fig. 4.2.6A). In the infectivity complementation, none of the mutants exhibited a significant defect (Fig. 4.2.6B). The cell-cell fusion activity of mutant 1 was increased by 20 %, whereas that of mutants 2-4 was reduced by 20-25% (Fig. 4.2.6C). Thus, the Pro and Glu residues do not represent critical residues in PFD/1.

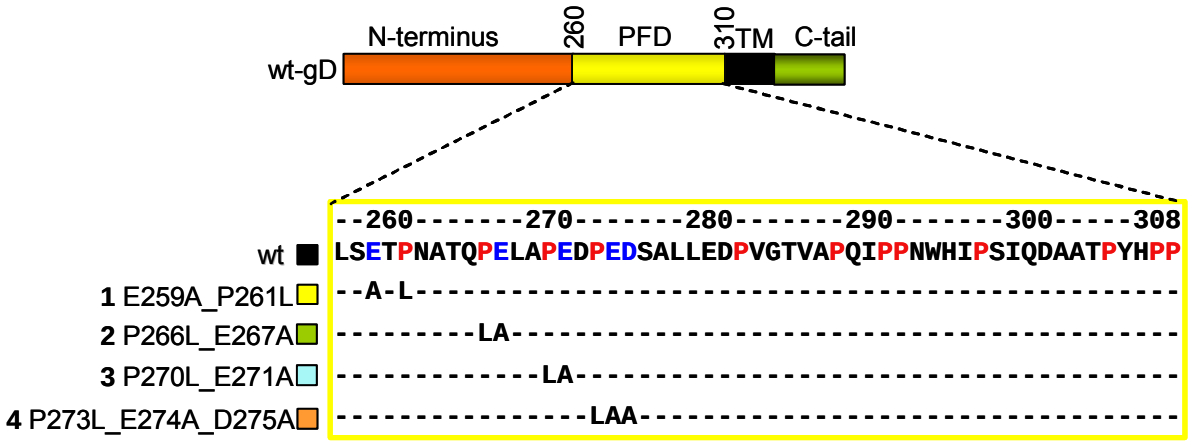

Fig. 4.2.5 a) Schematic diagram of gD. **b)** The pro-fusion domain (PFD) sequence is shown on the top. All prolines present in PFD sequence are highlighted red, other residues mutated are highlighted blue. The amino acid substitutions introduced are shown in the below lines.

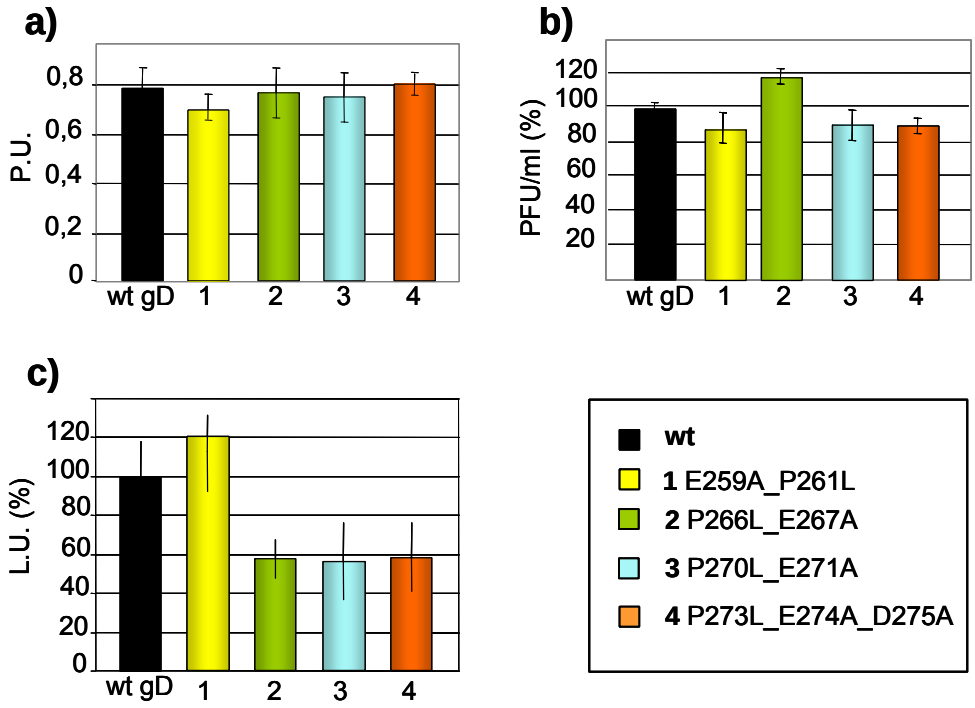

Fig.4.1.2B a) Cell surface expression of gD mutants quantified by CELISA. COS cells, were transfected with 125 ng of plasmids encoding wt or mutagenized forms of gD. Cells were fixed with 4% paraformaldehyde at 24 h after transfection and were reacted with mAb H170, anti-mouse IgG peroxidase, and *o*-phenylenediamine. Results are expressed as peroxidase units (P.U.) **b) Infectivity complementation.** COS cells were transfected with mutagenized or wt-gD and infected 4 h later with a gD stock of FgDβ (3 PFU/cell). Progeny virus was titrated at 24 h in gD-expressing cells (R6). **c) Luciferase-based cell–cell fusion assay.** Effector COS cells, seed in 24 well-plate, were transfected with 80 ng /well of plasmids encoding gH, gL, gB, and wt or mutagenized gD, plus 107 ng/well of plasmid encoding T7 polymerase. Target COS cells were transfected with T7-luciferase expressing plasmid. The negative control lacked gD (data not shown). The luciferase activity was expressed as luciferase units (L.U.).

4.2.2 CONCLUSIONS

PFD of HSV-1 gD is made of subdomains 1 and 2, comprising residues 260-285 and 285-310, respectively. Each subdomain partially contributed to virus entry, whereas only the subdomain 1 exhibited cell-cell fusion activity. The latter finding is in agreement with the report of Zago *et al.* [147]. Mutational analysis of Pro and Glu, the most characteristic sequence pattern of subdomain 1, did not highlight any critical role of these amino acids in the infectivity complementation and resulted in a modest reduction in the cell-cell fusion assay. The lack of phenotype of these mutants is in agreement with the observation that serial 5-aa deletions in this region failed to identify a specific sequence requirement [147]. The properties of the PFD/1 subdomain contrast with those of PFD/2, which carries some Pro that is critical for infectivity [53]. Their mutagenesis did not

alter PFD-binding to gD N terminus, implying a role at subsequent steps, likely in the triggering of fusion.

4.3 INTERACTION OF gB MUTANTS WITH gD AND gH, DETECTED BY MEANS OF PULL DOWN EXPERIMENTS

4.3.1 RESULTS

4.3.1.1 Generation of gB backbones.

Insertion of 5E1 epitope and deletion of part of the C-tail encoding endocytosis motifs.

To enable gB detection, we inserted an heterologous epitope, named 5E1 epitope, recognized by a specific MAb [133]. The epitope was inserted between aa 68 to 77, a poly-lysine domain known to be deletable. The resulting construct was gB_{5E1N} (Fig.4.3.1). The details of the constructions are given in M&M. Essentially, two restriction sites, BamHI and EcoRI, were inserted at residues 68 and 77, respectively, by site-directed mutagenesis. An amplimer was generated by extension of two synthetic partially overlapping oligonucleotides, cleaved with BamHI and EcoRI, and ligated in predigested gB.

Avitavile et al showed that removal of part of the cytoplasmic tail of gB encoding the endocytosis motifs results in a form of gB that exhibits a cell surface expression and, consequently, increased cell-cell fusion activity [73]. Here, removal of the endocytosis motifs located in the cytoplasmic tail, downstream of aa 867, was performed by insertion of a stop codon at aa 867 by site directed mutagenesis. The resulting construct was named $gB_{5E1N\Delta867}$. Fig. 4.3.2 and 4.3.3 show that, as expected, $gB_{5E1N\Delta867}$ exhibited a higher cell surface expression and fusion activity than wt-gB and gB_{5E1N}.

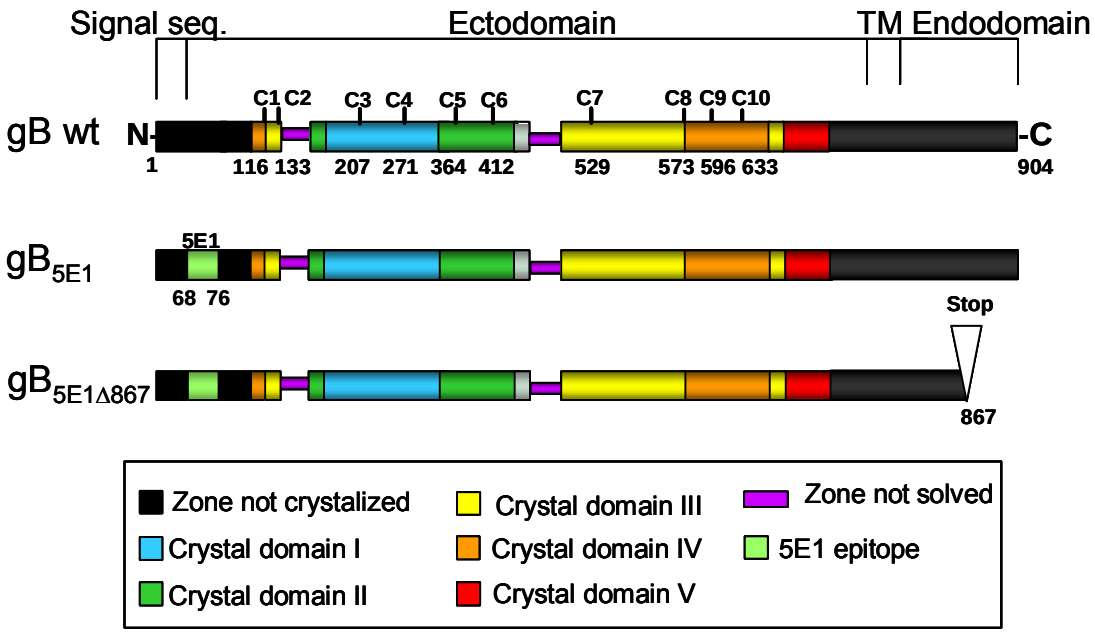

Fig 4.3.1 Schematic representation of HSV-1 gB. The top drawing depicts the domain architecture observed in the crystal structure of wt gB [84] and the locations of highly conserved cysteines. The bottom two lines show the modifications introduced to construct gB_{5E1N} and $gB_{5E1N\Delta867}$.

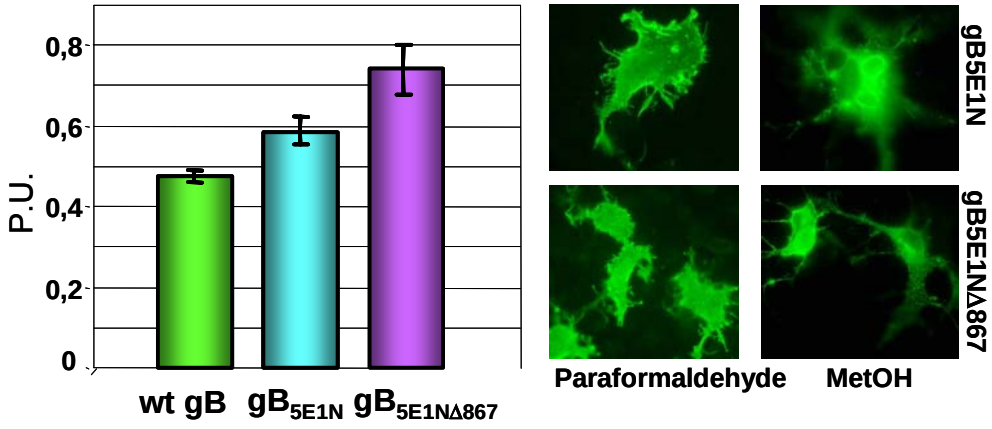

Fig.4.3.2 On the left cell surface expression quantified by CELISA. COS cells seeded in 48 well-plate were transfected with 125 ng per well of the plasmids encoding wt gB or gB5E1N or gB5E1ND867. 24 hours later cells were reacted with mAb H1817 and then fixed with 4% formaldehyde in PBS, followed by incubation with anti-mouse peroxidase and *o*-phenylenediamine. Background value was subtracted. Results are expressed as peroxidase units (P.U.). On the right cell surface and intracellular localization of mutant gB proteins by immunofluorescence. COS cells were transfected with plasmids encoding gB_{5E1N} and $gB_{5E1N\Delta867}$. At 24 h after transfection cells were fixed with 4 % paraformaldehyde or methanol and stained with Mab 5E1 followed by an anti-mouse IgG-FITC conjungate.

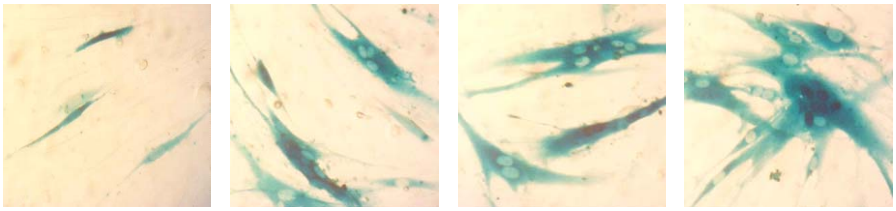

Fig.4.3.3 Digital micrographs of BHK cells forming syncytia after cotransfection with plasmids encoding HSV-fusogenic glycoproteins**.** Cells were transfected with 80 ng of plasmids encoding wt-gH, wt-gL, wt-gD, β galactosidase plus wt gB or gB_{5E1N} or $gB_{5E1N\Delta867}$. The negative control lacked gB. 48 h after transfection cells were fixed with 0.2% glutaraldehyde and 0.2% paraformaldehyde in PBS and then stained with 5-bromo-4-chloro-3-indolyl-galactopyranoside (X-Gal).

Insertion of restrictions sites adjacent to cysteines.

gB ectodomain, after cleavage of the signal sequence, carries 10 cysteines, herein named C1, C2, etc. The spacing between gB cysteines is one of the most conserved pattern across the Herpesviridae family. To generate mutants by homologous replacement of HSV gB sequences with HHV-8 gB sequences, we inserted restriction sites adjacent to cysteines. Each construct was mutated in two or three consecutive cysteines, as follows. C1-C3-C4, C3-C4, C4-C5, C5-C6, C6-C7, herein named gB_{C1C3C4}, gB_{C3C4}, gB_{C4C5}, gB_{C5C6}, gB_{C6C7}.

The mutations adjacent to C3 and C4 were silent. The mutations adjacent to C1, C5, C6, C7 introduced the substitutions listed in table 4.3.1. With respect to the C5C6 mutants, two versions were generated, named gB_{C5VC6} and gB_{C5MC6}, respectively. They substitutions they carry are listed in Table 4.3.1. The mutants gB_{C1C3C4}, gB_{C3C4}, gB_{C4C5}, gB_{C5C6}, gB_{C6C7} were characterized with respect to their ability to be expressed at the cell surface and to be mediate cell-cell fusion. The results are summarized in Table 4.3.1 and shown in Fig. 4.3.4 and 4.3.5. Briefly, none of the mutants was hampered in cell surface expression. Except gB_{C5VC6}, none of the mutants was hampered in cell-cell fusion assay (Fig. 4.3.5).

Name of the construct	Restriction sites inserted	Amino acid substitution	Cell surface expression	Cell-cell fusion
gB_{C1C3C4}	HindIII, XbaI, HpaI	N112S	+	+
gB_{C3C4}	XbaI, HpaI	Silent Mutations	+	+
gB_{C4C5}	HpaI, Asp718	P361R, S362Y, V363L	+	+
gB_{C5VC6}	XbaI, XhoI	T365S, M366R, I412L, G413E	+	-
gB_{C5MC6}	HpaI, Asp718	P361R, S362Y, V363L, I412L, G413E	+	+
gB_{C6C7}	XhoI, EcoRV	I412L, G413E, E530D, L531I	+	+

Tab. 4.3.1 List of the constructs in wich restriction sites were inserted adjacent to cysteines in the ectodomain of HSV-1 gB. The name of the constructs refer to the number of the cysteine in mature gB, e.i. in gBC4C5 were added two restriction sites, one near the fourth cysteine and one near the fifth one. Cell surface expression was detected by immuno-fluorescence of COS cells transfected with the constructs (see fig.4.3.4). Cell-cell fusion assay was performed co-transfecting BHK cells with expression plasmids encoding wt-gD, wt-gH, wt-gL, plus listed mutated gB and pcDNA 3.1Myc-His/Lac vector (Invitrogen) for constitutive expression of β-Gal (see fig. 4.3.5).

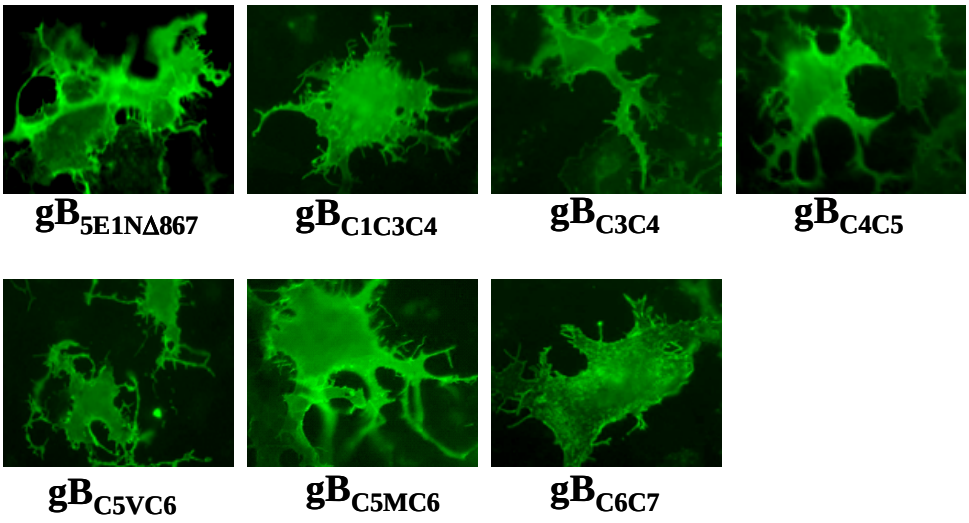

Fig. 4.3.4. Cell surface localization of gB mutants. COS cells were grown on glass coverslips and transfected with plamids encoding $gB_{5E1N\Delta867}$ or the other mutants. At 24 h after transfection the cells were fixed with paraformaldehyde 4% in PBS. Fixed cells were incubated for 1 h at room temperature with anti-5E1 MAb (1:5000), followed by anti-mouse fluorescein-conjugated immunoglobulin G (Jackson Laboratory).

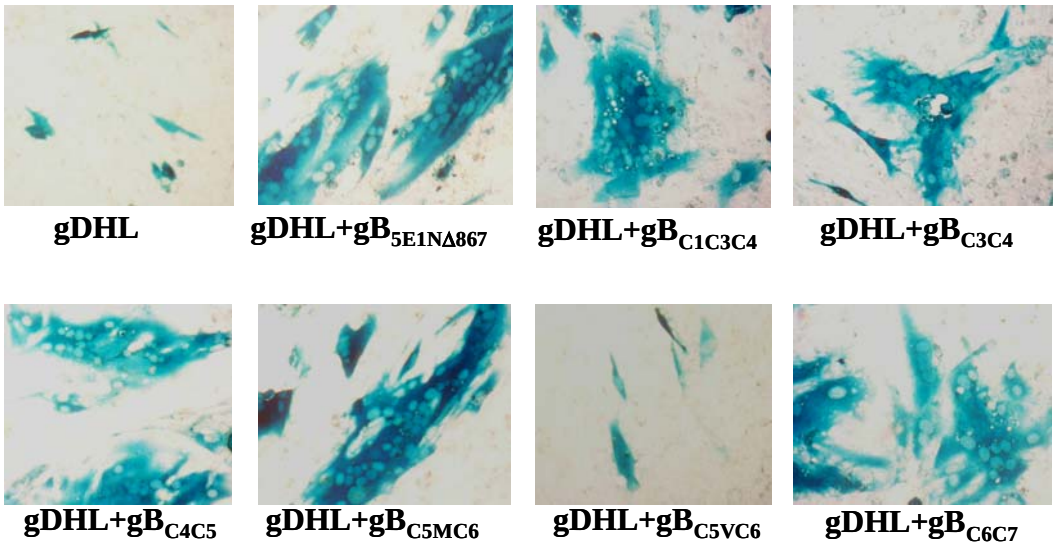

Fig. 4.3.5 Cell-cell fusion assay. BHK cells were cotransfected with plasmids encoding wt-gD, wt-gH, wt-gL, β-galactosidase and $gB_{5E1\Delta867}$ or one of the other gB mutants. The negative control lacked gB, the Erb2 plasmid was used to make the amounts of DNA equal. 48 h after transfection the cells were fixed with 0.2% glutaraldehyde and 0.2% paraformaldehyde in PBS. Syncytia were detected by light microscopy observation of ß-Gal expressing cells after staining with 5-bromo-4chloro-3-indolyl-ß-galactopyranoside (X-Gal). Digital micrograph were taken with Kodak DC120 digital camera.

4.3.1.2 Generation of gB mutants by homologous replacement of HSV gB portions with the corresponding portions from HHV-8 gB (HSV-HHV8 gB chimeras).

The strategy adopted here to generate gB mutants expected to maintain a proper conformation was to substitute the sequence bracketed by two (or three) consecutive cysteines, with the homologous sequences from HHV-8 gB (see alignment in Fig.4.3.6). Indeed, preliminary modelling studies, performed using the SWISSMODEL server (http://swissmodel.expasy.org//SWISS-MODEL.htm) indicated that the homologous replacement mutants generated below can be modelled on HSV gB structure with high confidence score.

The homologous replacement mutants were named according to the cysteines that bracketed the substituted region, followed by H8, which stands for HHV8. To exemplify, in the mutant named gB13H8, the C1-C3-bracketed region was replaced with the corresponding HHV-8 C1-C3-bracketed region (see Fig 4.3.7). Briefly, the mutants were generated as exemplified here for gB13H8. First HSV gB was cleaved with the HindIII and XbaI restriction endonucleases for which the sites were inserted, adjacent to C1 and C3. An amplimer was generated on

HHV-8 gB template. The primers carried the HindIII and XbaI restriction sites useful for insertion. The digested amplimer was ligated to HindIII-XbaI predigested gB. All mutants were sequenced for accuracy.

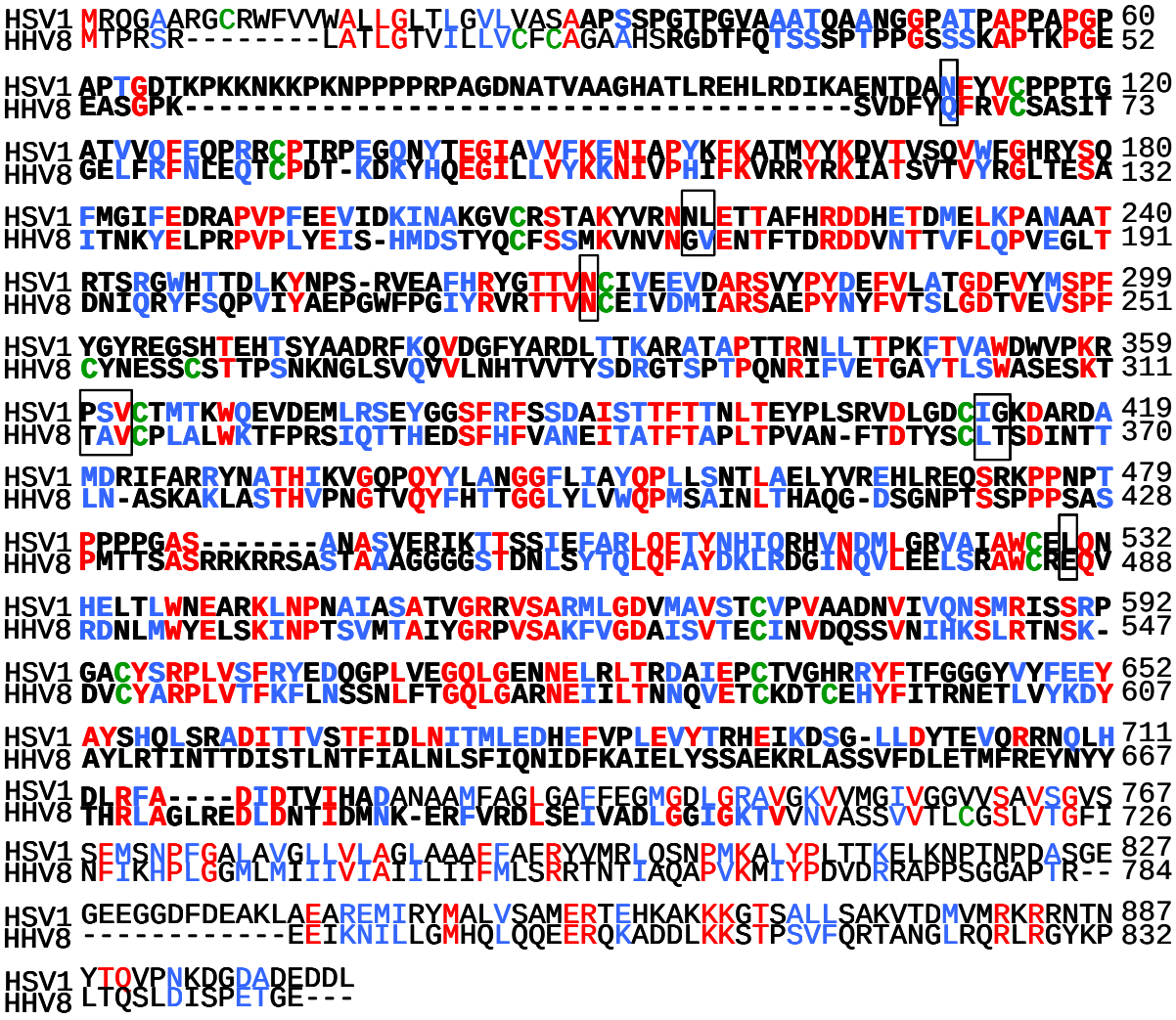

Fig.4.3.6. Amino acid sequences of HSV-1 and HHV8 gBs were aligned. The residues of the two ecodomains are in bold letters. Identical residues are red except for cysteines that are all green. Homologous residues are blue. The squares indicate the positions of the inserted restriction sites thus in some cases the amino acids mutated.

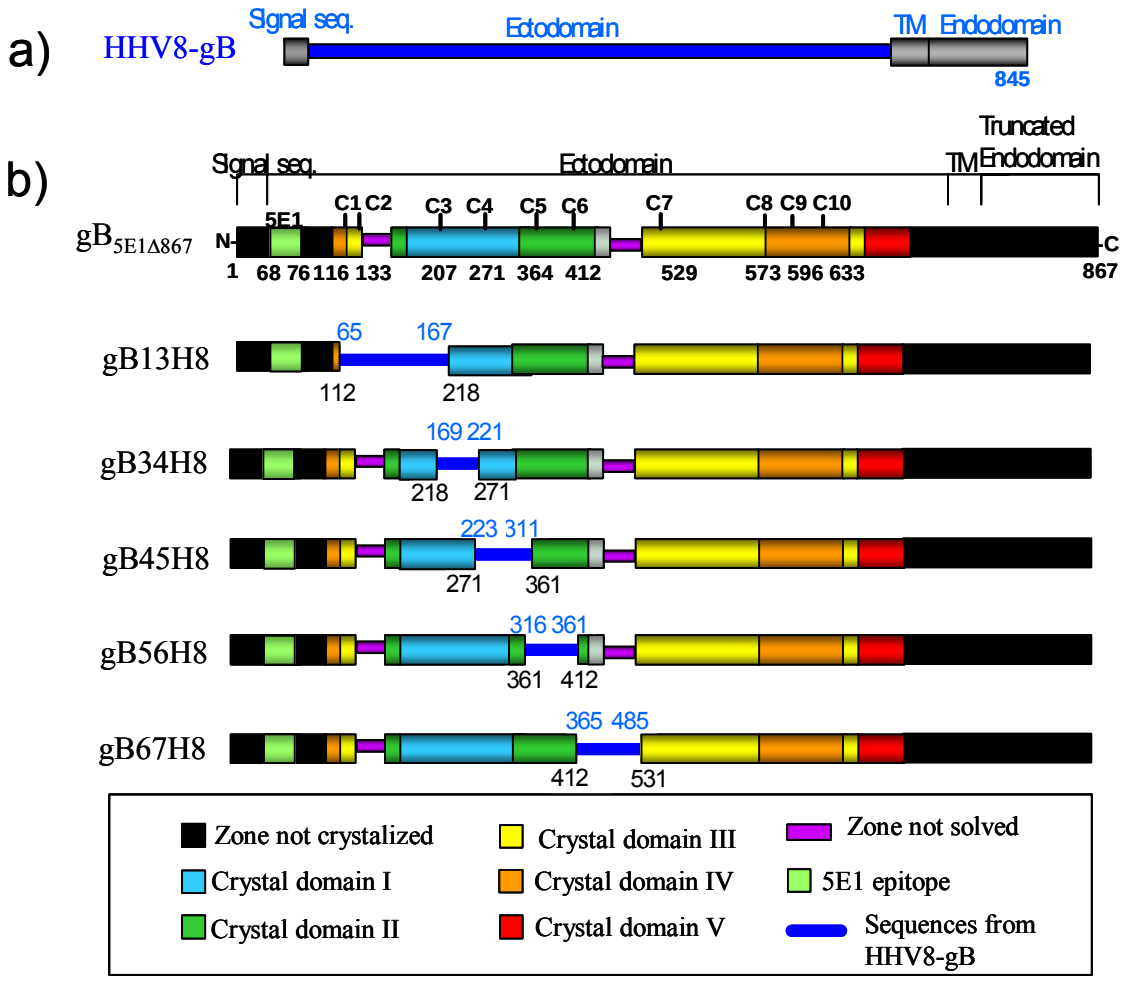

Fig. 4.3.7 a) Schematic representation of HHV8 gB. **b)** Schematic representation of $gB_{5E1N\Delta867}$ and HSV-HHV8 chimeras. Crystal domains are depiticted in the same way used by authors of the HSV-gB solved structure [84], for detail see the legend at the bottom. In HSV-HHV8 chimeras are indicated the residues from HHV8 gB in blue and the position of the insertion in HSV-gB in black. The residue positions are ever referred to that of wt-gB and not $gB_{5E1\Delta867}$.

4.3.1.3 Characterization of HSV-HHV8 gB chimeras.

The HSV-HHV8 gB chimeras generated above were characterized with respect to

(i) cellular localization, as detected by IFA

(ii) Cell-cell fusion

(iii) Infectivity complementation

(iv) Complex formation with gD and gH, detected by pull-down experiments.

(i) For all mutants, the chimeric gB failed to localize at the cell surface. In permeabilized cells, the distribution appeared to be reticular, typical of endoplasmic reticulum (Fig 4.3.8)

(ii) All mutants failed to induce cell-cell fusion when cotransfected with gD, gH, gL, a results consistent with the lack of cell surface expression (Fig 4.3.9).

(iii) All mutants failed to mediate virus infection, as measured in a virus infectivity complementation assay (results not shown).

(iv) As illustrated above, the model of HSV entry into the cell that is being probed in our laboratory envisions that gD forms complexes with gB and gH.gL. here we tested the ability of HSV-HHV-8 gB chimeras to form complexes with gD and/or with gH.gL. Rather than studying complex formation by co-immunoprecipitation studies, here we developed a pull-down approach, as follows. The One-strep-tag sequence (IBA) was engineered at the C terminus of gD (gDstrep) or of gH (gHstrep). 293 cells were transfected with gDstrep, one of the gB chimera, gH.gL. Alternatively cells were transfected with gD, one of gB chimera, gHstrep, gL. Replicate cultures were transfected with mixtures of three glycoproteins, rather than of four glycoprotein, in order to highlight the ability of the glycoporteins to give rise to interaction, even in the absence of some partners. Twenty four h after transfection, cells were lysed with detergent containing buffer ($EA1^{+}$), centrifuged. The supernant was cleared through a ProteinA-sepharose resin, and absorbed to strep-Tactin resin. The absorbed proteins were eluted with SDS-containg sample buffer and separated by SDS-PAGE. The proteins were identified by western blotting. In this assay, if gDsrep (or gHstrep) forms complexes with the other glycoproteins, the complexes are retained by the resin, and subsequently, visualized by WB. Examples of the results obtained are shown in Fig. 4.3.9 and 4.3.10. The results worth of note were as follows, (a) all gB chimeras were capable to form a complex with gD, both in the absence and in the presence of gH. (b) some of the gB chimeras were capable to form a complex with gH. The exceptions were gB34H8 and gB45H8. This result identified the HSV gB region

bracketed by C3-C5 as putative region of interaction between gB and gH.

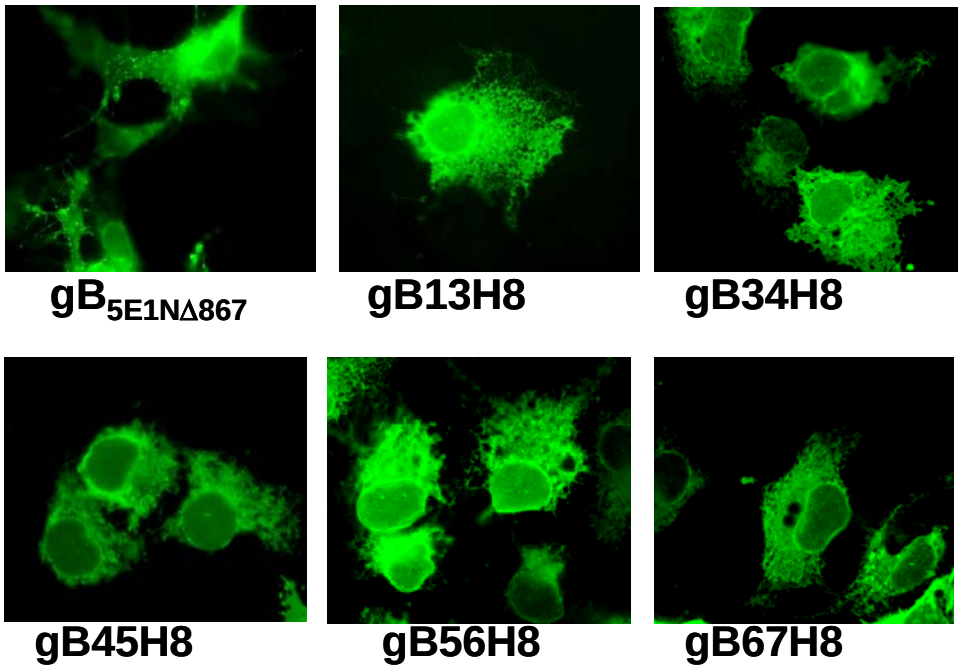

Fig.4.3.8 Cellular localization of HSV-HHV8 chimeras. Cells were transfected with plasmids encoding $gB_{5E1N\Delta867}$ or HSV1-HHV8 gB chimeras. 24 h after transfection cells were fixed in paraformaldehyde or methanol and stained with MAb 5E1 followed by anti-mouse-FITC conjugate. HSV1-HHV8 gB chimeras were not detectable in not permeabilized cells (not shown). All micrographs show permeabilized cells.

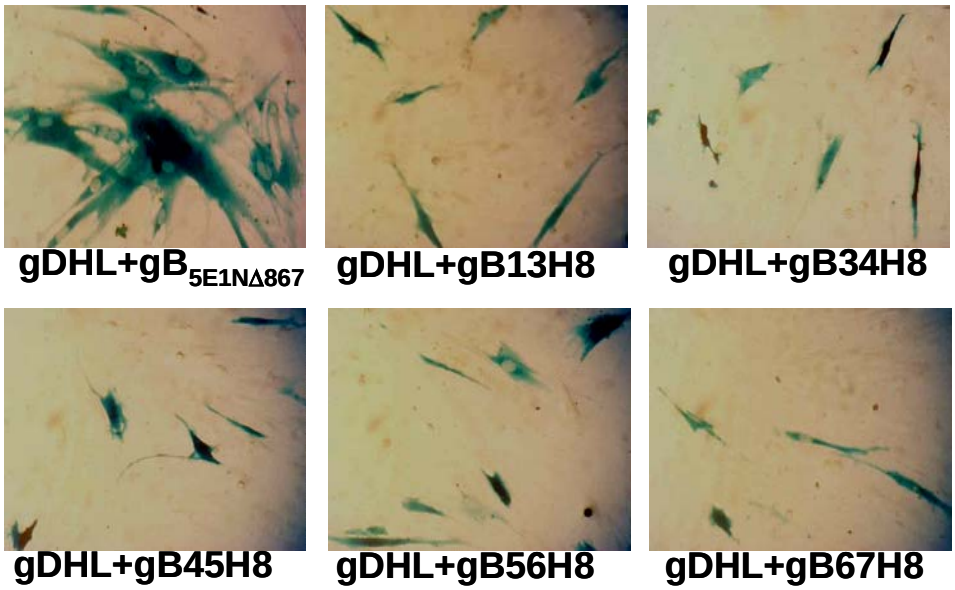

Fig.4.3.9 Digital micrographs of BHK cells submitted to cell-cell fusion assay. BHK cells were transfected with 80 ng of plasmids encoding wt gH, gL, gD, β galactosidase plus $gB_{5E1N\Delta867}$ or HSV1-HHV8 gB chimeras. 48 h after transfection cells were fixed with 0.2% glutaraldehyde and 0.2% paraformaldehyde in PBS then stained with 5-bromo-4-chloro-3-indolyl-galactopyranoside (X-Gal).

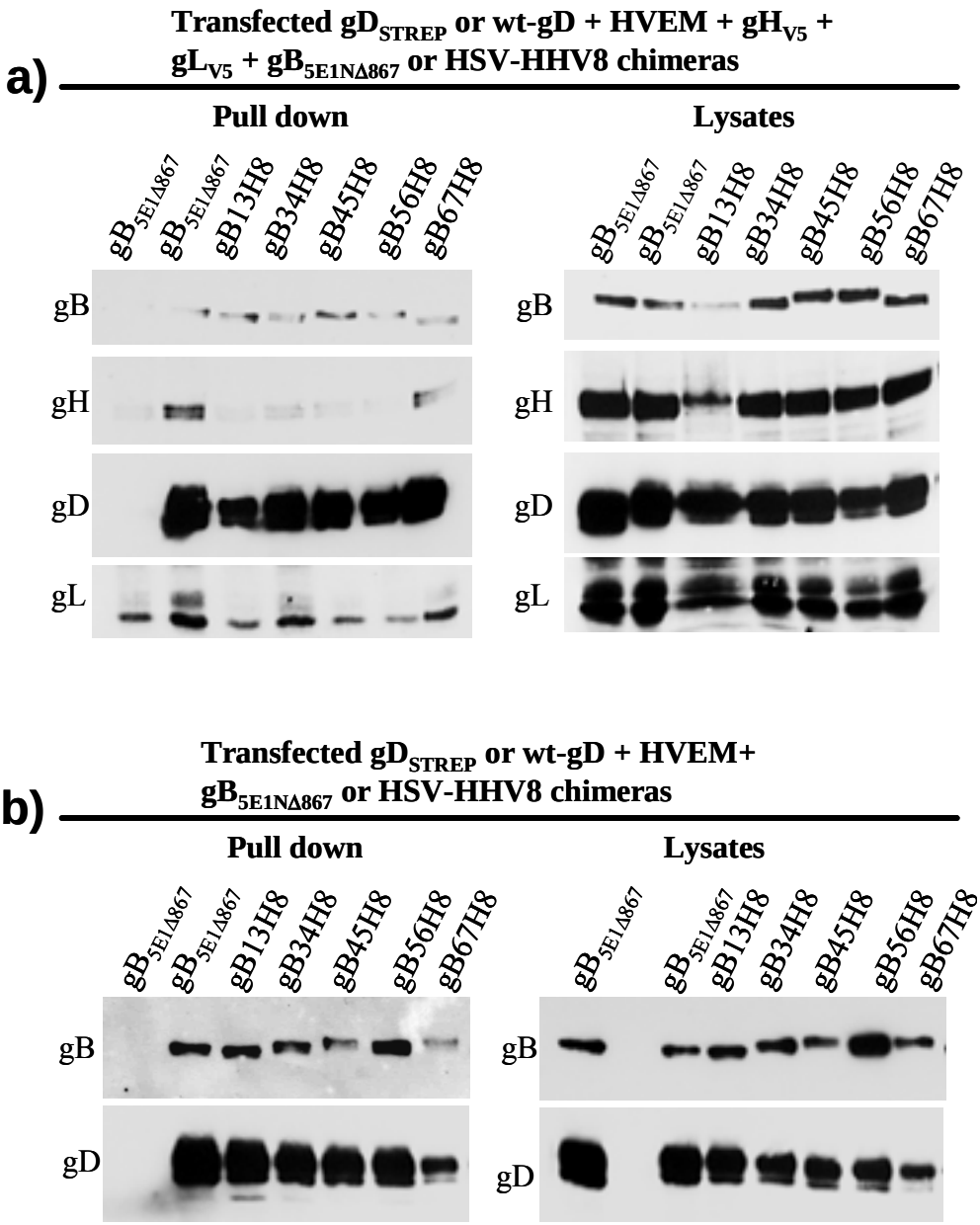

Fig.4.3.9 293T cells were cotransfected with plasmids that express wt-gD or gD$_{STREP}$, HVEM, gB$_{5E1ND867}$ or HSV-HHV8 gB chimeras, and (only in a)) gH$_{V5}$ and gL$_{V5}$. After 24 h the cells were lysed. Expressed proteins present into lysates were analysed by Western blotting (right panel, 'Lyates'). Lysates were centrifuged and the supernatants were incubated prior with ProteinA-Sepharose and then with *Strep*-Tactin Resin. The proteins bound to the beads were analysed by Western blotting (left panel, 'pull down'). To detect gD was used MAb H170, to detect gB$_{5E1ND867}$ or gB chimeras MAb H1817 and to detect gH$_{V5}$ and gL$_{V5}$ anti-V5 antibody (Invitrogen). The negative control was the pull down in the absence of proteins with a *Strep*-tag (first lane). All HSV-HHV8 gB chimeras were recruited by gD$_{STREP}$. both in the presence (a)) and in the absence (b))of gH.gL.

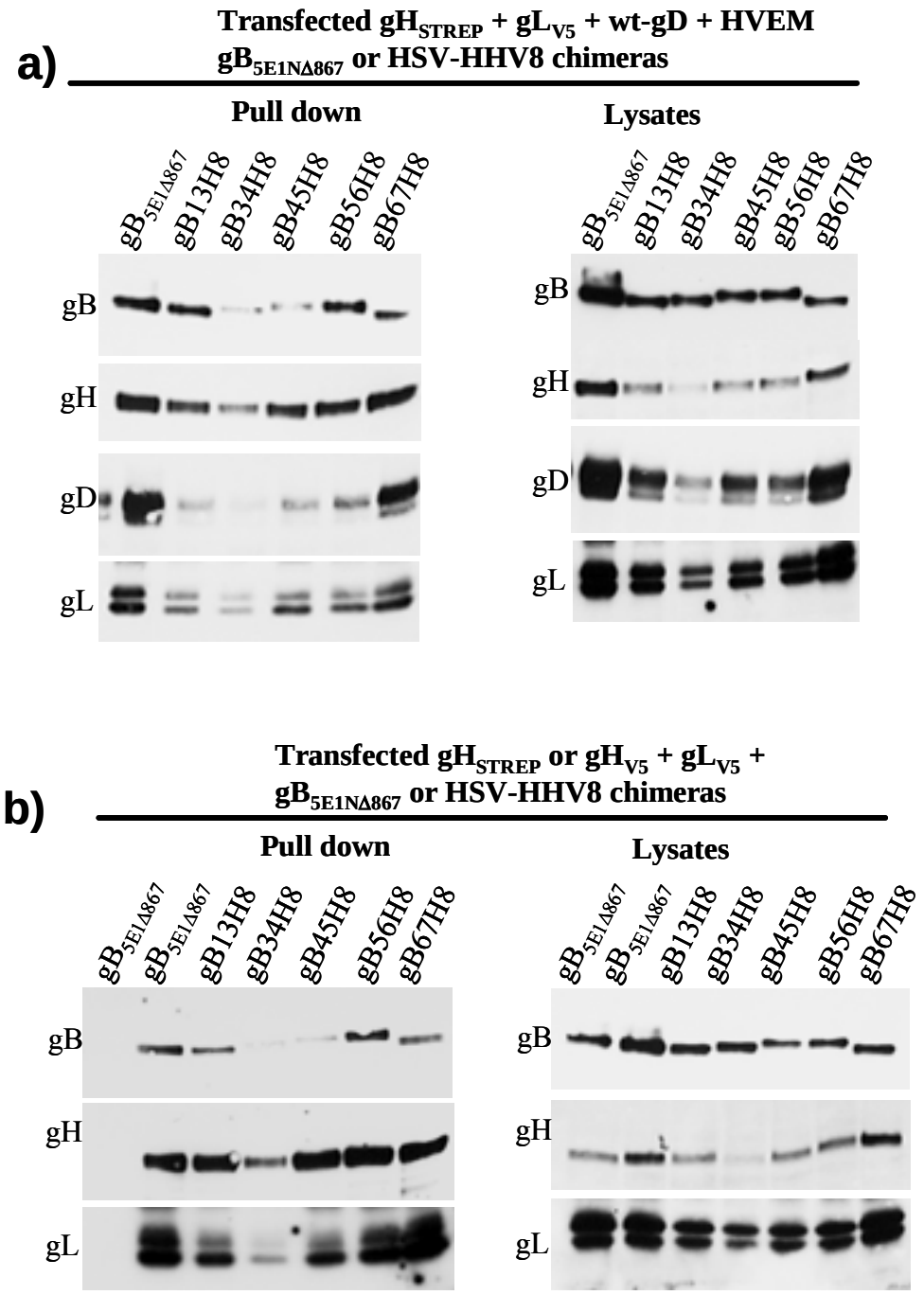

Fig.4.3.9 293T cells were cotransfected with plasmids that express gH_{STREP} or gH_{V5}, gL_{V5}, $gB_{5E1NΔ867}$ or HSV-HHV8 gB chimeras, and (only in a)) wt-gD and HVEM. After 24 h the cells were lysed. Expressed proteins present into lysates were analysed by Western blotting (right panel, 'Lyates'). Lysates were centrifuged and the supernatants were incubated prior with ProteinA-Sepharose and then with *Strep*-Tactin Resin. The proteins bound to the beads were analysed by Western blotting (left panel, 'pull down'). To detect gD was used MAb H170, to detect $gB_{5E1NΔ867}$ or gB chimeras MAb H1817 and to detect gH_{V5} and gL_{V5} anti-V5 antibody (Invitrogen). The negative control was the pull down in the absence of proteins with a *Strep*-tag (first lane). The chimeras named gB34H8 and gB45H8 were recruited by gH_{STREP}. at a lower amount than other chimeras or $gB_{5E1NΔ867}$ both in the presence (a)) and in the absence (b))of gD and HVEM.

4.3.2 CONCLUSIONS

In the past, there have been numerous efforts from a number of laboratory to identify functional regions in gB. The efforts included random linker insertion throughout the gB ectodomain, or site directed mutagenis of predicted helical regions. The vast majority of the studies were carried out prior to resolution of the crystal structure. All these studies were marred by the afct that it was not known whether the mutants maintained the structure of the wt allele. The strategy adopted here to obviate these problem was (i)conservation of conserved cysteines; (ii) homologous substitutions of HSV gB portions with allelic gB regions from HHV-8. Despite this conservative strategy, the mutants failed to be transpoerted to the plasma membrane, and were retained in ER. This property suggests problems in proper folding. Lack of transport to the cell surface has made it impossible to characterize the mutants with respect to their fusion ability in the cell-cell fusion assay.

A most novel property of gB investigated here has been the ability of gb to form complexes with the ther glycoproteins required for HSV entry into the cells, namely gD and gH.gL. The conservative strategy applied here has indeed lead to the identification of a gB region most likely involved in the interaction with gH.gL, or critical to complex formation. The region is the segment bracketed by C3-C5. Inspection of gB crystal structure shows that the C3-C5 segment is part odf domain I, the domain that carries the candidate fusion loop of gB. Such candidate fusion loop appears to be critical for gB interaction with cell membranes. Much of the uncertainties in interpreting these data stems from the fact that the soved gB structure very likely represents the post-fusion structure. For the ebst known viral fusion glycoproteins, it is known that the higly hydrophobic fusion peptide is masked when the glycoprotein adopts a prefusion conformation, and is expsed when the glycoprotein adopts a post-fusion conformation. This leads us to speculate that the possible interaction between gB fusion loop and gH may exert the effect of masking the fusion loop, when gB adopts the prefusion conformation.

REFERENCES

5. REFERENCES

1. Roizman, B. and N. Frenkel, *The transcription and state of herpes simplex virus DNA in productive infection and in human cervical cancer tissue.* Cancer Res, 1973. **33**(6): p. 1402-16.
2. Roizman, B., et al., *Herpesviridae. Definition, provisional nomenclature, and taxonomy. The Herpesvirus Study Group, the International Committee on Taxonomy of Viruses.* Intervirology, 1981. **16**(4): p. 201-17.
3. Roizmann, B., et al., *The family Herpesviridae: an update. The Herpesvirus Study Group of the International Committee on Taxonomy of Viruses.* Arch Virol, 1992. **123**(3-4): p. 425-49.
4. Davison,A.J., Eberle, R., Hayward, G.S. et al. (2005). Familiy *Herpesviridae*. In *Virus Taxonomy, VIIIth Report of the International Committee on Taxonomy ofViruses*, ed. C.M. Fauquet, M.A. Mayo, J. Maniloff, U. Desselberger and A.L. Ball, pp 193-212. London: Academic Press/Elsevier
5. Whitley, R.J., *Herpes simplex virus*, in *Fields Virology*, D.M. Knipe, et al., Editors. 2001, Lippincott Williams & Wilkins: Philadelphia. p. 2461-2509.
6. Lafferty, W.E., et al., *Herpes simplex virus type 1 as a cause of genital herpes: impact on surveillance and prevention.* J Infect Dis, 2000. **181**(4): p. 1454-7.
7. Mertz, G.J., S.L. Rosenthal, and L.R. Stanberry, *Is herpes simplex virus type 1 (HSV-1) now more common than HSV-2 in first episodes of genital herpes?* Sex Transm Dis, 2003. **30**(10): p. 801-2.
8. Whitley, R., Kimberlin, D.V., Prober, C.G (2007). *Pathogenesis, clinical disease, host reponse, and epidemiology: alphaherpes virus*. In *Human Herpesviruses, Biology, Therapy, and Immunoprophylaxis*, ed. Arvin, A., Campadelli-Fiume, G., Mocarski, E., Moore, P.S., Roizman, B., Whitley, R. and Yamanishi, K. pp 589-656. Cambridge University Press.
9. Roizman, B. and Furlong, D. (1974). *The replication of herpes viruses*. In *Comprehensive Virology*, ed. H. Fraenkel-Conrat, H., and R. R. Wagner, pp. 229-403 New York, NY: Plenum Press.
10. Zhou, G., G. Liang, and L. Li, *[Complete nucleotide sequence of the nonstructural gene of alphavirus YN87448 strain isolated in China and its relationship to other Sindbis viruses]*. Zhonghua Shi Yan He Lin Chuang Bing Du Xue Za Zhi, 1999. **13**(4): p. 314-20.
11. Zhou, G. and B. Roizman, *Wild-type herpes simplex virus 1 blocks programmed cell death and release of cytochrome c but not the translocation of mitochondrial apoptosis-inducing factor to the nuclei of human embryonic lung fibroblasts.* J Virol, 2000. **74**(19): p. 9048-53.

12. Roizman, B. and D.M. Knipe, *Herpes simplex viruses and their replication*, in *Fields Virology*, D.M. Knipe, et al., Editors. 2001, Lippincott Williams & Wilkins: Philadelphia. p. 2399-2459.
13. Grunewald, K., et al., *Three-dimensional structure of herpes simplex virus from cryo-electron tomography.* Science, 2003. **302**(5649): p. 1396-8.
14. Roizman, B. and P.E. Pellet, *The family Herpesviridae: a brief introduction*, in *Fields Virology*, D.M. Knipe, et al., Editors. 2001, Lippincott Williams & Wilkins: Philadelphia. p. 2381-2397.
15. Chernomordik, L.V. and M.M. Kozlov, *Membrane hemifusion: crossing a chasm in two leaps.* Cell, 2005. **123**(3): p. 375-82.
16. Weissenhorn, W., A. Hinz, and Y. Gaudin, *Virus membrane fusion.* FEBS Lett, 2007. **581**(11): p. 2150-5.
17. Jardetzky, T.S. and R.A. Lamb, *Virology: a class act.* Nature, 2004. **427**(6972): p. 307-8.
18. Kielian, M., *Class II virus membrane fusion proteins.* Virology, 2006. **344**(1): p. 38-47.
19. Roche, S., et al., *Crystal structure of the low-pH form of the vesicular stomatitis virus glycoprotein G.* Science, 2006. **313**(5784): p. 187-91.
20. Roche, S., et al., *Structure of the prefusion form of the vesicular stomatitis virus glycoprotein G.* Science, 2007. **315**(5813): p. 843-8.
21. Herold, B.C., et al., *Glycoprotein C of herpes simplex virus type 1 plays a principal role in the adsorption of virus to cells and in infectivity.* J Virol, 1991. **65**(3): p. 1090-8.
22. Nicola, A.V. and S.E. Straus, *Cellular and viral requirements for rapid endocytic entry of herpes simplex virus.* J Virol, 2004. **78**(14): p. 7508-17.
23. Nicola, A.V., et al., *Herpes simplex virus type 1 enters human epidermal keratinocytes, but not neurons, via a pH-dependent endocytic pathway.* J Virol, 2005. **79**(12): p. 7609-16.
24. Milne, R.S., et al., *Glycoprotein D receptor-dependent, low-pH-independent endocytic entry of herpes simplex virus type 1.* J Virol, 2005. **79**(11): p. 6655-63.
25. Montgomery, A.M., et al., *Human neural cell adhesion molecule L1 and rat homologue NILE are ligands for integrin alpha v beta 3.* J Cell Biol, 1996. **132**(3): p. 475-85.
26. Warner, M.S., et al., *A cell surface protein with herpesvirus entry activity (HveB) confers susceptibility to infection by mutants of herpes simplex virus type 1, herpes simplex virus type 2, and pseudorabies virus.* Virology, 1998. **246**(1): p. 179-89.
27. Lopez, M., et al., *Nectin2α (PRR2α or HveB) and nectin2δ are low-efficiency mediators for entry of herpes simplex virus mutants carrying the Leu25Pro substitution in glycoprotein D.* J Virol, 2000. **74**(3): p. 1267-74.
28. Cocchi, F., et al., *The ectodomain of a novel member of the immunoglobulin superfamily related to the poliovirus receptor has the*

attibutes of a bonafide receptor for herpes simplex viruses 1 and 2 in human cells. J Virol, 1998. **72**: p. 9992-10002.
29. Geraghty, R.J., et al., *Entry of alphaherpesviruses mediated by poliovirus receptor-related protein 1 and poliovirus receptor.* Science, 1998. **280**(5369): p. 1618-20.
30. Shukla, D., et al., *A novel role for 3-O-sulfated heparan sulfate in herpes simplex virus 1 entry.* Cell, 1999. **99**(1): p. 13-22.
31. Campadelli-Fiume, G., et al., *The novel receptors that mediate the entry of herpes simplex viruses and animal alphaherpesviruses into cells.* Rev Med Virol, 2000. **10**(5): p. 305-19.
32. Spear, P.G., R.J. Eisenberg, and G.H. Cohen, *Three classes of cell surface receptors for alphaherpesvirus entry.* Virology, 2000. **275**(1): p. 1-8.
33. Cocchi, F., et al., *The V domain of herpesvirus Ig-like receptor (HIgR) contains a major functional region in herpes simplex virus-1 entry into cells and interacts physically with the viral glycoprotein D.* Proc Natl Acad Sci U S A, 1998. **95**(26): p. 15700-5.
34. Haarr, L., et al., *Transcription from the gene encoding the herpesvirus entry receptor nectin-1 (HveC) in nervous tissue of adult mouse.* Virology, 2001. **287**(2): p. 301-9.
35. Matsushima, H., et al., *The expression of nectin-1alpha in normal human skin and various skin tumours.* Br J Dermatol, 2003. **148**(4): p. 755-62.
36. Richart, S., et al., *Entry of herpes simplex virus type 1 into primary sensory neurons in vitro is mediated by Nectin-1/HveC.* J. Virol., 2003. **77**(5): p. 3307-11.
37. Linehan, M.M., et al., *In vivo role of nectin-1 in entry of herpes simplex virus type 1 (HSV-1) and HSV-2 through the vaginal mucosa.* J Virol, 2004. **78**(5): p. 2530-6.
38. Krummenacher, C., et al., *Herpes simplex virus glycoprotein D can bind to poliovirus receptor-related protein 1 or herpesvirus entry mediator, two structurally unrelated mediators of virus entry.* J Virol, 1998. **72**(9): p. 7064-74.
39. Krummenacher, C., et al., *Comparative usage of herpesvirus entry mediator A and nectin-1 by laboratory strains and clinical isolates of herpes simplex virus.* Virology, 2004. **322**(2): p. 286-99.
40. Perez, A., et al., *A new class of receptor for herpes simplex virus has heptad repeat motifs that are common to membrane fusion proteins.* J Virol, 2005. **79**(12): p. 7419-30.
41. Bender, F.C., et al., *Herpes simplex virus glycoprotein B binds to cell surfaces independently of heparan sulfate and blocks virus entry.* J Virol, 2005. **79**(18): p. 11588-97.
42. Satoh, T., et al., *PIRLα is a herpes simplex virus-1 entry co-receptor that associates with glycoprotein B*. In press.
43. Carfi, A., et al., *Herpes simplex virus glycoprotein D bound to the human receptor HveA.* Mol Cell, 2001. **8**(1): p. 169-79.

44. Krummenacher, C., et al., *Structure of unliganded HSV gD reveals a mechanism for receptor-mediated activation of virus entry.* Embo J, 2005. **24**(23): p. 4144-53.
45. Connolly, S.A., et al., *Structure-based mutagenesis of herpes simplex virus glycoprotein D defines three critical regions at the gD-HveA/HVEM binding interface.* J Virol, 2003. **77**(14): p. 8127-40.
46. Yoon, M., et al., *Mutations in the N termini of herpes simplex virus type 1 and 2 gDs alter functional interactions with the entry/fusion receptors HVEM, nectin-2, and 3-O-sulfated heparan sulfate but not with nectin-1.* J Virol, 2003. **77**(17): p. 9221-31.
47. Zhou, G., et al., *The domains of glycoprotein D required to block apoptosis induced by herpes simplex virus 1 are largely distinct from those involved in cell- cell fusion and binding to nectin1.* J Virol, 2003. **77**(6): p. 3759-67.
48. Manoj, S., et al., *Mutations in herpes simplex virus glycoprotein D that prevent cell entry via nectins and alter cell tropism.* Proc Natl Acad Sci U S A, 2004. **101**(34): p. 12414-21.
49. Connolly, S.A., et al., *Potential nectin-1 binding site on herpes simplex virus glycoprotein d.* J Virol, 2005. **79**(2): p. 1282-95.
50. Zhou, G. and B. Roizman, *Construction and properties of a herpes simplex virus 1 designed to enter cells solely via the IL-13alpha2 receptor.* Proc Natl Acad Sci U S A, 2006. **103**(14): p. 5508-13.
51. Browne, H., et al., *Analysis of the role of the membrane-spanning and cytoplasmic tail domains of herpes simplex virus type 1 glycoprotein D in membrane fusion.* J Gen Virol, 2003. **84**(Pt 5): p. 1085-9.
52. Cairns, T.M., et al., *Structure-function analysis of herpes simplex virus type 1 gD and gH-gL: clues from gDgH chimeras.* J Virol, 2003. **77**(12): p. 6731-42.
53. Cocchi, F., et al., *The soluble ectodomain of herpes simplex virus gD contains a membrane-proximal pro-fusion domain and suffices to mediate virus entry.* Proc Natl Acad Sci U S A, 2004. **101**(19): p. 7445-50.
54. Fusco, D., C. Forghieri, and G. Campadelli-Fiume, *The pro-fusion domain of herpes simplex virus glycoprotein D (gD) interacts with the gD N terminus and is displaced by soluble forms of viral receptors.* Proc Natl Acad Sci U S A, 2005. **102**(26): p. 9323-8.
55. Zhou, G. and B. Roizman, *Separation of receptor-binding and profusogenic domains of glycoprotein D of herpes simplex virus 1 into distinct interacting proteins.* Proc Natl Acad Sci U S A, 2007. **104**(10): p. 4142-6.
56. Forrester, A., et al., *Construction and properties of a mutant of herpes simplex virus type 1 with glycoprotein H coding sequences deleted.* J Virol, 1992. **66**(1): p. 341-8.
57. Fuller, A.O., R.E. Santos, and P.G. Spear, *Neutralizing antibodies specific for glycoprotein H of herpes simplex virus permit viral attachment to cells but prevent penetration.* J Virol, 1989. **63**(8): p. 3435-43.

58. Gianni, T., et al., *The ectodomain of herpes simplex virus glycoprotein H contains a membrane alpha-helix with attributes of an internal fusion peptide, positionally conserved in the herpesviridae family.* J Virol, 2005. **79**(5): p. 2931-40.
59. Gianni, T., L. Menotti, and G. Campadelli-Fiume, *A heptad repeat in herpes simplex virus 1 gH, located downstream of the alpha-helix with attributes of a fusion peptide, is critical for virus entry and fusion.* J Virol, 2005. **79**(11): p. 7042-9.
60. Gianni, T., et al., *Heptad repeat 2 in herpes simplex virus 1 gH interacts with heptad repeat 1 and is critical for virus entry and fusion.* J Virol, 2006. **80**(5): p. 2216-24.
61. Gianni, T., et al., *Hydrophobic alpha-helices 1 and 2 of herpes simplex virus gH interact with lipids, and their mimetic peptides enhance virus infection and fusion.* J Virol, 2006. **80**(16): p. 8190-8.
62. Galdiero, S., et al., *Analysis of synthetic peptides from heptad-repeat domains of herpes simplex virus type 1 glycoproteins H and B.* J Gen Virol, 2006. **87**(Pt 5): p. 1085-97.
63. Parry, C., et al., *Herpes simplex virus type 1 glycoprotein H binds to alphavbeta3 integrins.* J Gen Virol, 2005. **86**(Pt 1): p. 7-10.
64. Galdiero, M., et al., *Site-directed and linker insertion mutagenesis of herpes simplex virus type 1 glycoprotein H.* J Virol, 1997. **71**(3): p. 2163-70.
65. Claesson-Welsh, L. and P.G. Spear, *Amino-terminal sequence, synthesis, and membrane insertion of glycoprotein B of herpes simplex virus type 1.* J Virol, 1987. **61**(1): p. 1-7.
66. Highlander, S.L., et al., *Oligomer formation of the gB glycoprotein of herpes simplex virus type 1.* J Virol, 1991. **65**(8): p. 4275-83.
67. Laquerre, S., S. Person, and J.C. Glorioso, *Glycoprotein B of herpes simplex virus type 1 oligomerizes through the intermolecular interaction of a 28-amino-acid domain.* J Virol, 1996. **70**(3): p. 1640-50.
68. Spear, P.G., *Entry of alphaherpesviruses into cells.* Semin Virol, 1993. **4**: p. 167-80.
69. Bzik, D.J., et al., *Nucleotide sequence of a region of the herpes simplex virus type 1 gB glycoprotein gene: mutations affecting rate of virus entry and cell fusion.* Virology, 1984. **137**(1): p. 185-90.
70. Pellett, P.E., et al., *Anatomy of the herpes simplex virus 1 strain F glycoprotein B gene: primary sequence and predicted protein structure of the wild type and of monoclonal antibody-resistant mutants.* J Virol, 1985. **53**(1): p. 243-53.
71. Rasile, L., et al., *Effects of deletions in the carboxy-terminal hydrophobic region of herpes simplex virus glycoprotein gB on intracellular transport and membrane anchoring.* J Virol, 1993. **67**(8): p. 4856-66.
72. Fan, Z., et al., *Truncation of herpes simplex virus type 2 glycoprotein B increases its cell surface expression and activity in cell-cell fusion, but these properties are unrelated.* J Virol, 2002. **76**(18): p. 9271-83.

73. Avitabile, E., et al., *Coexpression of UL20p and gK inhibits cell-cell fusion mediated by herpes simplex virus glycoproteins gD, gH-gL, and wild-type gB or an endocytosis-defective gB mutant and downmodulates their cell surface expression.* J Virol, 2004. **78**(15): p. 8015-25.
74. Beitia Ortiz de Zarate, I., K. Kaelin, and F. Rozenberg, *Effects of mutations in the cytoplasmic domain of herpes simplex virus type 1 glycoprotein B on intracellular transport and infectivity.* J Virol, 2004. **78**(3): p. 1540-51.
75. Avitabile, E., G. Lombardi, and G. Campadelli-Fiume, *Herpes Simplex Virus Glycoprotein K, but Not Its Syncytial Allele, Inhibits Cell-Cell Fusion Mediated by the Four Fusogenic Glycoproteins, gD, gB, gH and gL.* Journal of Virology, 2003. **77**(12): p. 6836-6844.
76. Kousoulas, K.G., et al., *Mutations affecting conformation or sequence of neutralizing epitopes identified by reactivity of viable plaques segregate from syn and ts domains of HSV-1(F) gB gene.* Virology, 1984. **135**(2): p. 379-94.
77. Cai, W.Z., et al., *Linker-insertion nonsense and restriction-site deletion mutations of the gB glycoprotein gene of herpes simplex virus type 1.* J Virol, 1987. **61**(3): p. 714-21.
78. Manservigi, R., P.G. Spear, and A. Buchan, *Cell fusion induced by herpes simplex virus is promoted and suppressed by different viral glycoproteins.* Proc Natl Acad Sci U S A, 1977. **74**(9): p. 3913-7.
79. Turner, A., et al., *Glycoproteins gB, gD, and gHgL of herpes simplex virus type 1 are necessary and sufficient to mediate membrane fusion in a Cos cell transfection system.* J Virol, 1998. **72**(1): p. 873-5.
80. Kousoulas, K.G., B. Huo, and L. Pereira, *Antibody-resistant mutations in cross-reactive and type-specific epitopes of herpes simplex virus 1 glycoprotein B map in separate domains.* Virology, 1988. **166**(2): p. 423-31.
81. Highlander, S.L., et al., *Identification of mar mutations in herpes simplex virus type 1 glycoprotein B which alter antigenic structure and function in virus penetration.* J Virol, 1989. **63**(2): p. 730-8.
82. Pereira, L., et al., *Domain structure of herpes simplex virus 1 glycoprotein B: neutralizing epitopes map in regions of continuous and discontinuous residues.* Virology, 1989. **172**(1): p. 11-24.
83. Qadri, I., et al., *Mutations in conformation-dependent domains of herpes simplex virus 1 glycoprotein B affect the antigenic properties, dimerization, and transport of the molecule.* Virology, 1991. **180**(1): p. 135-52.
84. Heldwein, E.E., et al., *Crystal structure of glycoprotein B from herpes simplex virus 1.* Science, 2006. **313**(5784): p. 217-20.
85. Lemmon, M.A., *Phosphoinositide recognition domains.* Traffic, 2003. **4**(4): p. 201-13.
86. Hannah, B.P., et al., *Mutational evidence of internal fusion loops in herpes simplex virus glycoprotein B.* J Virol, 2007. **81**(9): p. 4858-65.

87. Bender, F.C., et al., *Antigenic and mutational analyses of herpes simplex virus glycoprotein B reveal four functional regions.* J Virol, 2007. **81**(8): p. 3827-41.
88. Duus, K.M., C. Hatfield, and C. Grose, *Cell surface expression and fusion by the varicella-zoster virus gH:gL glycoprotein complex: analysis by laser scanning confocal microscopy.* Virology, 1995. **210**(2): p. 429-40.
89. Kinzler, E.R. and T. Compton, *Characterization of human cytomegalovirus glycoprotein-induced cell-cell fusion.* J Virol, 2005. **79**(12): p. 7827-37.
90. Pertel, P.E., *Human herpesvirus 8 glycoprotein B (gB), gH, and gL can mediate cell fusion.* J Virol, 2002. **76**(9): p. 4390-400.
91. Akula, S.M., et al., *Kaposi's sarcoma-associated herpesvirus (human herpesvirus 8) infection of human fibroblast cells occurs through endocytosis.* J Virol, 2003. **77**(14): p. 7978-90.
92. Akula, S.M., et al., *Human herpesvirus 8 envelope-associated glycoprotein B interacts with heparan sulfate-like moieties.* Virology, 2001. **284**(2): p. 235-49.
93. Akula, S.M., et al., *Human herpesvirus 8 interaction with target cells involves heparan sulfate.* Virology, 2001. **282**(2): p. 245-55.
94. Baghian, A., et al., *Glycoprotein B of human herpesvirus 8 is a component of the virion in a cleaved form composed of amino- and carboxyl-terminal fragments.* Virology, 2000. **269**(1): p. 18-25.
95. Akula, S.M., et al., *Integrin alpha3beta1 (CD 49c/29) is a cellular receptor for Kaposi's sarcoma-associated herpesvirus (KSHV/HHV-8) entry into the target cells.* Cell, 2002. **108**(3): p. 407-19.
96. Rappocciolo, G., et al., *DC-SIGN is a receptor for human herpesvirus 8 on dendritic cells and macrophages.* J Immunol, 2006. **176**(3): p. 1741-9.
97. Kaleeba, J.A. and E.A. Berger, *Kaposi's sarcoma-associated herpesvirus fusion-entry receptor: cystine transporter xCT.* Science, 2006. **311**(5769): p. 1921-4.
98. Johnson, R.M. and P.G. Spear, *Herpes simplex virus glycoprotein D mediates interference with herpes simplex virus infection.* J Virol, 1989. **63**(2): p. 819-27.
99. Wild, P., et al., *Impairment of nuclear pores in bovine herpesvirus 1-infected MDBK cells.* J Virol, 2005. **79**(2): p. 1071-83.
100. Mettenleiter, T.C. and T. Minson, *Egress of alphaherpesviruses.* J Virol, 2006. **80**(3): p. 1610-1; author reply 1611-2.
101. Farnsworth, A., et al., *Herpes simplex virus glycoproteins gB and gH function in fusion between the virion envelope and the outer nuclear membrane.* Proc Natl Acad Sci U S A, 2007. **104**(24): p. 10187-92.
102. Farnsworth, A., K. Goldsmith, and D.C. Johnson, *Herpes simplex virus glycoproteins gD and gE/gI serve essential but redundant functions during acquisition of the virion envelope in the cytoplasm.* J Virol, 2003. **77**(15): p. 8481-94.

103. Desai, P.J., *A null mutation in the UL36 gene of herpes simplex virus type 1 results in accumulation of unenveloped DNA-filled capsids in the cytoplasm of infected cells.* J Virol, 2000. **74**(24): p. 11608-18.
104. Fuchs, W., et al., *Essential function of the pseudorabies virus UL36 gene product is independent of its interaction with the UL37 protein.* J Virol, 2004. **78**(21): p. 11879-89.
105. Kopp, M., et al., *The pseudorabies virus UL11 protein is a virion component involved in secondary envelopment in the cytoplasm.* J Virol, 2003. **77**(9): p. 5339-51.
106. Silva, M.C., et al., *Human cytomegalovirus UL99-encoded pp28 is required for the cytoplasmic envelopment of tegument-associated capsids.* J Virol, 2003. **77**(19): p. 10594-605.
107. Fuchs, W., et al., *The UL48 tegument protein of pseudorabies virus is critical for intracytoplasmic assembly of infectious virions.* J Virol, 2002. **76**(13): p. 6729-42.
108. Klupp, B.G., et al., *Functional analysis of the pseudorabies virus UL51 protein.* J Virol, 2005. **79**(6): p. 3831-40.
109. Mossman, K.L., et al., *Evidence that herpes simplex virus VP16 is required for viral egress downstream of the initial envelopment event.* J Virol, 2000. **74**(14): p. 6287-99.
110. Nozawa, N., et al., *Herpes simplex virus type 1 UL51 protein is involved in maturation and egress of virus particles.* J Virol, 2005. **79**(11): p. 6947-56.
111. AuCoin, D.P., et al., *Betaherpesvirus-conserved cytomegalovirus tegument protein ppUL32 (pp150) controls cytoplasmic events during virion maturation.* J Virol, 2006. **80**(16): p. 8199-210.
112. Crump, C.M., C. Yates, and T. Minson, *Herpes simplex virus type 1 cytoplasmic envelopment requires functional Vps4.* J Virol, 2007. **81**(14): p. 7380-7.
113. Piper, R.C. and J.P. Luzio, *Late endosomes: sorting and partitioning in multivesicular bodies.* Traffic, 2001. **2**(9): p. 612-21.
114. Raiborg, C., T.E. Rusten, and H. Stenmark, *Protein sorting into multivesicular endosomes.* Curr Opin Cell Biol, 2003. **15**(4): p. 446-55.
115. Babst, M., *A protein's final ESCRT.* Traffic, 2005. **6**(1): p. 2-9.
116. Piper, R.C. and D.J. Katzmann, *Biogenesis and function of multivesicular bodies.* Annu Rev Cell Dev Biol, 2007. **23**: p. 519-47.
117. Hershko, A. and A. Ciechanover, *The ubiquitin system.* Annu Rev Biochem, 1998. **67**: p. 425-79.
118. Hicke, L. and R. Dunn, *Regulation of membrane protein transport by ubiquitin and ubiquitin-binding proteins.* Annu Rev Cell Dev Biol, 2003. **19**: p. 141-72.
119. Dupre, S., C. Volland, and R. Haguenauer-Tsapis, *Membrane transport: ubiquitylation in endosomal sorting.* Curr Biol, 2001. **11**(22): p. R932-4.
120. Hicke, L., *Protein regulation by monoubiquitin.* Nat Rev Mol Cell Biol, 2001. **2**(3): p. 195-201.

121. Reggiori, F. and H.R. Pelham, *Sorting of proteins into multivesicular bodies: ubiquitin-dependent and -independent targeting.* Embo J, 2001. **20**(18): p. 5176-86.
122. Melman, L., et al., *Proteasome regulates the delivery of LDL receptor-related protein into the degradation pathway.* Mol Biol Cell, 2002. **13**(9): p. 3325-35.
123. Gottlinger, H.G., *The HIV-1 assembly machine.* Aids, 2001. **15 Suppl 5**: p. S13-20.
124. Demirov, D.G. and E.O. Freed, *Retrovirus budding.* Virus Res, 2004. **106**(2): p. 87-102.
125. Morita, E. and W.I. Sundquist, *Retrovirus budding.* Annu Rev Cell Dev Biol, 2004. **20**: p. 395-425.
126. Ott, D.E., et al., *Ubiquitination of HIV-1 and MuLV Gag.* Virology, 2000. **278**(1): p. 111-21.
127. Whitney, J.A., et al., *Cytoplasmic coat proteins involved in endosome function.* Cell, 1995. **83**(5): p. 703-13.
128. Calistri, A., et al., *Intracellular trafficking and maturation of herpes simplex virus type 1 gB and virus egress require functional biogenesis of multivesicular bodies.* J Virol, 2007. **81**(20): p. 11468-78.
129. Campadelli-Fiume, G., et al., *The multipartite system that mediates entry of herpes simplex virus into the cell.* Rev Med Virol, 2007. **17**(5): p. 313-26.
130. Ghosh, R.N., et al., *Cell-based, high-content screen for receptor internalization, recycling and intracellular trafficking.* Biotechniques, 2000. **29**(1): p. 170-5.
131. Ejercito, P.M., E.D. Kieff, and B. Roizman, *Characterization of herpes simplex virus strains differing in their effects on social behaviour of infected cells.* J Gen Virol, 1968. **2**(3): p. 357-64.
132. Ligas, M.W. and D.C. Johnson, *A herpes simplex virus mutant in which glycoprotein D sequences are replaced by beta-galactosidase sequences binds to but is unable to penetrate into cells.* J Virol, 1988. **62**(5): p. 1486-94.
133. Stefan, A., et al., *Development of recombinant diagnostic reagents based on pp85(U14) and p86(U11) proteins to detect the human immune response to human herpesvirus 7 infection.* J Clin Microbiol, 1999. **37**(12): p. 3980-5.
134. Menotti, L., et al., *The murine homolog of human-Nectin1δ serves as a species non-specific mediator for entry of human and animal αherpesviruses in a pathway independent of a detectable binding to gD.* Proc Natl Acad Sci U S A, 2000. **97**(9): p. 4867-72.
135. Rovero, S., et al., *DNA vaccination against rat her-2/Neu p185 more effectively inhibits carcinogenesis than transplantable carcinomas in transgenic BALB/c mice.* J Immunol, 2000. **165**(9): p. 5133-42.

136. Okuma, K., et al., *Host range of human T-cell leukemia virus type I analyzed by a cell fusion-dependent reporter gene activation assay.* Virology, 1999. **254**(2): p. 235-44.
137. Showalter, S.D., M. Zweig, and B. Hampar, *Monoclonal antibodies to herpes simplex virus type 1 proteins, including the immediate-early protein ICP 4.* Infect Immun, 1981. **34**(3): p. 684-92.
138. Isola, V.J., et al., *Fine mapping of antigenic site II of herpes simplex virus glycoprotein D.* J Virol, 1989. **63**(5): p. 2325-34.
139. Pereira, L., et al., *Differential immunologic reactivity and processing of glycoproteins gA and gB of herpes simplex virus types 1 and 2 made in Vero and HEp-2 cells.* Proc Natl Acad Sci U S A, 1981. **78**(8): p. 5202-6.
140. Lopez, M., et al. *CD155 Workshop: Identification of a new class of IgG superfamily antigens expressed in hemopoiesis.* in *In T. Kishimoto, H. Kikutani, A. E. G. von dem Borne, S. M. Goyert, D. Y. Mason, M. Miyasaka, A. Moretta, K. Okumura, S. Shaw, T. A. Springer, K. Sugamura, and H. Zola (ed.), Leukocyte Typing VI, White cells differentiation antigens*. 1997: Garland Publishing, Inc., New York, N.Y.
141. Pertel, P.E., et al., *Cell fusion induced by herpes simplex virus glycoproteins gB, gD, and gH-gL requires a gD receptor but not necessarily heparan sulfate.* Virology, 2001. **279**(1): p. 313-324.
142. Schmidt, T.G. and A. Skerra, *The Strep-tag system for one-step purification and high-affinity detection or capturing of proteins.* Nat Protoc, 2007. **2**(6): p. 1528-35.
143. Schwede, T., et al., *SWISS-MODEL: An automated protein homology-modeling server.* Nucleic Acids Res, 2003. **31**(13): p. 3381-5.
144. Kerppola, T.K., *Visualization of molecular interactions by fluorescence complementation.* Nat Rev Mol Cell Biol, 2006. **7**(6): p. 449-56.
145. Michnick, S.W., *Exploring protein interactions by interaction-induced folding of proteins from complementary peptide fragments.* Curr Opin Struct Biol, 2001. **11**(4): p. 472-7.
146. Magliery, T.J., et al., *Detecting protein-protein interactions with a green fluorescent protein fragment reassembly trap: scope and mechanism.* J Am Chem Soc, 2005. **127**(1): p. 146-57.
147. Zago, A., C.R. Jogger, and P.G. Spear, *Use of herpes simplex virus and pseudorabies virus chimeric glycoprotein D molecules to identify regions critical for membrane fusion.* Proc Natl Acad Sci U S A, 2004. **101**(50): p. 17498-503.